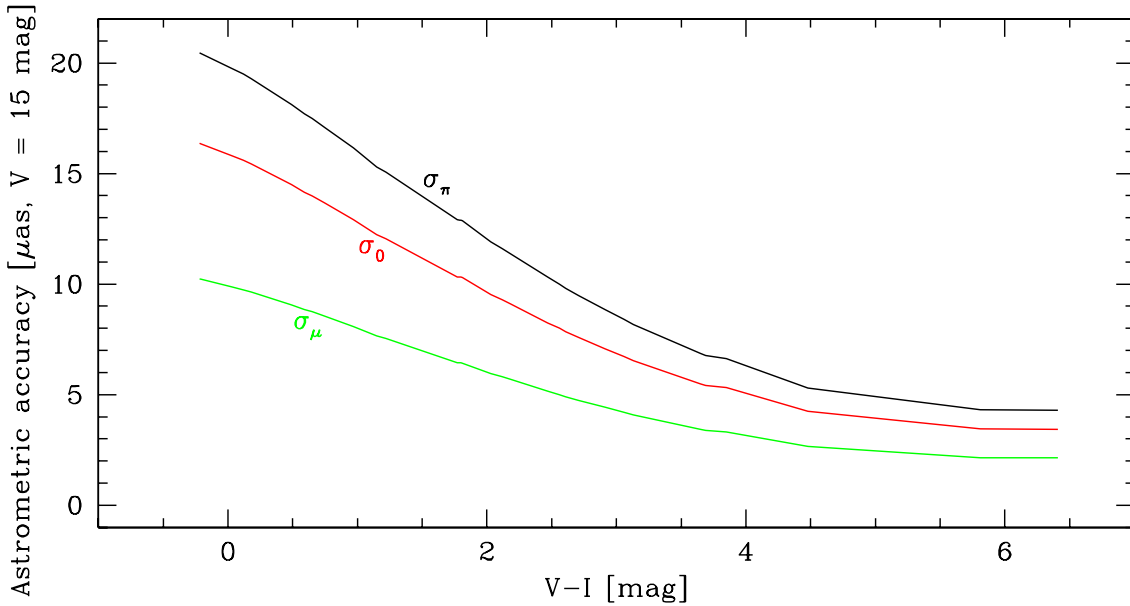


Progress in astrometric accuracy from Hipparchus to Tycho Brahe, Hipparcos, and Gaia. ESA's space astrometry mission Gaia pushes astrometric measurements to the limits.

Gaia's main goal is to collect high-precision astrometric data (i.e. positions, parallaxes, and proper motions) for the brightest 1 billion objects in the sky. These data, complemented with multi-band, multi-epoch photometric and spectroscopic data collected from the same observing platform, will allow astronomers to reconstruct the formation history, structure, and evolution of the Galaxy. In the Gaia Concept and Technology Study Report (published by ESA in 2000), it was shown that meeting these main mission objectives will require the observation of a complete sample of stars down to 20-th magnitude combined with end-of-life astrometric accuracies of  $\sim 20\text{--}25 \mu\text{as}$  (or better) at  $V = 15$  mag.

Order-of-magnitude estimates of Gaia's expected end-of-life astrometric accuracy can easily be obtained by using back-of-the-envelope calculations involving overall, system-level parameters such as primary mirror size, detector efficiency, and mission lifetime. In the current phase of the project, however, a fully-fledged astrometric accuracy tool is indispensable for carefully assessing the impact of various design alternatives on the scientific value of the mission product, for optimizing instrument parameters such as the mirror coating reflectivity, and for safeguarding the mission objectives in general. It has been the responsibility of the Gaia Project Scientist Support Team to set up, maintain, and expand such a general astrometric accuracy model.

The astrometric accuracy model currently in place provides a simplified yet realistic end-to-end simulation of the Gaia observation process, ranging from photon emission at the astronomical source at the one end, through the effects introduced by, e.g. the revolving scanning law and CCD TDI operation, to single-transit centroiding measurements of the line spread function, and the averaging of these results over the operational mission lifetime, at the other end. The model also includes, among other things, wave-front errors due to aberrations and image smearing due to transverse motion of sources in the focal plane and charge diffusion in the CCD detectors. The longer-term goal of this modelling effort is to include all effects affecting the final mission accuracies and to expand the model to include photometric and radial-velocity accuracy assessments.



Results from the GAAT astrometric accuracy tool: predicted sky-averaged end-of-life astrometric accuracies, at  $V = 15$  mag and as a function of  $V-I$  colour index (black: parallaxes  $\pi$  in  $\mu\text{as}$ ; red: positions in  $\mu\text{as}$ ; green: proper motions  $\mu$  in  $\mu\text{as yr}^{-1}$ ).

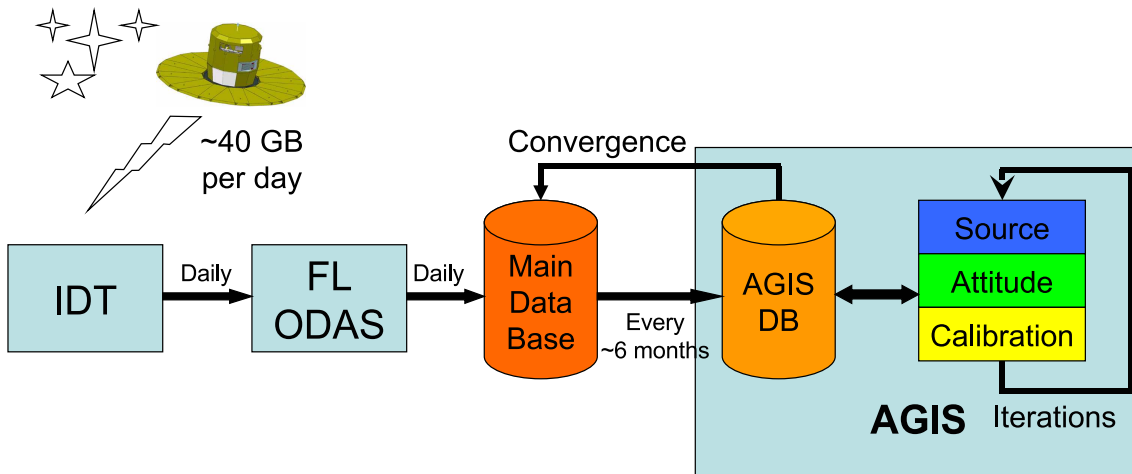
Gaia's scientific mission objectives can be summarized as the "observation of all 1 billion stars brighter than 20-th magnitude with end-of-life astrometric accuracies of  $20 - 25 \mu\text{as}$  at  $V = 15$  mag". Roughly speaking, Gaia's astrometric capabilities are a function of the satellite's operational strategy (mainly scanning law and mission lifetime) and the properties of its optical and detector system (e.g. CCD TDI integration). The present detailed design of the satellite is such that all mission objectives are met.

Gaia's scanning law is a central element in the data acquisition strategy during the 5-year operational lifetime of the satellite and the end-of-mission astrometric accuracies depend on its properties. Given technical boundary conditions, the scanning law has been defined in such a way that the precession speed of the spin axis on the sky is minimised and the uniformity of the end-of-mission sky coverage is maximised. In spite of this, the characteristics of this uniform revolving scanning law imply that astrometric accuracies vary with direction on the sky. Moreover, for any given direction, there is a significant difference between attainable position, proper-motion, and parallax accuracy. Generally, end-of-life (random) position and proper-motion errors will be, respectively, 25% and 50% smaller than end-of-life (random) parallax errors.

The properties of Gaia's optical and detector system are such that for stars brighter than  $\sim 12$  mag photon noise is negligible. The end-of-mission astrometric accuracies for these stars will amount to a few  $\mu\text{as}$ , the so-called accuracy noise floor. For magnitudes between 12 and 20, photon noise determines the line-spread-function centroiding accuracies, and the expected end-of-life astrometric accuracies are  $20 - 25 \mu\text{as}$  at 15-th magnitude and a few hundred  $\mu\text{as}$  at 20-th magnitude. At fainter magnitudes star-detection statistics enter and astrometric accuracies reach milli-arcsecond levels.

At a given magnitude (e.g.  $V = 15$  mag), astrometric accuracy also depends on apparent star colour – i.e. intrinsic star colour combined with interstellar reddening – through, for example, the wavelength-dependent properties of the modulation transfer function ("image quality") and quantum efficiency of the CCDs and the transmission of the optics. Generally, redder stars have smaller astrometric errors (see figure above).

A detailed astrometric accuracy tool (called GAAT) taking into account, among other things, all effects mentioned above, has been developed in the Gaia Project Scientist Support Team (see the information sheet on "Astrometric Accuracy Assessment"). Results of this tool give confidence that the present design of the satellite is viable and that the scientific mission objectives will be met.



Simplified schematic overview of Gaia's astrometric data reduction system. The main processing modules are IDT, FL-ODAS, and AGIS which will iteratively generate the final astrometric mission products.

The objective of Gaia's astrometric data reduction system is the construction of the core mission products: The five standard astrometric parameters, position ( $\alpha, \delta$ ), parallax ( $\varpi$ ), and proper motion ( $\mu_{\alpha^*}, \mu_\delta$ ) for all observed stellar objects brighter than  $G = 20$  mag with targeted micro-arcsec accuracies (e.g.  $< 10 \mu\text{as}$  [ $G < 10$  mag],  $< 25 \mu\text{as}$  [ $G = 15$  mag],  $< 300 \mu\text{as}$  [ $G = 20$  mag])). To this end, all the available  $\sim 70$  observations per object gathered during Gaia's 5 year lifetime will have to be combined in a single, global, and self-consistent manner.

The figure depicts a simplified schematic overview of the system. The  $\sim 40$  GB of daily telemetry data coming from the satellite are first processed by the Initial Data Treatment (IDT) which determines from the raw CCD measurement data astrometric image parameters ("centroids"). A second main task is the so-called "cross-matching" that links observation data to celestial objects. These outputs of IDT form the main input to the One Day Astrometric Solution (ODAS) which is part of Gaia's First-Look system. ODAS produces from one day's worth of data estimates for source positions, satellite attitude and calibration parameters at the level of sub-milli-arcsec accuracy. The results of the daily processings of IDT and ODAS are written to the Main Database.

Gaia's core data processing module is the Astrometric Global Iterative Solution (AGIS) system. AGIS treats the wanted source parameters, the satellite's attitude and calibration parameters as unknowns and tries to find the best global match in a least-square sense between all measurement data and an observational model that is formulated in terms of these unknowns. Numerically this is done through an iterative adjustment of the parameters from a starting point to an approximation to the sought solution of the least-squares problem. The system is considered converged and iterations are stopped if the adjustments become sufficiently small. At this point the results are written back to the Main Database. The fact that attitude and calibration parameters are optimized together with the source parameters in the same scheme is a necessity since they cannot be determined to the required level of micro-arcsec accuracy in any other way. This elegant aspect of the astrometric data reduction is the reason why Gaia is sometimes referred to as a self-calibrating mission.

Only single, non-variable stars which fit the standard 5-parameter astrometric model – in number perhaps up to 500 Million – will take part in such a "primary" AGIS cycle. For the remaining objects (binary, multiple systems, etc.) only provisional values will be computed by AGIS in a subsequent "secondary" cycle which only optimizes source parameters using the attitude and calibration solutions from the preceding primary cycle. Astrometry for secondary objects may be further improved by dedicated software in CU4 ("Object Processing").

Unlike IDT and ODAS which run daily, AGIS is executed only about every 6 months on an ever increasing data volume. IDT, ODAS, and AGIS are developed in the framework of Gaia's Data Processing & Analysis Consortium (DPAC) Coordination Unit 3. During operations all systems will run on dedicated processing hardware installed at ESA's European Space Astronomy Centre (ESAC) in Spain near Madrid. Owing to the large data volume (100 TB) that Gaia will produce and the iterative nature of the processing the computing challenges are formidable: The AGIS processing alone is estimated to require some  $10^{21}$  FLOPs which translates to runtimes of months on a baselined 10 FLOP/s local computing system at ESAC. The usage of external Cloud computing services is being studied as a possible alternative.



Mission operations at the European Space Operation Centre (ESOC), Germany.

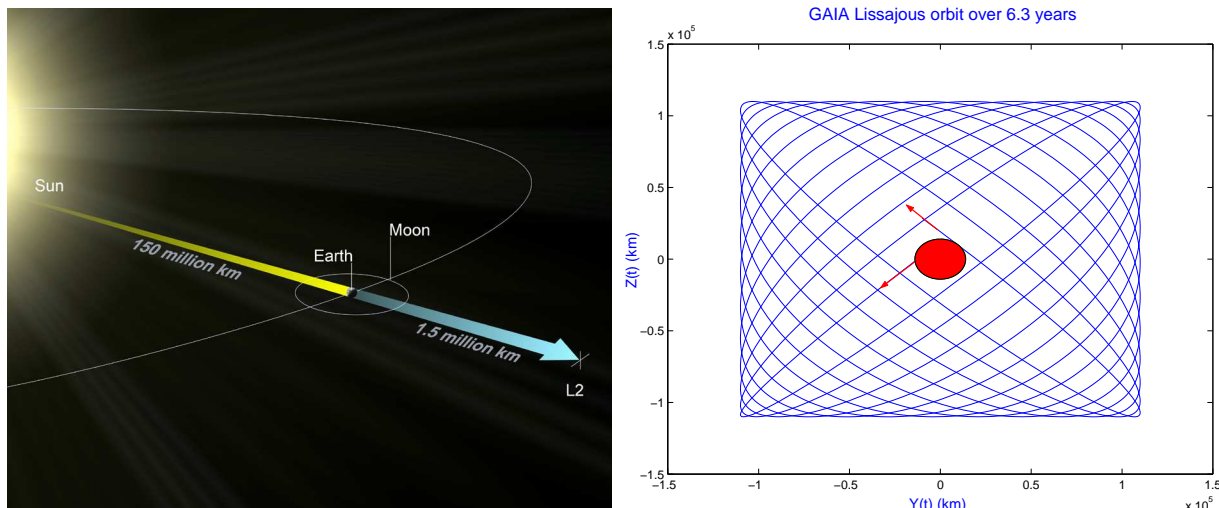
Gaia will be launched from Kourou by a Soyuz-Fregat launch vehicle. The chosen orbit is around the L2 Lagrange point of the Sun-Earth system, some 1.5 million km from Earth. The satellite will then be injected from a low-earth parking orbit into the L2 transfer orbit. After separation from the launcher, solar array deployment, spin rate and axis control will be performed autonomously by the spacecraft.

During the transfer only small orbit correction manoeuvres will be performed, controlling the effects of errors induced along the highly sensitive orbit. The spacecraft will be spin stabilized during the transfer. After typically one month, an orbit insertion manoeuvre of about  $180 \text{ m s}^{-1}$  will inject the spacecraft onto the stable manifold of the operational L2 orbit. Complete check-out of the spacecraft and the instruments will precede the start of nominal operations. Consumables are allocated for 6.5 years.

Mission operations will be carried out by ESOC, Germany. These will comprise spacecraft operations (mission planning, spacecraft monitoring and control, and all orbit and attitude determination and control) as well as scientific instrument operations (functional quality control and collection of the science telemetry). ESOC will provide a 'ground segment' that comprises all facilities, hardware, software, documentation and staff, required to conduct the mission operations. Two ground stations (Cebreros, Spain, and New Norcia, Australia) will be used.

The ground operations facilities consist of: (a) the ground stations and the communications network (hardware and software); (b) the mission control centre (infrastructure, computer hardware); (c) the flight control system (data processing and flight dynamics software); (d) the spacecraft simulator. All mission and flight control facilities, except the ground stations, will be located at ESOC, including the interfaces for the provision of science telemetry to the scientific data reduction teams.

The scanning law will remain unmodified throughout the mission. Nominal spacecraft control during the routine mission phase will be 'off line' - contacts between the Mission Control Centre at ESOC and the spacecraft, except for collecting payload and housekeeping telemetry, will primarily be used for pre-programming of the autonomous operations functions on the spacecraft (up-link of master schedule), and for science data collection. The science data will be distributed to the scientific processing centre at ESAC directly via high-speed communication lines.



Left: The second Lagrange point lies on the Sun-Earth line, in the direction opposite to the Sun, at a distance of 1.5 million km from the Earth. L2 is a semi-stable region of gravity where spacecraft can be maintained for several years with cheap orbit manoeuvres. Right: Example of a Lissajous orbit projected on the plane perpendicular to the Earth-L2 line, as seen from the Earth. The initial conditions are chosen such that the orbit wanders outside the Earth shadow (red circle at the centre) until the occurrence of the next eclipse more than six years later.

Gaia will operate in the vicinity of the second Lagrange point (L2), approximately 1.5 million km from the Earth, along the Sun-Earth line in the direction opposite to the Sun. The region around L2 is a gravitational saddle point, where spacecraft can be maintained at roughly constant distance from the Earth for several years by small and cheap manoeuvres.

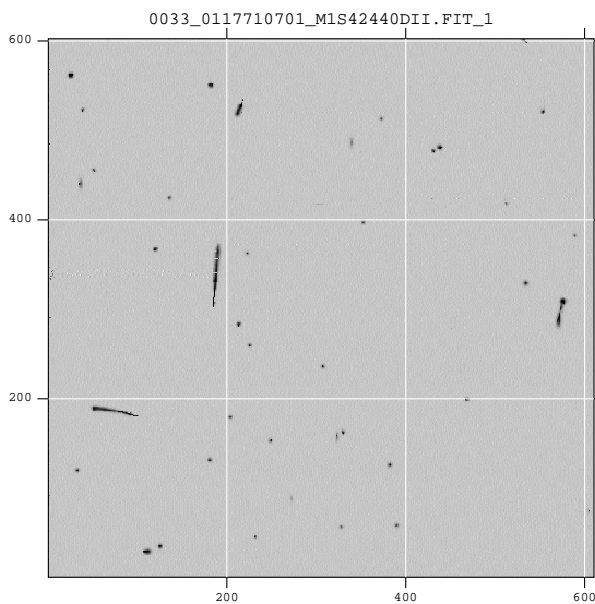
Around L2 there is a circular zone of radius  $\sim 13,000$  km where the Sun is always eclipsed by the Earth. Here the solar panels of a spacecraft would be unable to generate sufficient power since they would not receive enough sunlight. In addition, even entering this region for a few minutes would generate a detrimental thermal shock in the spacecraft. Therefore, Gaia will be placed in a large Lissajous orbit ( $\sim 300,000$  km) around L2 to ensure that it stays away from the eclipse zone for at least six years. The constant pull exerted by the Sun and the Earth will cause Gaia to swing around L2 on a nearly periodic circuit and six months will be needed to complete a full cycle (see figure above.)

The selection of the orbit arises from a trade-off between communication, operations, cost, thermal and radiation environment, and accessibility with current rockets. Around L2 one benefits from a virtually unchanging environment with very stable thermal conditions, an essential asset for the success of the mission. The optics are so sensitive to minute changes of temperature that a variation of less than one thousandth of a degree over a few hours would disturb the alignment of the mirrors and degrade the quality of the images.

Gaia will first be launched into low-Earth orbit and then injected into a smooth transfer orbit for a quiet trip of  $\sim 1$  month to its final Lissajous orbit about L2, where the observations will commence for a mission lasting at least five years.

Gaia will not be alone around L2 since this remote location is now favoured by several missions: ESA's Herschel-Planck and the NASA/ESA James Webb Space Telescope (will) operate from L2. In 2001, NASA's WMAP mission was the first to use an L2 orbit as its permanent observing station.

Lagrange points (L1 to L5) are named after the French-Italian mathematician Joseph-Louis Lagrange (1736-1813) who discovered them in the eighteenth century as equilibrium solutions of the three-body problem.



Background particle events (galactic cosmic rays) in an XMM-Newton image. About 60 events were registered on the  $2.4\text{ cm} \times 2.4\text{ cm}$  CCD in an integration time of 2.6 s, corresponding to a background rate of 4 events per  $\text{cm}^2$  per s.

When operating electronic equipment in space, one of the most important considerations is always the energetic particle radiation environment. For Gaia, which will operate at L2, this environment will be particularly critical because the large astrometric focal plane, carrying 106 CCD detectors, will be very difficult to shield. Radiation damage to the CCDs will degrade their performance and hence the overall performance of Gaia.

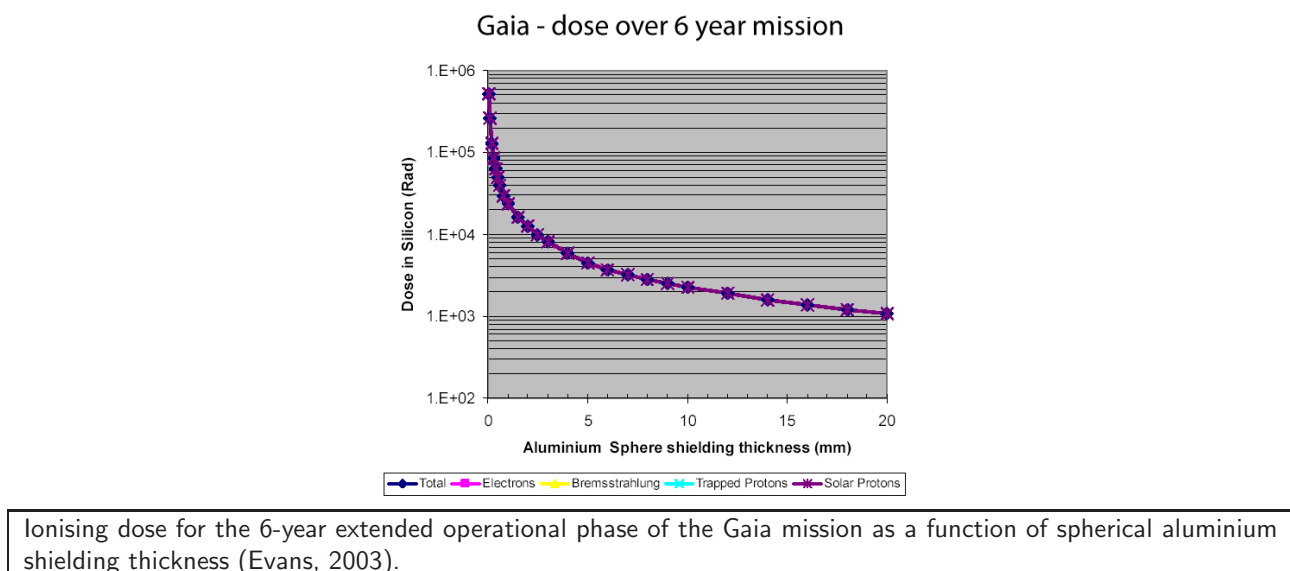
There are three main sources of damaging particles:

- *Galactic Cosmic Rays (GCR)*: Very high energy particles (typically hundreds of MeV) trapped in the galactic magnetic field. These are mainly generated by supernovae and are just passing through our Solar System. The rate observed varies between about 4–8 particles per  $\text{cm}^2$  per second depending upon the phase of the solar cycle and they comprise approximately 90% protons, 9% He ions and 1% heavier ions. It is not possible to shield against galactic cosmic rays effectively because their energy is high enough to penetrate many centimetres of shielding.
- *Solar particles*: Particles ejected directly from the Sun. The solar particle flux varies from essentially zero during solar quiet times to thousands of particles per  $\text{cm}^2$  per second during periods of high solar activity (solar flares). Like galactic cosmic rays, solar particles are predominantly protons and helium ions. However, the peak energy of the solar proton spectrum is several orders of magnitude lower than that of the galactic cosmic ray spectrum, so that shielding can be effective in reducing the dose to sensitive components.
- *Trapped particle environment*: These are protons and electrons trapped in the Earth's magnetic field to form the 'radiation belts'. This environment is not relevant for Gaia which will be situated at L2.

During solar-quiet (observing) periods, there will always be a particle flux of between 4 and 8 galactic cosmic rays per  $\text{cm}^2$  per second passing through the Gaia CCDs. There are two main ways in which these background particle events will affect Gaia astrometric observations:

- Astronomical sources are detected autonomously by the Star Mappers. Particle events which are incorrectly identified as sources, will be assigned windows, tracked across the focal plane and transmitted to the ground. This is clearly a waste of resources and a reliable on-board rejection algorithm is required.
- Particle events detected in a CCD, close to a source Point Spread Function (PSF) will introduce PSF distortion and hence centroiding errors. These errors need to be quantified and mitigation techniques assessed (such as the use of PSF matched filters in the centroiding algorithm). Once identified, a PSF contaminated by a particle detection may be corrected or rejected.

Of more concern is the longer term damage caused to the CCDs during solar flares. This effect is considered in the Information Sheet *Radiation Environment and Gaia CCDs*.



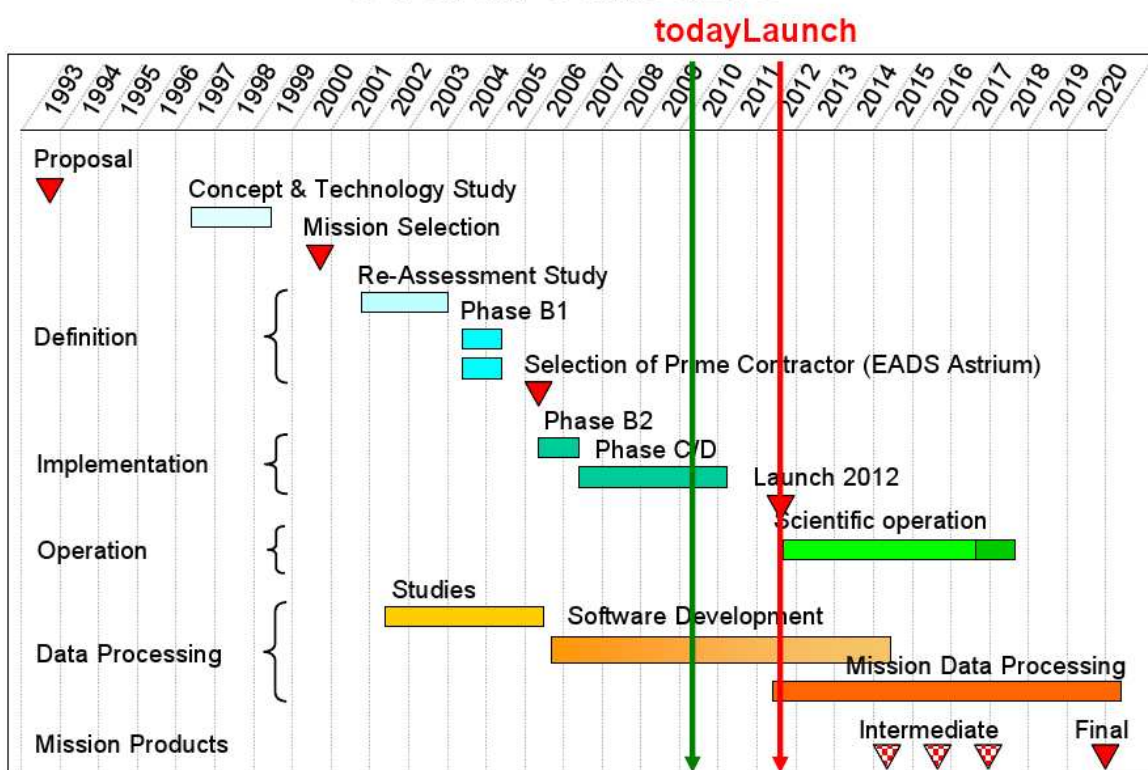
The energetic particle radiation environment at L2 has been described in the Information Sheet *Radiation Environment at L2*. This Information Sheet deals with the damaging effect of this environment on Gaia CCDs. Essentially all damage to Gaia CCDs will occur during solar flares when the solar particle flux is thousands per cm<sup>2</sup> per second. As any particle passes through a CCD it causes two kinds of damage:

- *Ionizing damage*: In passing through the insulating layers of the electrode structure, a particle liberates electrons from atoms. Over the course of a mission this leads to a static charging of the electrode insulators which means that CCD operating voltages essentially drift with time. Ionizing radiation tests will be conducted on the Gaia demonstrator CCDs to establish how susceptible they are, but it is currently estimated that voltages will drift by less than 0.5 V over the mission lifetime of 5 years.
- *Non-ionizing or Displacement damage*: As a particle passes through the epitaxial silicon, there is a chance that it will collide with a silicon atom so as to displace it from its location in the crystal lattice, generating a point defect. Such defects introduce energy levels in the semiconductor bandgap into which electrons from the conduction band can drop and become trapped. Owing to its thermal energy, a trapped electron may jump back up into the conduction band (out of the trap), but this process has an associated exponential de-trapping time constant which is a strong function of temperature. During the course of the mission, the huge fluxes of solar protons during solar flares will introduce a significant density of traps into the buried channel (where the electrons are carried through the CCD). As the resultant trapping increases, the efficiency with which electrons can be transferred from pixel to pixel decreases, i.e. the Charge Transfer Inefficiency increases. During the Gaia mission, this will lead directly to a distortion of the PSF and hence a reduction in centroiding (astrometric) accuracy.

There are several ways to reduce the effects of radiation-induced charge trapping. For example, incorporating a supplementary buried channel into the CCD design causes electrons to be transported through the CCD in a narrow stream so that they encounter fewer empty traps. Another option is to operate at higher temperatures so that electrons escape from traps very quickly. Unfortunately this is only effective when the CCDs are being read out relatively slowly. Increasing the temperature also increases dark current which contributes to the noise. A better solution for Gaia is to operate at low temperatures so that traps stay filled for longer - once a trap contains an electron it cannot trap another. An operating temperature of  $-115^{\circ}\text{C}$  is about optimum and this has been selected as the operating temperature for Gaia CCDs. Unfortunately, most traps will still release electrons after a few seconds so a charge injection structure is incorporated to periodically re-fill them. However, it is never possible to eliminate all trapping because real traps are invariably complexes comprising several different energy levels with different de-trapping time constants.

By adding shielding around detectors, it is possible to eliminate a significant soft component of the solar proton spectrum and hence reduce the total mission damage dose. This is effective up to about 3 cm of Aluminium shielding, beyond which, significant further increases in shield thickness yield only small reductions in total dose. The X-ray observatories XMM-Newton and Chandra both employ about 3 cm of shielding around their CCDs. Early Gaia designs incorporated minimal shielding and radiation models indicated that the damage to the CCDs would be 100 times higher than previous missions. In addition, the large area of Gaia CCDs makes them more sensitive to radiation damage than earlier devices. Therefore, designing mass efficient means of shielding the Gaia CCDs against particle radiation has been one of the many technical challenges facing the project.

# Overall schedule



The figure shows the overall Gaia mission timeline at the present time. Approval for go-ahead of the construction phase of Gaia was given in early 2006, with a launch foreseen around 2012.

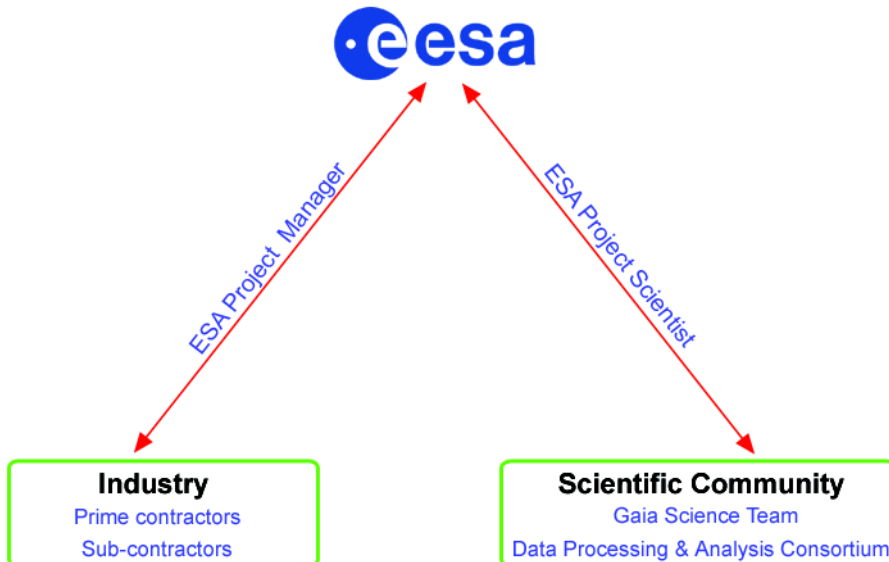
The first ideas for Gaia began circulating in the early 1990's, culminating in a proposal for a cornerstone mission within ESA's science programme submitted in 1993, a workshop in Cambridge in June 1995 to discuss possibilities and, following a 2-year Concept & Technology Study Phase, selection of the Gaia mission by the ESA Science Programme Committee in 2000.

The results of the Concept & Technology Study indicated that a launch in 2009–10 was feasible, and that a period of technological development would be required in advance of the detailed design and construction phase, in order to gain full confidence in the required technology. This technology phase was scheduled to run between 2002–04. Gaia was originally foreseen to be launched by Ariane 5, but a further industrial study was carried out in early 2002 to assess accommodation within the smaller (and cheaper) Soyuz launcher. The studies were completed, a workable design with only small accuracy degradation was identified, and the Gaia mission was reconfirmed within the ESA science programme in mid-2002.

A series of industrial technology studies ran between 2002–05, in parallel with many further feasibility and assessment studies by European scientists involved in the Gaia programme. The data simulation chains, prototype analysis algorithms, and a prototype reduction system were studied during this period. With reasonable confidence in the critical hardware (detectors, optics, etc) and the critical scientific elements, ESA issued a competitive call for the industrial phase in mid-2005. In early 2006, the contract for Phases B2/C/D was agreed between ESA and the industrial prime contractor, EADS Astrium SAS.

A final phase of detailed design lasted until early 2007. Currently, the satellite construction, integration and testing is in full swing. In parallel, the scientific community has begun its serious preparatory phase for handling the huge amounts of data that will flow from the satellite after launch.

After launch, the satellite will take one month to journey to L2, its operational environment. Operations and observations will extend for five years, during which period the data analysis will be ongoing. A final phase of 3 years will be required to tie up the data analysis in advance of data release to the scientific community. Just over 2 decades will have elapsed between the original concept for this ground-breaking mission and the final results.



The key players in a mission, ESA, Industry and the Scientific Community, communicate through well-defined interfaces. The scientific community, represented by the Gaia Science Team and the Data Processing and Analysis Consortium, interface with ESA through the Gaia Project Scientist. Industry, as well as ESOC and launch interfaces, are under the responsibility of the Gaia Project Manager.

The management model adopted for Gaia assumes that the entire satellite, including payload and operations, is under ESA responsibility. The substantial scientific activities are carried out under the responsibility of scientists in the ESA Member States – these include activities related to instrumental and satellite design and optimisation, scientific performance assessment, and preparation and eventual implementation of the data reduction tasks leading to the production of the final mission science products. This approach is driven by the complexity and ‘system nature’ of the payload, and also by the effort demanded of the scientific community for the data analysis.

Acceptance of Gaia within the ESA Science Programme was followed by a technology development phase, during which critical aspects of the technologies required for Gaia were studied and assessed, and a detailed mission definition phase. These activities ran until mid-2005. At the end of this period, ESA issued an open ‘Invitation to Tender’ based on a comprehensive ‘System Requirements Document’, detailing the top-level requirements demanded of the Gaia satellite and payload – this document was prepared based on the findings of the technology development phase. After review, a single prime contractor was selected to carry out the ‘implementation phase’ (the detailed design, component procurement, and satellite integration, assembly and testing). The spacecraft development and procurement will thereafter be carried out by the single industrial prime contractor, supported by sub-contractors responsible for different sub-systems of the satellite. The industrial contract is funded and managed by ESA.

The scientific activities of the Gaia mission are conducted by members of the scientific community, nationally funded. Teams were organised into focussed working groups during the study phase, and are now structured into the Gaia Data Processing and Analysis Consortium during the implementation phase (2006 onwards). Overall activities and scientific priorities are monitored and coordinated by the Gaia Science Team. These groups together establish a schedule of tasks consistent with the satellite development. One of the main priorities has been to develop a prototype of the data analysis system that will be used to analyse the data sent down from the satellite, and to estimate the processing resources and computing architecture needed to perform this huge task. During the industrial phase B2, ESA will issue an Announcement of Opportunity to formalise the structure of the Data Processing and Analysis Consortium. The Gaia Science Team will remain in place until the final mission results are available, sometime around 2019 according to present planning.



The easy-to-access Hipparcos data has proved attractive to educators, researchers and the public. Gaia will provide more and wider opportunities to support educational and technical training activities, in addition to the role it will play in informing the public about science and exploration.

Space science missions, and in particular astronomical studies of the visible Universe, have an extraordinary interest for the public at all levels. In addition to the primary ESA goals of basic research and applied technological developments, this means that related educational goals, such as helping to ensure that a continuing supply of scientists, engineers, and technologists will be available to meet the needs of the twenty-first century, can build on Gaia. The images, scientific discoveries and new appreciation of the scale and diversity of nature provided by astronomy captivate people's imaginations, inform teachers, and excite students and the public about science and exploration.

Gaia is exceptionally well-suited for this educational, awareness and technical training requirement. It will provide opportunities and challenges at all levels, from the evolution of the Galaxy and the search for extra-solar planets, through applied gravitation, to the technical challenges in accessing large data sets. Every one of these is of direct and topical interest, and produces knowledge of very wide and continuing general applicability.

Among many examples of Gaia science which are directly appropriate for general educational opportunities, Gaia will provide the first detailed knowledge of the content and evolution of our own Milky Way, and its kinematics, allowing a natural forum for explanation of Newtonian and General Relativity gravitational theory, chaos theory, and orbits. This can be provided naturally at the pictorial level – a movie of the sky – through to the highly technical – metric mapping, gravitational distortions of space-time – appropriate to all ages and interests, and all levels of educational requirements. At a wider level, by providing a precise measure of the distribution of dark matter near the Sun, and throughout the Galaxy, Gaia will set the boundaries of our understanding of the nature of matter, luminous and dark. The direct links with particle physics and fundamental physics are well known, and of wide general appeal. The scale of the Gaia data set and its resulting data processing requirements will also provide outstanding opportunities for computational research.

Complementary to these formal educational capabilities, Gaia addresses science of vast general appeal. The general public is genuinely fascinated by astronomical discoveries, and their important general implications for people's understanding of their place in the Universe. Thus activities ranging from the motivation of the creative arts, through galleries and the public media, to informed political debate, will naturally follow from public understanding of its scientific mission goals.

**Objectives:**

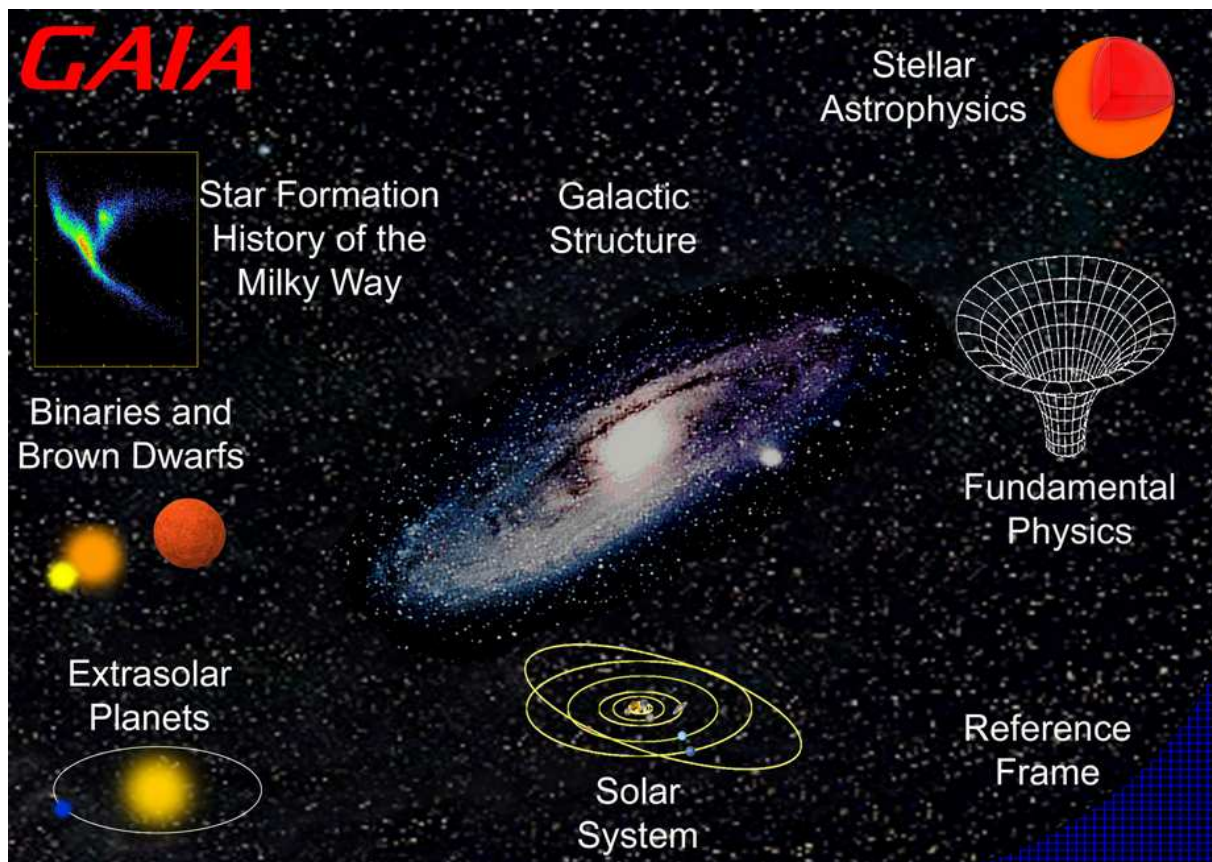
- Galaxy origin and formation;
- Physics of stars and their evolution;
- Galactic dynamics and distance scale;
- Solar System census;
- Large-scale detection of all classes of astrophysical objects including brown dwarfs, white dwarfs, and planetary systems;
- Fundamental physics

**Measurement Capabilities:**

- **Catalogue:**  $\sim 1$  billion stars;  $0.34 \times 10^6$  to  $V = 10$  mag;  $26 \times 10^6$  to  $V = 15$  mag;  $250 \times 10^6$  to  $V = 18$  mag;  $1000 \times 10^6$  to  $V = 20$  mag; completeness to about 20 mag
- **Sky density:** mean density  $\sim 25\,000$  stars  $\text{deg}^{-2}$ ; maximum density  $\sim 3 \times 10^6$  stars  $\text{deg}^{-2}$
- **Accuracies:** median parallax errors: 7  $\mu\text{as}$  at 10 mag; 20-25  $\mu\text{as}$  at 15 mag; 200-300  $\mu\text{as}$  at 20 mag
- **Distance accuracies:** from preliminary Galaxy model estimates: 3 million better than 1 per cent; 5 million better than 2 per cent; 10 million better than 5 per cent; 30 million better than 10 per cent
- **Tangential velocity accuracies:** from Galaxy models: 5 million better than  $0.5 \text{ km s}^{-1}$ ; 10 million better than  $1 \text{ km s}^{-1}$ ; 25 million better than  $3 \text{ km s}^{-1}$ ; 40 million better than  $5 \text{ km s}^{-1}$ ; 60 million better than  $10 \text{ km s}^{-1}$
- **Radial velocity accuracies:**  $1\text{--}10 \text{ km s}^{-1}$  to  $V = 16\text{--}17$  mag, depending on spectral type
- **Photometry:** to  $V = 20$  mag in broadband light, and spectrally-dispersed light, with some 20 independent spectral samples between 330–1000 nm

**Scientific Goals:**

- **The Galaxy:** origin and history of our Galaxy — tests of hierarchical structure formation theories — star formation history — chemical evolution — inner bulge/bar dynamics — disk/halo interactions — dynamical evolution — nature of the warp — star cluster disruption — dynamics of spiral structure — distribution of dust — distribution of invisible mass — detection of tidally disrupted debris — Galaxy rotation curve — disk mass profile
- **Star formation and evolution:** *in situ* luminosity function — dynamics of star forming regions — luminosity function for pre-main sequence stars — detection and categorization of rapid evolutionary phases — complete and detailed local census down to single brown dwarfs — identification/dating of oldest halo white dwarfs — age census — census of binaries and multiple stars
- **Distance scale and reference frame:** parallax calibration of all distance scale indicators — absolute luminosities of Cepheids — distance to the Magellanic Clouds — definition of the local, kinematically non-rotating metric
- **Local Group and beyond:** rotational parallaxes for Local Group galaxies — kinematical separation of stellar populations — galaxy orbits and cosmological history — zero proper motion quasar survey — cosmological acceleration of Solar System — photometry of galaxies — detection of supernovae
- **Solar System:** deep and uniform detection of minor planets — taxonomy and evolution — inner Trojans — Kuiper Belt Objects — disruption of Oort Cloud
- **Extra-solar planetary systems:** complete census of large planets to 200–500 pc — orbital characteristics of several thousand systems
- **Fundamental physics:**  $\gamma$  to  $\sim 2 \times 10^{-6}$ ;  $\beta$  to  $3 \times 10^{-4} - 3 \times 10^{-5}$ ; solar  $J_2$  to  $10^{-7} - 10^{-8}$ ;  $\dot{G}/G$  to  $10^{-12} - 10^{-13} \text{ yr}^{-1}$ ; constraints on gravitational wave energy for  $10^{-12} < f < 4 \times 10^{-9} \text{ Hz}$ ; constraints on  $\Omega_M$  and  $\Omega_\Lambda$  from quasar microlensing
- **Specific objects:**  $10^6 - 10^7$  resolved galaxies; 20 000 extragalactic supernovae; 500 000 quasars; 250 000 solar system objects;  $\gtrsim 50\,000$  brown dwarfs; 15 000 extra-solar planets; 200 000 disk white dwarfs; 100 astrometric and 1000 photometric microlensed events;  $10^7$  resolved binaries within 250 pc



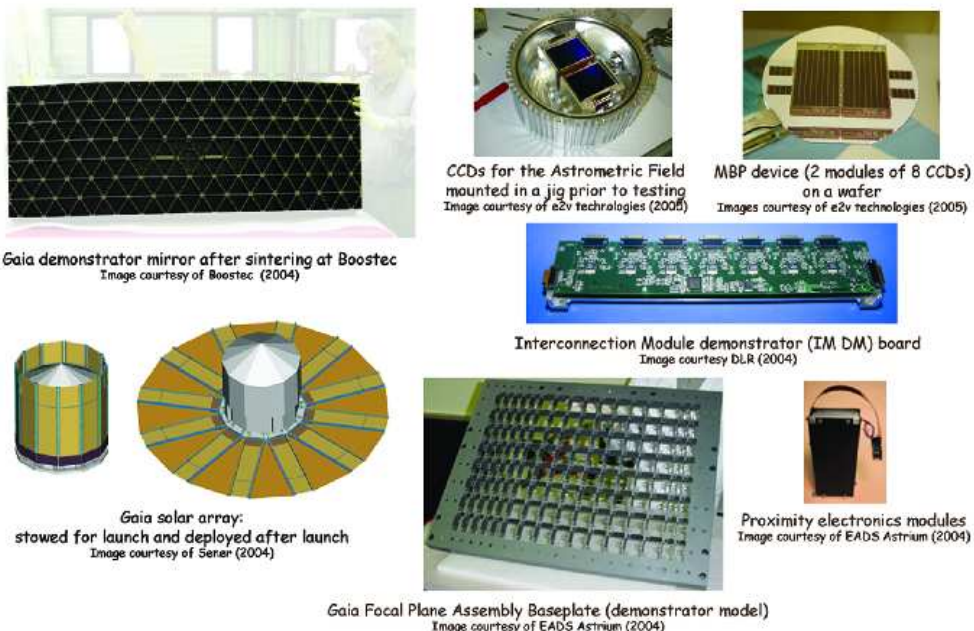
Many areas of science will be addressed by the Gaia mission as indicated in this schematic figure.

Gaia will measure the positions, distances, space motions, and many physical characteristics of some one billion stars in our Galaxy and beyond. For many years, the state of the art in celestial cartography has been the Schmidt surveys of Palomar and ESO, and their digitized counterparts. Gaia will provide the detailed 3-d distributions and space motions of all these stars, complete to 20-th magnitude. The measurement precision, reaching a few millionths of a second of arc, will be unprecedented. This will allow our Galaxy to be mapped, for the first time, in three dimensions. Some millions of stars will be measured with a distance accuracy of better than 1 per cent; some 100 million or more to better than 10 per cent.

Gaia's resulting scientific harvest is of almost inconceivable extent and implication. It will provide detailed information on stellar evolution and star formation in our Galaxy. It will clarify the origin and formation history of our Galaxy. The Gaia results will precisely identify relics of tidally-disrupted accretion debris, probe the distribution of dark matter, establish the luminosity function for pre-main sequence stars, detect and categorize rapid evolutionary stellar phases, place unprecedented constraints on the age, internal structure and evolution of all stellar types, establish a rigorous distance scale framework throughout the Galaxy and beyond, and classify star formation and kinematical and dynamical behaviour within the Local Group of galaxies.

Gaia will pinpoint exotic objects in colossal and almost unimaginable numbers: many thousands of extra-solar planets will be discovered (from both their astrometric wobble and from photometric transits) and their detailed orbits and masses determined; tens of thousands of brown dwarfs and white dwarfs will be identified; tens of thousands of extragalactic supernovae will be discovered; Solar System studies will receive a massive impetus through the observation of hundreds of thousands of minor planets; near-Earth objects, inner Trojans and even new trans-Neptunian objects, including Plutinos, may be discovered.

Gaia will follow the bending of star light by the Sun and major planets over the entire celestial sphere, and therefore directly observe the structure of space-time – the accuracy of its measurement of General Relativistic light bending may reveal the long-sought scalar correction to its tensor form. The PPN parameters  $\gamma$  and  $\beta$ , and the solar quadrupole moment  $J_2$ , will be determined with unprecedented precision. All this, and more, through the accurate measurement of star positions.



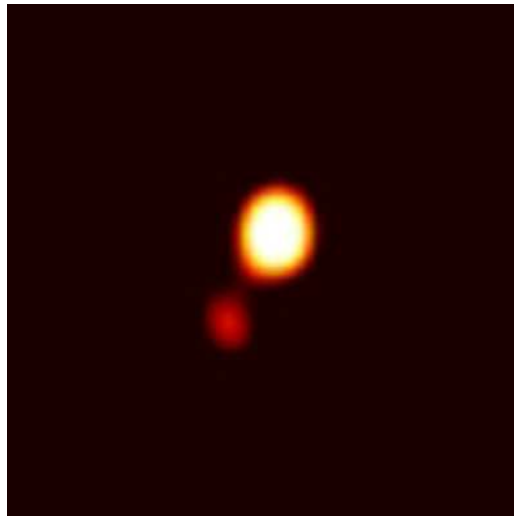
Technology activities completed between 2002–2005 included studies on deployable solar arrays, large area SiC mirrors, and small-pixel high-performance CCDs.

During the first studies of the Gaia project by ESA between 1998–2002, several technological activities were identified to be carried out prior to the construction of Gaia, in order to ensure that the spacecraft and payload development would be feasible, and the associated costs reliable. Work on these technological developments started in 2002, and extend to the end of 2005. A total of about 10 MEuros was assigned to them, representing a carefully coordinated effort of the industrial and scientific teams which will lead to much greater confidence in embarking on the construction phase of the Gaia mission.

Activities, which typically included a study and preliminary design phase followed by ‘breadboarding’, were carried out in the following areas: \* three-side-buttable, small pixel, high performance CCDs and the focal plane assembly for the astrometric instruments, the radial velocity spectrometer and the photometer; \* highly integrated, high-speed low-noise detection chains for the astrometric focal planes; \* payload data handling electronics architecture optimisation; \* large area SiC mirrors; \* ultra-stable large size SiC structure as applied to the payload primary structure; \* large-size deployable solar array sunshield assembly; \* phased-array antenna for high data rates in the L2 orbit; \* optimised on-board compression algorithm for the science data; \* study of ground verification calibration approach and required facilities; \* inch-worm actuators for the refocusing mechanism; \* data base architecture, including storage, archive and processing of the satellite data.

All these preparatory activities were under ESA responsibility, with a technical officer in the European Space Research and Technology Centre (ESTEC) supervising the industrial contracts, and reporting regularly to the study manager. Several European industrial firms were involved in these technical studies. In addition, two major industrial teams – the System Level Technical Assistance and Definition Study teams (EADS Astrium and Alcatel/Alenia) were responsible for the overall Gaia system design under ESA contract. They also monitored the development of these technical studies to ensure consistency with the overall goals of Gaia.

At the end of the technology study phase in mid-2005, Gaia entered the detailed design phase (which commenced at the start of 2006), under a single prime contractor for the satellite development and the ESA project manager. The detailed design, construction, and testing phase will last some 6 years, leading to a planned launch in 2012.



A brown dwarf orbiting its stellar companion, a faint main-sequence star. The image was obtained by adaptive-optics imaging on the Gemini North Telescope. The separation between the two components is of the order of 3 AU, which is a typical distance for this kind of system. Image courtesy Gemini Observatory/Melanie Freed, Laird Close, Nick Siegler University of Arizona/ Hokupa'a-QUIRC image, University of Hawai'i, IfA.

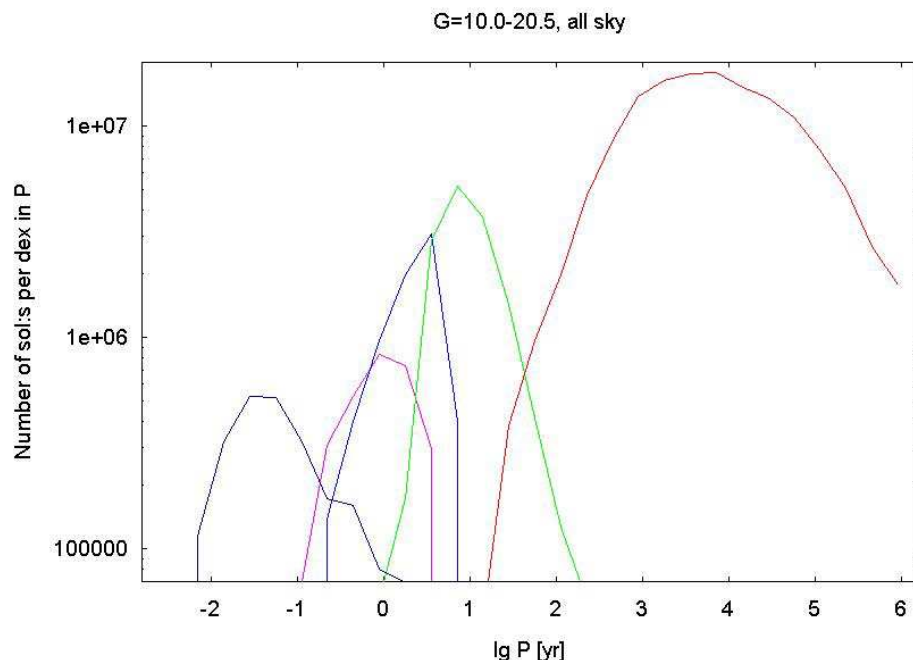
Although brown dwarfs are at least as numerous as stars, our knowledge of their intrinsic physical properties, of their formation processes, and of the characteristics of the brown-dwarf population as a whole is comparatively poor. This situation is mainly due to the fact that brown-dwarf astronomy is a relatively new branch of science: the first brown dwarf ever was observed as recently as 1995 and the first dynamical brown-dwarf mass was only measured in the year 2000.

The main reason that so little is known about these objects is their low luminosity, which renders even nearby specimens faint. Another reason is the degeneracy between the effects of age and mass on observed brown-dwarf colours and magnitudes. In this respect, brown dwarfs in binaries provide critical information, because of the possibility of measuring dynamical masses. However, brown dwarfs in binaries can also help to answer more general questions such as *What is the origin of free-floating brown dwarfs? Is the formation process of brown dwarfs in binaries related to the formation of binary brown dwarfs? How do the binary-distribution characteristics (mass ratio, separation, etc.) of brown dwarfs differ from their stellar counterparts?*

A puzzling discovery is that, while planets are now routinely observed orbiting F-, G-, and K-dwarfs, few of these types of stars have brown-dwarf companions. Most of the brown dwarfs in binaries are found orbiting late-M-type stars, but while the distribution of separations peaks around 30 AU in FGK-type binaries, few brown dwarfs are detected at separations larger than 15 AU in low-mass systems. The origin of these differences is not known.

From present-day knowledge, it is estimated that about  $\sim 15\%$  of low-mass stars in the solar neighbourhood have brown-dwarf companions. There also seem to be numerous systems in which both components are brown dwarfs. With estimates of the M-star population representing about 50 million stars in the Gaia Catalogue, the present-day knowledge suggests that Gaia will observe several million systems in which one component is a *bona fide* brown dwarf. Among these, Gaia will detect a sizeable fraction of separated components. At distances less than 50 pc, and assuming the presently known distribution of separations,  $\sim 6000$  systems could be detected as separated components.

Although the long periods and faint magnitudes of brown dwarfs will not permit Gaia to measure viable orbits for many systems, the Gaia data will represent an unprecedented pool of measurements for follow-up observations and accurate mass determinations. Together with accurate parallaxes (better than 1% relative accuracy at distances  $< 50$  pc), Gaia will allow the above-mentioned questions to be addressed in detail.



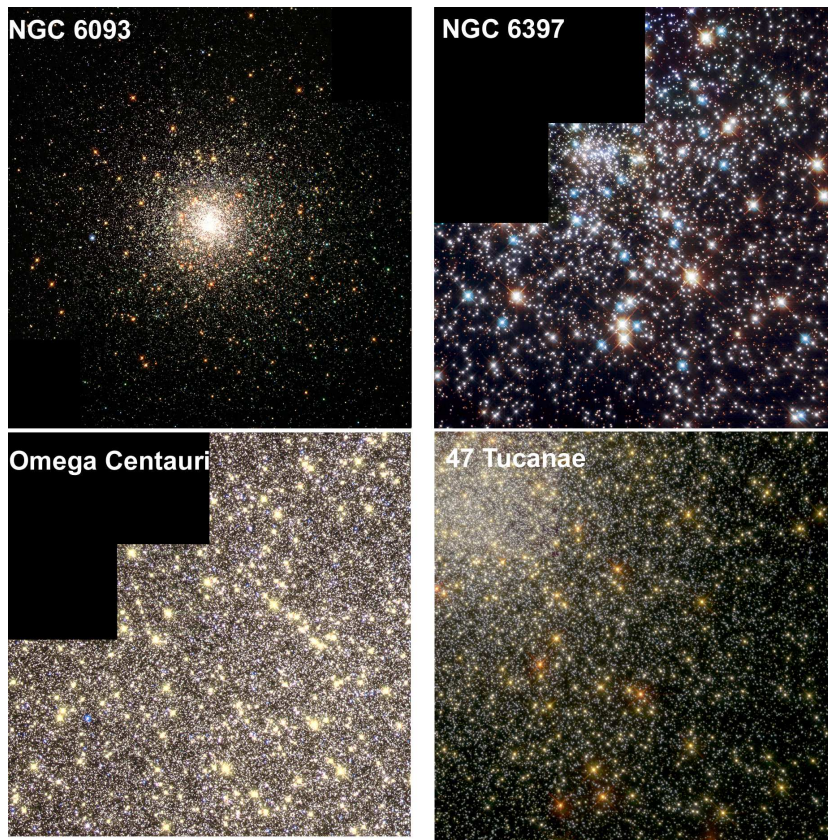
Estimated numbers of binary solutions from Gaia as a function of period. From left to right:  $\sim 7 \times 10^5$  radial-velocity orbits,  $8 \times 10^5$  radial-velocity-plus-astrometry orbits,  $2 \times 10^6$  astrometry orbits,  $4 \times 10^6$  non-linear proper-motion systems, and  $4 \times 10^7$  resolved binaries. Gaia will also provide solutions for millions of eclipsing binaries with periods below  $10^{-2}$  yr.

One of Gaia's unique features is the well-defined sampling and subsequent observations of tens of millions of binaries over the entire sky. Even though by the time Gaia will be operational, large ground-based telescopes and interferometers may have resolutions and light-collecting areas exceeding those of Gaia, thus enabling detailed studies of individual binaries and multiples, relatively few objects will have been observed with such instruments. Moreover, the observed targets will have been selected basically at random and thus do not form a complete sample in any sense.

As a result of its aperture size, Gaia will resolve all binaries with separations above some 20 mas which have moderate magnitude differences between the components. Many such systems exist and these will form the bulk of the 'Gaia Binary Catalogue'. Since distances of Gaia binaries will typically exceed a kilo-parsec, orbital periods of most of them will be too long for orbit determination. Nevertheless, direct observational data in the form of the distributions of separations and magnitude differences will already provide a unique handle on the basic  $f(a)$  (semi-major axes) and  $f(q)$  (mass ratio) distributions.

One of Gaia's strengths is its extreme sensitivity to non-linear (proper) motions. Large fractions of the astrometric binaries with periods in the range 0.03 – 30 yr will be recognised immediately. If the period of such systems is below 7 – 8 yr, it will be possible to determine a photocentre orbit. At the bright end (up to 15-th magnitude), radial-velocity observations will define large numbers of shorter-period binaries. At the shortest periods, Gaia will (photometrically) observe millions of eclipsing binaries, mostly too faint for radial-velocity observations. In summary, Gaia will observe binaries with periods between hours and millions of years, but the actual 'detection-efficiency' will be a complex function of period, distance, and absolute magnitude.

The figure above shows results from detailed simulations. The five curves give the expected total number of binary-star solutions from five solution methods. From left to right: the radial-velocity observations that give short-period orbits are only available for the brightest stars. The next two curves refer to combined radial-velocity-plus-astrometry and the astrometry-only orbits. The 'non-linear proper motion' detections peak at a period of 10 yr since these systems are resolved at longer periods. To these five solution types should be added a large number of eclipsing binaries with periods below  $10^{-2}$  yr. The 'all-sky/all magnitude' curves shown above are a combination of results from all distances. Looking at a nearby sample ( $< 500$  pc), many resolved binaries have periods short enough for orbit determination, i.e. there is good overlap between the solution methods, and hence binaries of all periods may be observed. For more distant samples, there are no resolved orbits, and as shown by the dip in the figure, binaries with a period of about 100 yr will be hard to detect with Gaia.



Globular clusters will be extensively observed by Gaia, giving precise distances and ages for these objects which are among the oldest objects in the Milky Way. Their distances provide a clue to Population-II distance scales and their ages give a lower limit for the age of the Universe. Images NGC 6093 and Omega Centauri, copyright NASA & The Hubble Heritage Team (STScI/AURA); NGC 6397, copyright ESA & Francesco Ferraro; 47 Tucanae, copyright NASA & Ron Gillard (STScI).

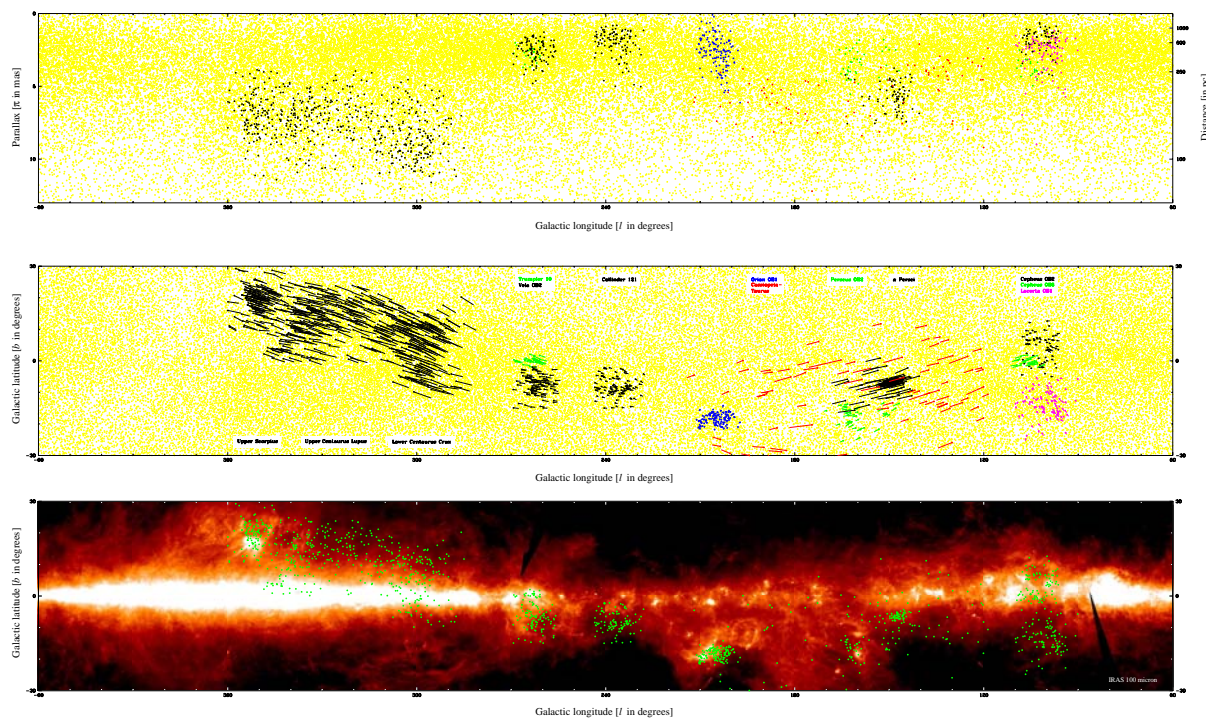
Gaia will have a major impact upon our knowledge of the distance scale in the Universe by providing accurate distances and physical parameters for all types of observable primary distance indicators in the Milky Way and in the closest galaxies of the Local Group. It will generate a complete sampling of these indicators versus the corrections due to metal, oxygen, or helium contents, colour, population, age, etc. In particular, Gaia will extensively observe many Galactic open and globular clusters and countless Cepheids and RR Lyraes, thus providing solid calibrations for cluster-sequence fitting and period-luminosity relations.

Major efforts have been made during the past decade to observe distance indicators in external galaxies (for example, the Hubble Space Telescope key project). Nowadays, the dominant contribution to the uncertainty on these distances, and hence on the most important cosmological parameter describing the Universe – the Hubble constant – is the uncertainty in the distance to the Large Magellanic Cloud (LMC).

Gaia will provide a firm foundation to the sequence of steps leading to the determination of distances of far-away galaxies and, as a consequence, to the determination of the Hubble constant by measuring individual trigonometric distances to the Cepheids and brightest stars of the LMC. Moreover, Gaia will establish a first check of the universality of the period-luminosity relationship for pulsating variables, with direct distances of all Galactic and LMC Cepheids and with mean Gaia distances for Cepheids in the closest galaxies of the Local Group.

Gaia will also provide an extensive picture of the whole Hertzsprung–Russell diagram, undoubtedly leading to new or renewed insight (Mirae period-luminosity relation, eclipsing binaries, white-dwarf luminosity function, etc.).

Moreover, Gaia will touch a second crucial parameter for the description and understanding of the Universe: its age. The accurate determination of the distances of the oldest objects in the Galaxy, namely subdwarf stars and globular clusters, combined with a fit to theoretical models of stellar evolution, will lead to a precise estimation of their ages. These age estimates naturally provide a lower limit to the age of the Universe, since these objects formed some time after the Big Bang.

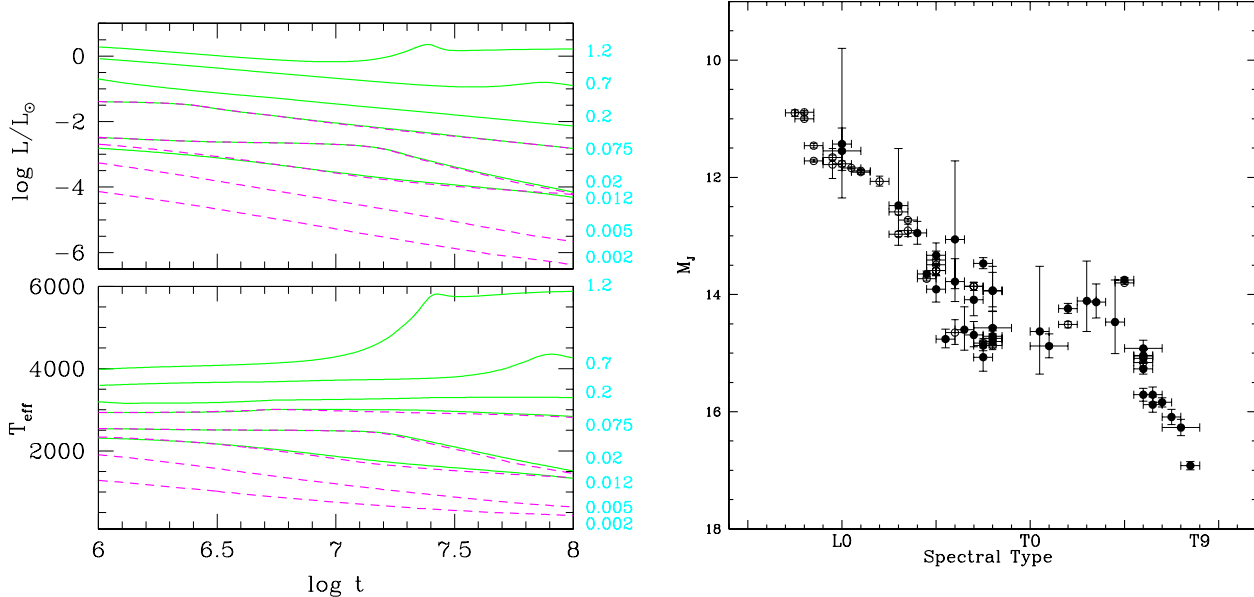


Kinematic selection of nearby OB associations using Hipparcos positions, parallaxes, and proper motions (de Zeeuw et al., 1999, AJ, 117, 354): (upper panel) parallaxes of the OB-association members, superimposed on all stars observed by Hipparcos in the range  $-30^\circ < b < 30^\circ$ ; (middle panel) positions and proper motions of the members in Galactic coordinates; (lower panel) positions of the members superimposed on the IRAS  $100-\mu\text{m}$  background.

The most conspicuous component of the Milky-Way galaxy is its flat disc which contains nearly  $10^{11}$  stars of all spectral types and ages orbiting the Galactic centre. The Sun is located at about 8.5 kpc from the Galactic centre. The disc displays spiral structure, and also contains interstellar material, predominantly atomic and molecular hydrogen, and a significant amount of dust. The disc of the Milky Way contains, besides numerous open clusters and associated super-clusters/moving groups, various manifestations of recent star formation events, including OB associations and the large-scale Gould Belt (see figure above). The inner kilo-parsec of the disc also contains the bulge, which is less flattened, may contain a bar, and consists mostly of moderately-aged stars. At its centre lies a supermassive black hole of  $\sim 4 \times 10^6 M_\odot$ . The disc and bulge are surrounded by a halo of about  $10^9$  old and metal-poor stars, as well as  $\sim 160$  globular clusters and a small number of satellite dwarf galaxies. This entire system is embedded in a massive halo of dark material of unknown composition and poorly known spatial distribution.

The distributions of stars in the Galaxy over position and velocities are linked through gravitational forces, and through the star formation rate as a function of position and time. The initial distributions are modified, perhaps substantially, by small- and large-scale dynamical processes. These processes include instabilities which transport angular momentum (for instance bars and warps) and mergers with other galaxies.

Understanding our Galaxy requires measurement of distances and space motions for large and unbiased samples of stars of different mass, age, metallicity, and evolutionary stage. Gaia's global survey of the entire sky down to 20-th magnitude is the ideal – and only – approach to define and measure such samples. The huge number of stars, the impressive astrometric accuracy, and the faint limiting magnitude of Gaia will quantify our understanding of the structure and motions of stars within the bulge, the spiral arms, the disc, and the outer halo, and will revolutionise dynamical studies of our Galaxy.



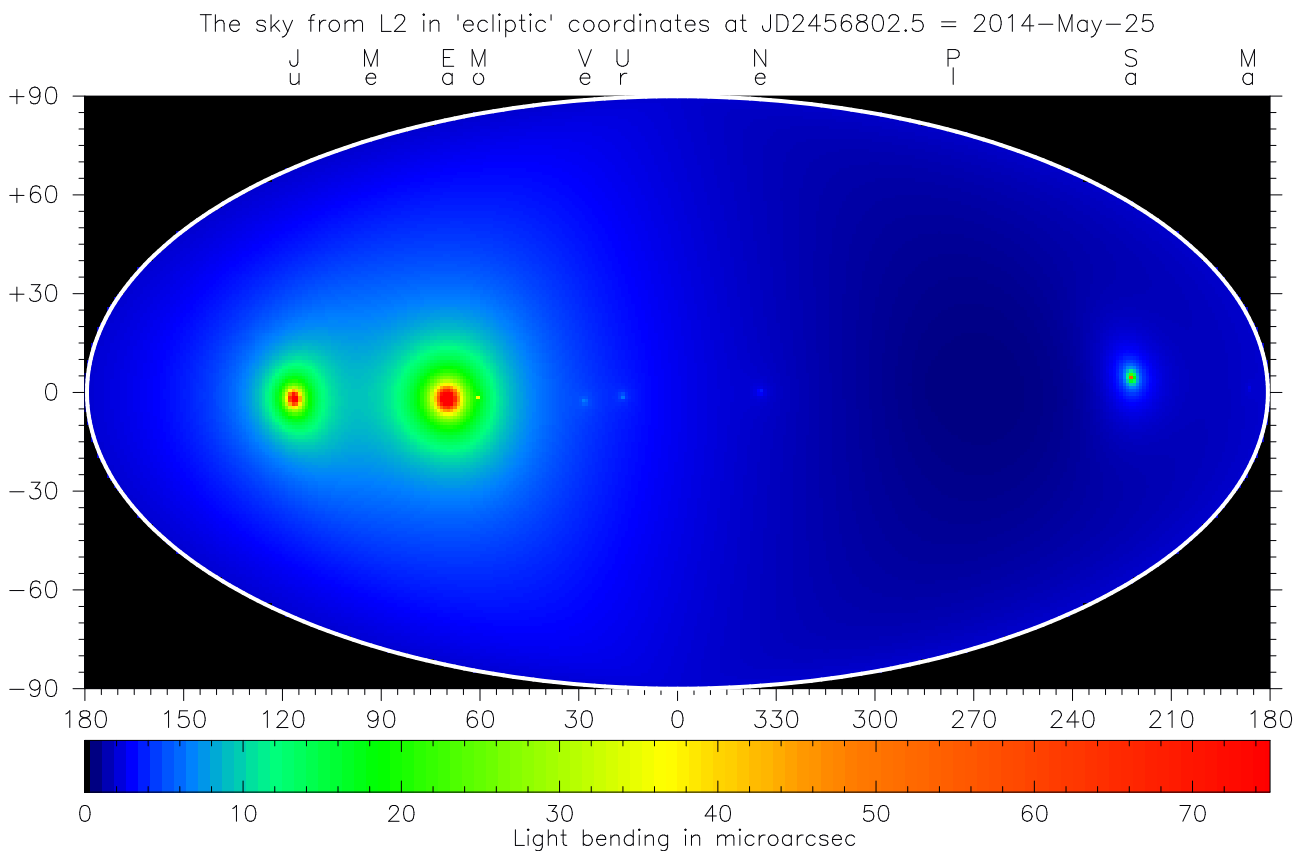
Left: the evolution of the luminosity (top) and effective temperature (bottom) as function of time (in yr) of brown dwarfs for different masses (shown on the right of this figure, in blue, in units of the solar mass). The solid green lines assume no dust formation; the dashed pink lines permit dust formation and retain it in the atmosphere. Gaia will measure accurate properties for young brown dwarfs in numerous clusters and star-forming regions (Baraffe et al. 2002, A&A, 382, 563). Right: absolute J-band magnitudes of field brown dwarfs obtained from ground-based astrometry and photometry. Late-L and T dwarfs are very faint in the optical, so Gaia will only be able to detect a limited sample of old field brown dwarfs out to several parsec. Yet even for these, Gaia will measure distances to better than 1% (Vrba et al. 2004, AJ, 127, 2948).

In observing the entire sky down to 20-th magnitude, Gaia will observe large numbers of isolated brown dwarfs in the solar neighbourhood. Structural models show that brown dwarfs cool and fade rapidly after formation, so that the distance out to which Gaia can detect them is a function of their mass and age. Gaia should see Pleiades-age ( $\sim 100$  Myr) brown dwarfs out to around 400 pc and younger brown dwarfs, such as those in the Orion Nebula Cluster (1–3 Myr), out to about 1 kpc. This volume encompasses numerous young clusters and star-forming regions such as Chamaeleon, where brown dwarfs are known to exist. For an  $I = 20$  mag brown dwarf at 200 pc, Gaia will obtain a distance accuracy of about 4% and transverse velocities to around  $0.2 \text{ km s}^{-1}$ .

One of the main contributions of Gaia to substellar astrophysics will be a detailed spatial and kinematic map of brown dwarfs in clusters of known age and metallicity (determined from Gaia parallaxes of higher-mass stars), permitting a comprehensive study of mass segregation and ejection of brown dwarfs. These are key ingredients to understanding the formation mechanism of substellar mass objects, whether it be via cloud fragmentation and gravitational collapse, premature ejection from an accreting envelope, or some other mechanism.

Brown dwarfs will be identified primarily from their absolute luminosities obtained from the precise Gaia parallaxes as well as from the on-board multi-band photometry. The latter will provide physical parameters of brown dwarfs, in particular the effective temperature, but perhaps also metallicity and the nature of cloud coverage. As brown dwarfs will be found in clusters of a range of ages, a significant contribution of Gaia will be an accurate observational determination of their cooling curves. The photometry and absolute magnitudes will furthermore help in the detection of spatially and astrometrically unresolved brown-dwarf binaries. From this information, we will be able to determine the substellar mass function and the three-dimensional spatial and age distribution of brown dwarfs, thus establishing their formation history in the context of the Galaxy.

Predictions of the number of brown dwarfs which Gaia will detect depend sensitively on their cooling function and their distribution. Rough estimates based on current knowledge are of the order of 50,000 over a wide range of masses and ages. The absolute luminosities, colours, and kinematics obtained from Gaia will provide us with detailed insight into the physical properties, formation, and evolution of this substellar population.

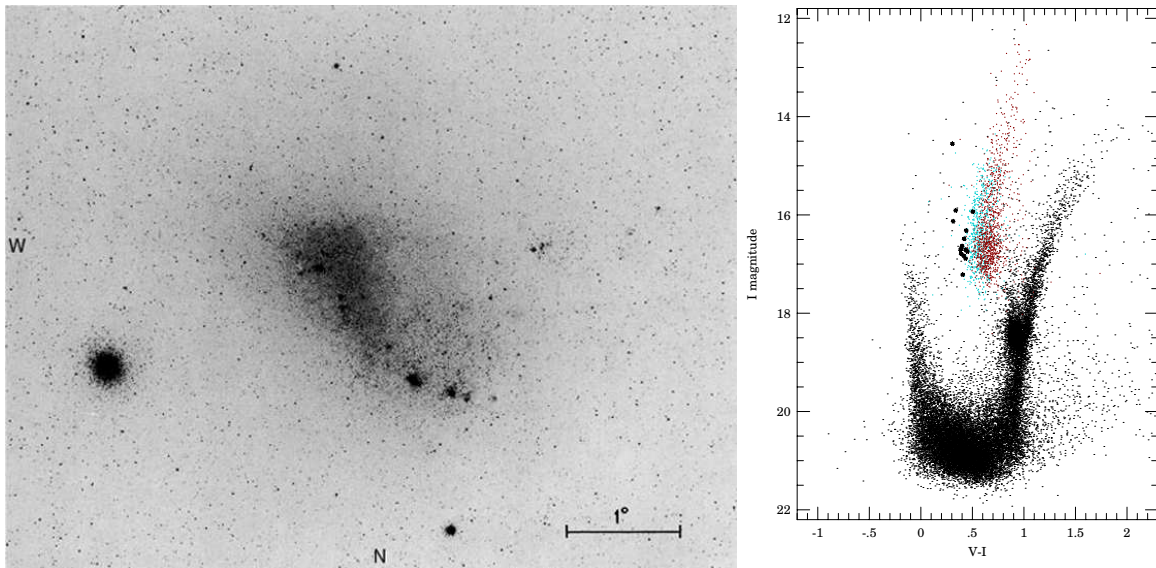


All-sky map (in ecliptic coordinates, for an L2-based observer) displaying the total amount of post-Newtonian light deflection due to all planets, and the Moon, at 25 May 2014 (two-letter object-name abbreviations appear above the top axis). The Sun has been suppressed because of its immense contribution, extending all over the sky, compared to the other bodies. The colour coding has been chosen such that significant light bending is predicted in all regions of the sky coloured different from blue.

Gaia will determine the positions, parallaxes, and proper motions for the brightest 1 billion objects in the sky. Expected astrometric accuracies are 20–25  $\mu\text{as}$  at 15-th magnitude and a few  $\mu\text{as}$  for the brightest stars (up to 12-th magnitude). At these accuracy levels, it is vital to treat the Gaia data in a general-relativistic context. For example, photons detected by Gaia are bent during the last hours of their long journey, while traversing the solar system, under the influence of the gravitational fields of the Sun, planets, moons, asteroids, etc. The amount of this post-Newtonian light deflection depends on the mass of the perturbing object, its distance to the observer (Gaia), and the angular separation at which the photon passes the object. A well-known example is a light ray grazing the limb of the Sun: an observer on Earth will notice a deflection of 1.75 arcsec.

In the context of Gaia, correcting for solar-system light bending is critical: for a spherical perturbing body with a mean mass density  $\rho$  (in  $\text{g cm}^{-3}$ ), the light deflection for a limb-grazing light ray is larger than  $\delta$  (in  $\mu\text{as}$ ) if its radius  $r > \rho^{-1/2} \cdot \delta^{1/2}$ . 624 km. Typically,  $\rho \sim 1 \text{ g cm}^{-3}$  for objects in the solar system, so that Gaia's astrometric measurements will be 'affected' to a significant extent ( $\delta \sim 1\text{--}10 \mu\text{as}$ ) by all bodies with radii larger than  $\sim 624$  km. (For Jupiter and Saturn, the quadrupole contributions of their gravitational fields should also be taken into account.)

In principle, this translates for Gaia, observing from L2, to the Sun and all planets (including the Earth and Moon) and to a number of the larger moons (notably Io, Europa, Ganymede, Callisto, and Titan; light deflection in these cases, however, is only significant at angular separations smaller than a few arcseconds). In practice, however, due to the geometry of the scanning law which effectively creates a 45°-radius zone of avoidance on the sky centered on the Sun, the contributions from Mercury and the Moon, for example, can always be neglected. Minor bodies (e.g. main-belt asteroids and Kuiper-Belt objects) and smaller moons are unimportant. The Sun, on the other hand, contributes significantly to light bending even 180° away from its center.



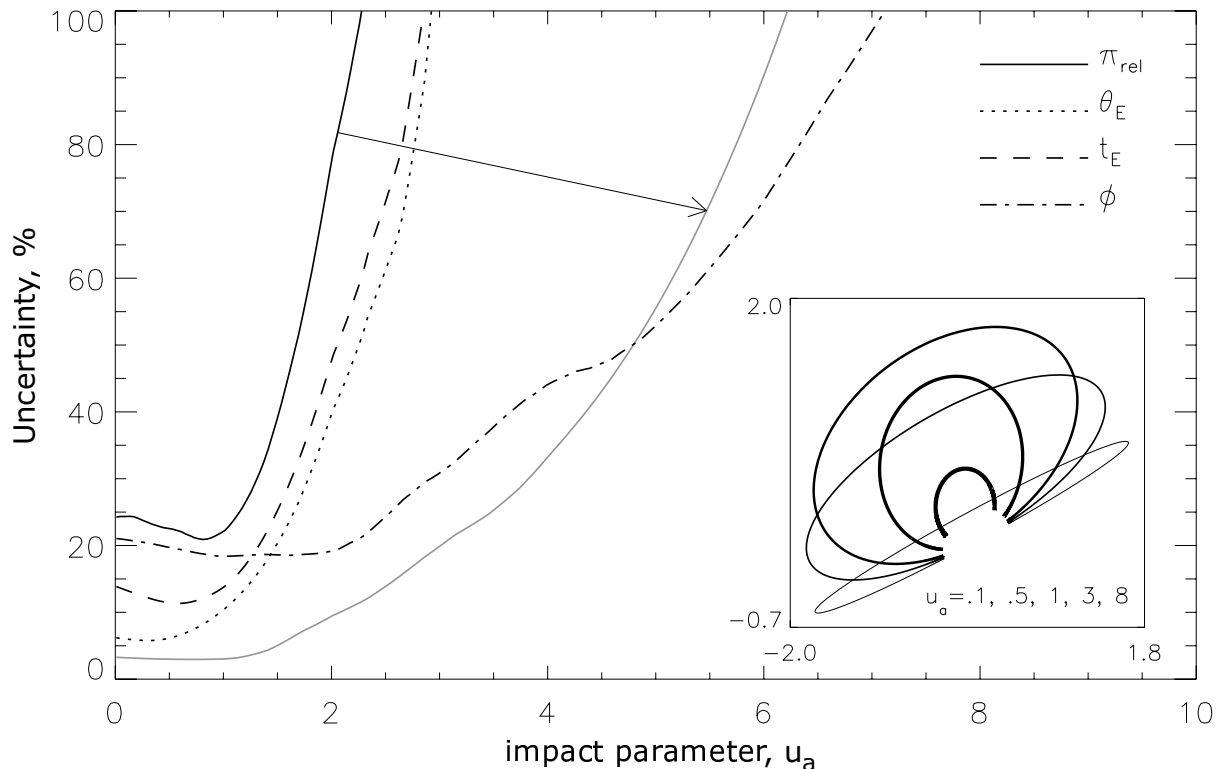
Left: the Small Magellanic Cloud as it appears on the sky. The big globular cluster (to the left) belongs to our own Galaxy. Image by Henize using the Mt. Wilson 10-inch refractor. Right: colour-magnitude diagram for an area of  $14 \times 57$  arcmin $^2$  in the SMC bar. There are 45,500 stars with  $I < 20$  mag. Overplotted are the Cepheids from OGLE, with fundamental, first overtone, and single-mode second overtone indicated separately by colour. Image from the OGLE consortium, courtesy of Andrzej Udalski. Gaia will observe millions of stars in the Large and Small Magellanic Clouds and will give even more detailed information.

The Magellanic Clouds are substantial galaxies in their own right, which provide the nearest examples of young intermediate-to-low chemical-abundance stellar populations for study. The Large Magellanic Cloud (LMC) and Small Magellanic Cloud (SMC) will provide millions of stars for Gaia analyses. The key scientific questions for Gaia involve the dynamics of the LMC-Galaxy and the LMC-SMC interactions, the luminosity calibration of stellar populations, the dynamics of star-forming regions, and the dynamical structure of the LMC 'bar'. At the LMC and SMC distance of roughly 50 kpc (parallax 20  $\mu$ as), individual bright stars, with  $I = 12\text{--}16$  mag, will have transverse velocities determined to approximately 1–2 km s $^{-1}$  ( $\sim 20 \mu$ as yr $^{-1}$ ). Gaia will allow kinematic mapping and membership analyses of young star-forming regions in the LMC and SMC with comparable precision to that presently available in the Milky Way. In other words, it will be possible to compare directly the kinematics and structure of star-forming regions in a large spiral disc with those in a mid-sized irregular galaxy.

The dynamical evolution of the solar neighbourhood is dominated by diffusion of stars in velocity space, crudely described as an age-velocity dispersion relation. This process is not well understood, but presumably involves energy input from spiral arms and molecular clouds. The Gaia kinematics in the LMC and SMC will quantify the age-kinematics relation in a very different environment, constraining the key dynamical processes.

One of the major puzzles in the structure of the LMC and the SMC is their asymmetric luminosity distribution. While the large-scale, radially-averaged luminosity profiles of both galaxies follow fairly smooth exponentials, both show significant bar-like asymmetries. This is most obvious in the LMC, and in stars of ages less than a few Gyr old. However, the LMC 'bar' is substantially offset from the dynamical centre, and seems unrelated to the stellar-dynamical  $m=2$  modes of cold discs. It appears to be sufficiently long-lived to have survived differential rotation for several rotation periods. It is presently unknown what the dynamical status of the bar is, or even if it is in the same plane as the main LMC disc. Gaia will provide three-dimensional dynamics across the whole bar and disc region, quantifying the dynamical relationship between these features. While an individual parallax to an LMC star will be imprecise (20 per cent error), the very large number of targets will map the spatial structure of the LMC/SMC system with high spatial resolution directly.

The masses of the LMC and SMC are poorly known. Current analyses involve approximate solutions fitting the poorly known transverse velocity, and assuming simple disc structure, for a small number of test particles. Gaia proper motions will map the membership of the clouds as far as they extend, including the 'inter-cloud' regions of young metal-poor star formation, the complex SMC 'wing', and stars associated with the HI Magellanic Stream. This will map the dark-halo structures of both the intact LMC and the apparently distorted SMC, determining the extent of their halos, the density of the Milky Way at 50 kpc, and the effects of the LMC-SMC interaction.



The percentage error in estimation of the microlensing parameters as a function of impact parameter. Accurate recovery of the relative parallax ( $\pi_{\text{rel}}$ ) is hard, whereas recovery of the angular Einstein radius ( $\theta_E$ ) and the Einstein crossing time ( $t_E$ ) is easier. (The lens distance is 150 pc, the source distance is 4 kpc, the transverse velocity is 20 km s<sup>-1</sup>, while the accuracy is 150  $\mu$ as.) The arrow shows improvement in the relative parallax estimate when photometric follow-up information is available. The inset shows the centroid shift evolution with increasing impact parameter (source parallactic and proper motion removed).

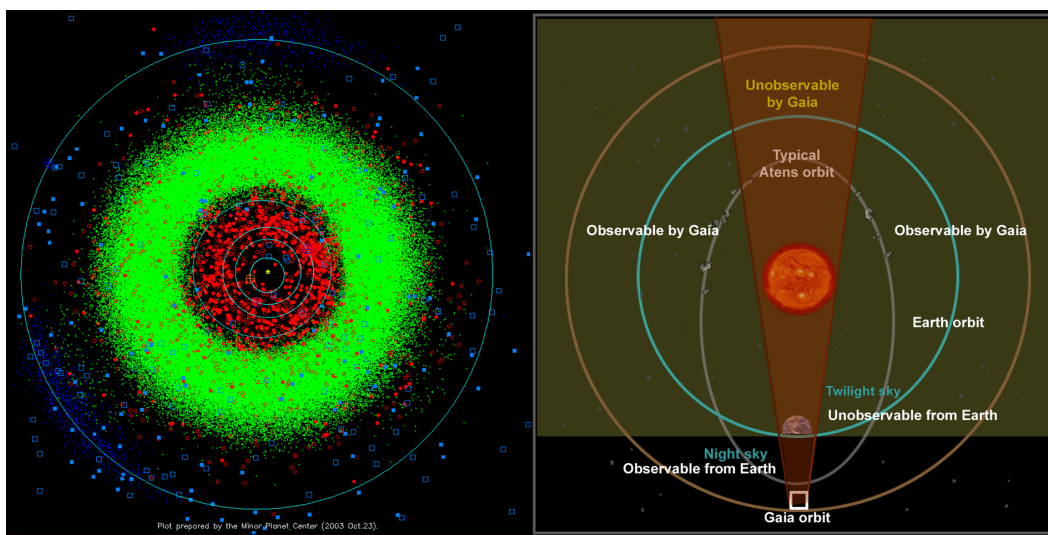
Gaia can observe gravitational microlensing by measuring the photometric amplification of a background source star at epochs when it is coincidentally aligned with a foreground lens. The all-sky averaged photometric optical depth associated with such an alignment is  $\sim 5 \times 10^{-7}$ , hence there will be  $\sim 7500$  photometric microlensing events during Gaia's 5-year mission lifetime, most of which will have only a few data points because of the poor sampling.

If photometry is combined with the measurements of the centroid of the two images of a microlensed source, then complete information about the distance and the mass of the lens can be obtained. The all-sky averaged astrometric microlensing optical depth is  $\sim 1.5\text{--}2.0 \times 10^{-5}$ . This means that between about 15,000 and 20,000 sources will have the variation of centroid shift at least  $5\sqrt{2}$  times larger than the typical astrometric accuracy together with a closest approach (source to the lens) during the lifetime of the Gaia mission.

The most valuable events are those for which the Einstein crossing time ( $t_E$ ), the angular Einstein radius ( $\theta_E$ ), and the relative parallax of the source with respect to the lens ( $\pi_{\text{rel}}$ ) can all be inferred from Gaia's data stream. The mass of the lens then follows directly. Gaia measurements alone will provide a sample of at least 500 stars with accurately determined masses. However, the numbers can be improved still further if Gaia observations are supplemented with ground-based photometry. A total of 1000 masses will be measured with the help of dedicated telescopes on the ground.

Astrometry can provide direct estimates of the angular Einstein radius ( $\theta_E$ ) and the lens proper motion angle. However, the values of impact parameter ( $u_a$ ) and Einstein crossing time ( $t_E$ ) are more difficult to obtain with astrometry alone. On the other hand, just a few data points on the light curve of a microlensed star will allow the time scale and the maximum amplification (and hence impact parameter) to be determined. A further increase in the number of mass measurements is possible if ground-based photometry is supplied.

One of the major scientific contributions of microlensing studies with Gaia will be the determination of the mass function in the solar neighbourhood. Microlensing is the only known technique which can measure the masses of objects irrespective of whether they happen to be components of a binary system or emit electromagnetic radiation.



Left: minor planets (indicated by green circles) in the inner solar system. Objects with perihelia within 1.3 AU are plotted as red circles. Orbits of major planets are shown in light blue. Image courtesy Minor Planet Center.  
 Right: Gaia is ideally situated to probe the asteroid blind spot between the Sun and Earth. As this schematic diagram shows, some regions of the sky that are unobservable from Earth can be observed by Gaia.

While tracking stars with its telescopes, Gaia will also observe solar system objects by the thousands, primarily asteroids of the main belt circling the Sun between the orbits of Mars and Jupiter. With its ability to detect faint and fast-moving objects, it is expected that Gaia will also detect several thousand Near-Earth Objects (NEOs), which are thought to be comets and asteroids that have been nudged by the gravitational attraction of nearby planets into orbits that allow them to enter the Earth's neighbourhood. Much further away, beyond the orbit of Neptune, bigger objects are clustered in the Kuiper belt. The largest of these will also be detected with Gaia.

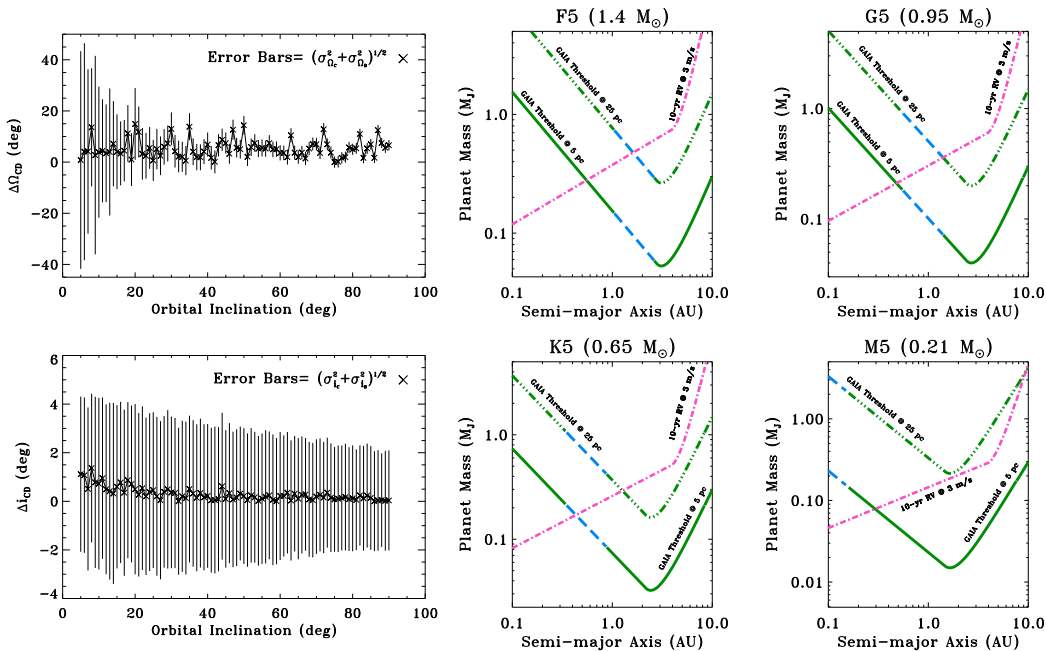
The scientific interest in asteroids is due largely to their status as the remnant debris left over from the process that formed the inner planets, including Earth. Asteroids are also the source of most meteorites that have struck the Earth's surface and many of these objects have already been subjected to chemical and physical analyses.

Due to its vantage point of observation at the Lagrange point L2 and its ability to observe down to an angular distance of 45 degrees from the Sun, Gaia will be ideally situated to probe the asteroid blind spot between the Sun and Earth and to discover small bodies orbiting the Sun inside the Earth's orbit, a region virtually unreachable from the Earth. In the course of its all-sky survey, Gaia will also observe the sky far from the ecliptic, where ground-based surveys of minor planets are predominantly active, an instance very favorable to the discovery of objects roaming the solar system on exotic orbits.

Gaia will accurately measure the positions and velocities of asteroids over the five years of the mission leading to a determination of their orbits with an unprecedented precision. Orbital parameters are essential to compute well in advance when and where a stellar occultation by a small body will be observable. Such events yield a wealth of information on the sizes and shapes, and when the masses are known, on the densities of these objects. Orbits are also a key element in identifying members of 'orbital families' sharing a common origin.

The tiny gravitational pull experienced by asteroids during close approaches between two bodies – thousands of such encounters are predicted to take place during Gaia's operational life – pushes them away from their path. This small deviation will be recorded in the Gaia astrometric measurements, leading to the mass of the perturber. About 150 asteroid masses will thus be determined to better than 50% by Gaia, as compared to the approximately 20 known today.

Beyond astrometry, Gaia's multi-epoch photometric data will reveal the surface properties of minor planets by telling us how much light is reflected in a particular colour. A refined classification of the population of minor bodies will emerge from this giant database, revealing the kinship between asteroids, NEOs, and meteorites. In addition, the variation of the physical parameters with the distance to the Sun will also be studied.



Left: coplanarity analysis for the  $v$  And system. Right: Gaia planet discovery space as a function of orbital radius, stellar spectral type and distance from the observer (green solid line: 5 pc; green dashed-dotted line: 25 pc). The blue dashed line represents the habitable zone of the star. The pink dashed line indicates the planet discovery space for 3  $m\ s^{-1}$ -precision radial-velocity measurements.

The size of the stellar sample out to 150–200 pc to be investigated for planets – comprising hundreds of thousands of objects – constitutes the most significant contribution Gaia will provide to the science of extra-solar planets. Indeed, the results derived from Gaia’s microarcsecond-precision astrometric measurements will help decisively improve our understanding of orbital parameters and actual mass distributions. Gaia will thus provide important data to constrain theoretical models of formation, migration, and dynamical evolution of planetary systems.

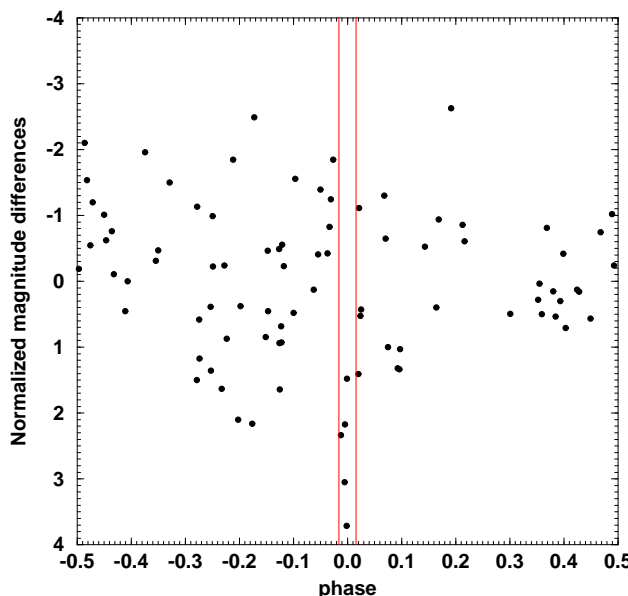
Within 200 pc of the Sun, and limiting counts to bright solar-type main-sequence stars, i.e. objects brighter than 13-th magnitude and with spectral types earlier than K5, about  $N_*$   $\sim 3 \times 10^5$  objects are predicted to exist. The table below shows how, given reasonable assumptions on the planetary frequency as a function of orbital radius, on the detection threshold, and on the accuracy of orbit determination, Gaia will be capable of discovering thousands of planets around these stars. Gaia will accurately measure the orbital characteristics and actual masses for a significant fraction of the detected systems.

$\Delta d$ (pc)	$N_*$	$\Delta a$ (AU)	$N_d$ (1)	$N_m$ (2)
0-100	$\sim 61\ 000$	1.3 - 5.3	$\geq 1600$	$\geq 640$
100-150	$\sim 114\ 000$	1.8 - 3.9	$\geq 1600$	$\geq 750$
150-200	$\sim 295\ 000$	2.5 - 3.3	$\geq 1500$	$\geq 750$

(1) Number of giant planets ( $N_d$ ) that could be detected by Gaia around solar-type stars, as a function of increasing distance from the Sun. (2) Number of detected planets ( $N_m$ ) for which orbital elements and masses can be measured to better than 20%. A uniform frequency distribution of 1.3% planets per 1-AU bin is assumed.

The frequency of multiple-planet systems, and their preferred orbital spacing and geometry, is not currently known. Star counts predict  $\sim 13\ 000$  stars to 60 pc. Gaia, with its high-precision astrometric survey of the solar neighbourhood, will observe each of these, searching for planetary systems composed of massive planets in a wide range of possible orbits, making precise measurements of their orbital elements, and establishing quasi-coplanarity (or non-coplanarity) for detected systems with favorable configurations.

Gaia observations of nearby stars, out to 25 pc, will also contribute to populating the database of stars to be observed by the future ESA/NASA Darwin/TPF mission. Gaia astrometry will confirm the existence of Jupiter signposts from radial-velocity measurements, and will extend spectroscopic surveys to the large database of nearby M dwarfs, complementing ground-based observations. The Gaia measurements will provide estimates of the actual planet masses, thus contributing to models establishing whether or not dynamical interactions would permit an Earth-like planet to form and survive in the habitable zone of any given star. Finally, Gaia will measure the inclinations of the orbital planes, complementing ground-based studies of exo-zodiacal cloud emission for the extra-solar system.



Transits of the star HD 209458 = HIP 108859 as seen in Hipparcos photometric observations, with the transit duration indicated by two vertical lines. The transits were predicted from ground-based observations after the Hipparcos mission.

In the search for extra-solar planets, three complementary techniques can be employed: *Radial-velocity* measurements can find planets in close orbits around their stars, but give no information about the inclination angle of the orbit, and therefore only the minimum mass of the planet can be established. *Astrometry* is suitable for detecting long-period planets, but requires precise measurements and long time spans. *Planetary transits* only occur in those systems with proper alignment of the orbit relative to Earth, but a transit reveals the planet's radius, if the exact inclination angle of the orbit can be determined. Detection or measurement both by astrometric and transit methods are feasible with Gaia; the astrometric method is described elsewhere.

The transit of an extra-solar planet across its parental stellar disc will often occur in Gaia observations and is of interest for detection or measurement for stars brighter than about 16-th mag. The photometric effect of a transit will be most significant in the measurements made in the 9 astrometric CCD strips (AF1–9). A precision of about 1 milli-magnitude per field crossing of Gaia's focal plane is expected for stars brighter than 14-th mag, much more accurate than from Hipparcos. This corresponds to a signal-to-noise ratio of 10 for a Jupiter-size planet around a Sun-like star. For 'known planets' around bright stars, Gaia photometry may yield significant additional information.

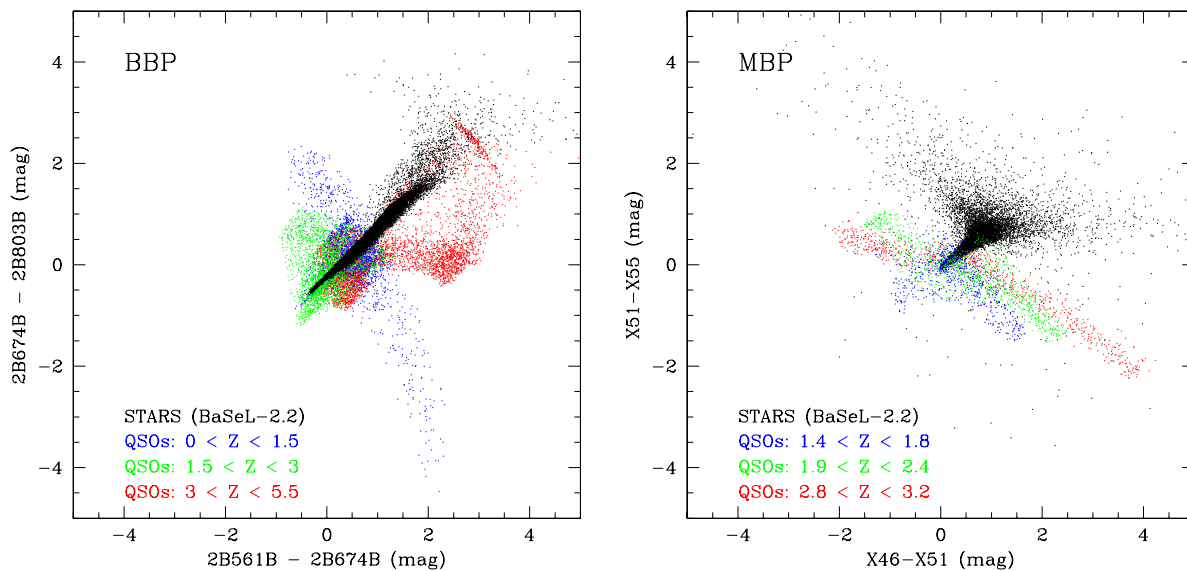
A photometric measurement for only one transit of the field in principle suffices to determine the radius of the planet when the stellar radius is known. However, the secure identification of a photometric dimming as being due to a planetary transit requires additional information, e.g. from astrometry or radial velocities or from other transits. Stars with surface spots may be recognised as such and may not be suited for detection of transits.

	F	G	K	M	Sum
$0 < a < 2\text{AU}$ :	3000	2000	1500	15	6500
$a > 2\text{AU}$ :	50	30	20	0	100

*The predicted number of planetary transits with Gaia for the four spectral types F, G, K, and M, for small and large orbital radii. A signal-to-noise ratio of at least 10 has been assumed.*

The number of detected planets (see table) is highly sensitive to the assumed distribution of planetary orbit sizes. From the distribution of currently detected extra-solar planets, it is possible to give a qualified estimate of the distribution for planets in small orbits. For larger orbits, the assumed distribution is an estimate based on our knowledge of the solar system and considering theories of planetary formation.

The advantage of Gaia observations over other surveys, either from space or from the ground, is that all sufficiently bright stars will be observed many times during the mission, thus providing a complete all-sky survey with a well-known selection function.



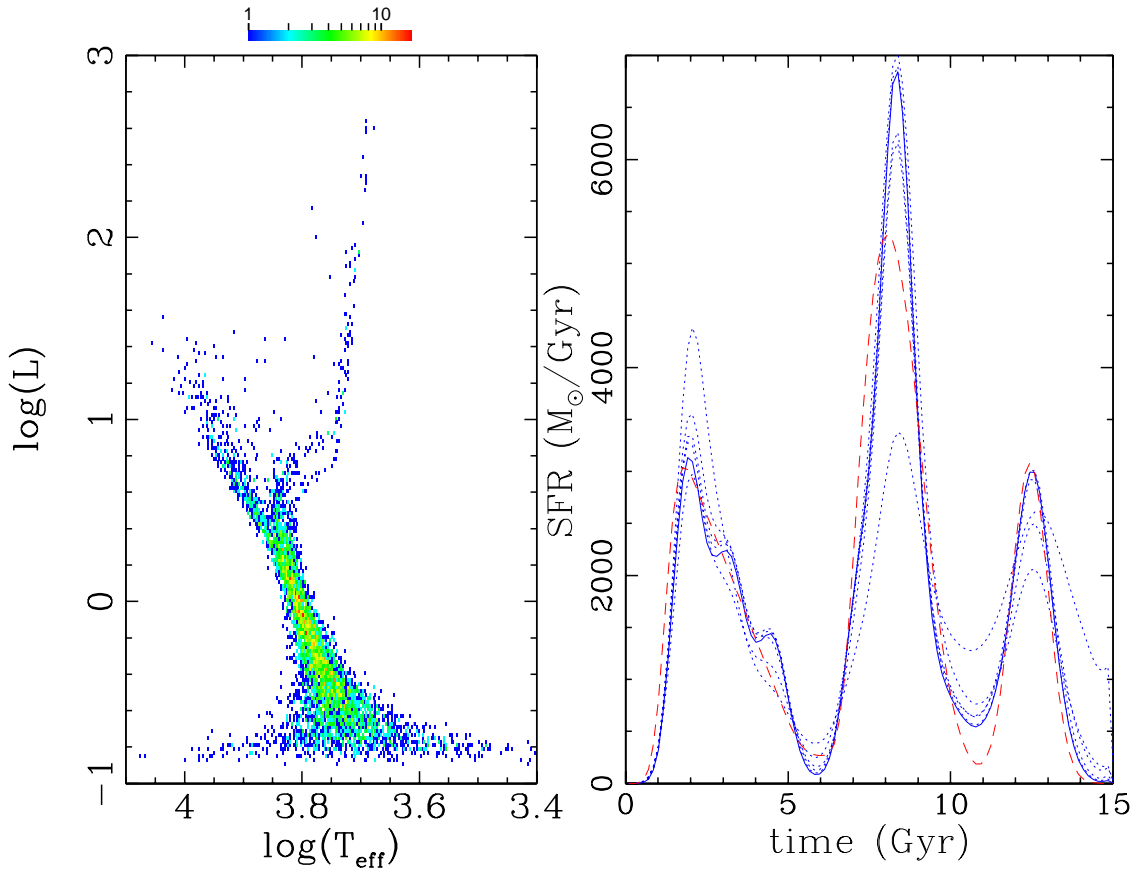
Examples of colour-colour diagrams showing star and QSO loci in simulated broad-band photometry (left) and medium-band photometry (right). In medium-band filters, QSO emission lines make strong signatures at specific redshifts (see right plot, where the signatures of the CIII], CIV and Ly-alpha emission lines are visible in the distribution of the blue, green, and red objects respectively). The figures refer to an obsolete photometric-filter system studied for Gaia during the assessment phase. The flight-model payload design features two low-dispersion photometers (BP and RP) returning spectra covering the entire wavelength range supported by the telescope plus CCD.

Gaia will provide astrometric and photometric observations for about 500,000 quasars (QSOs) down to 20-th magnitude over the whole sky, 5 times more than the number expected from the Sloan Digital Sky Survey. The Gaia data set will constitute the first all-sky survey of optically-selected active galactic nuclei (AGN) and QSOs.

AGN and QSOs are of prime importance in establishing the relativistic reference frame, one of the scientific objectives of the Gaia mission. Gaia's QSO sample will have a profound impact on studies of the large-scale structure of the Universe. Their spectroscopy will allow the gas content in distant galactic haloes and in intervening intergalactic clouds to be probed. In addition, about 2000 QSOs in the final sample are expected to be lensed by a foreground galaxy, and 50 per cent of these should directly be identified as multiply-imaged objects thanks to Gaia's reconstructed sky-mapper images. This number is an order of magnitude larger than the number of known lensed QSOs. The number and properties of lensed QSOs in a statistical sample contain information on the nature of distant lensing galaxies and on the geometry of the Universe. Thus, Gaia also offers the prospect of constraining the values of cosmological parameters.

Since QSOs only represent 0.05 per cent of the objects detected by Gaia, it is crucial to be able to discriminate them from the much more numerous stars. In principle, Gaia's data will offer three methods to reach this objective, based on three properties of QSOs: (i) their colours occupy a different locus from the one formed by stars in the multi-dimensional colour space built from Gaia's photometric data (see the figure above); (ii) their variability can be detected by photometric measurements collected during the 5-year mission lifetime; (iii) their lack of proper motion and parallax can be determined by the astrometric instruments. Which (combination of) method(s) will be used for QSO selection remain to be decided.

After having built sets of representative simulated QSO spectra, either characterised by their redshift, continuum slope, total equivalent width of emission lines, and reddening, or by weights for a set of spectral principal components, on-going studies aim at determining: (i) the parameter space over which QSOs can be discriminated against stars by photometric means alone; (ii) the rate of contamination of stars by QSOs if only photometry is used; (iii) the accuracy with which the redshift and other spectral parameters can be determined; (iv) the QSO limiting magnitude required to recover their spectra with good accuracy.

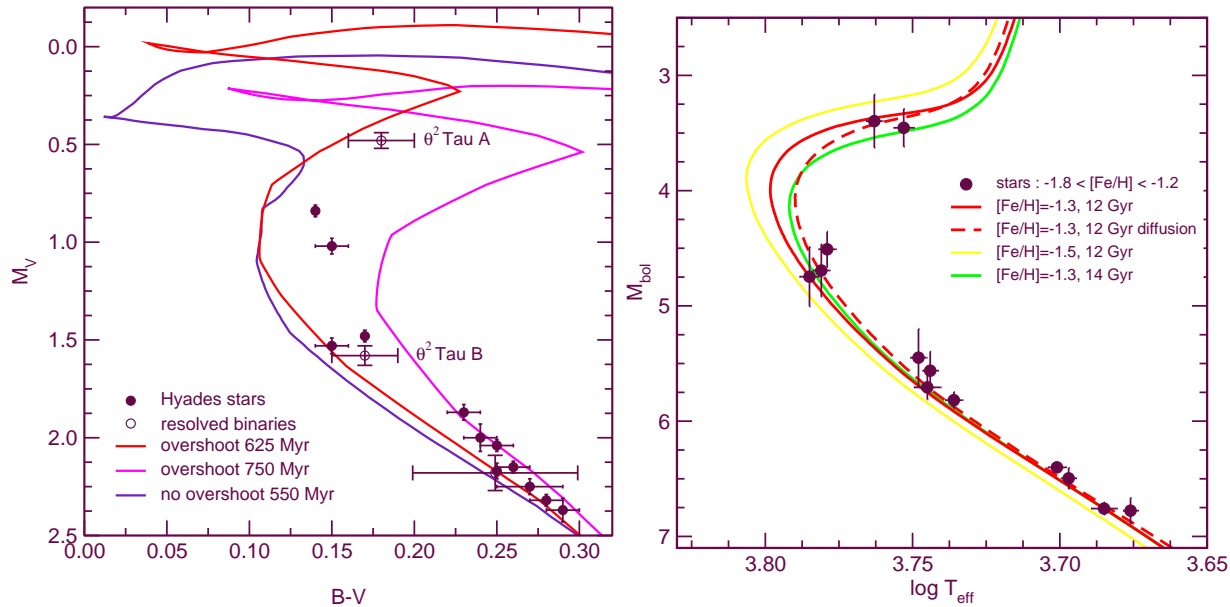


Left: synthetic Hertzsprung–Russell diagram appropriate for good-quality Gaia data. Right: derived star-formation history following inversion of the data in the left panel. Long-dashed red curve: true input star-formation history; dotted curves: successive intermediate iterations; solid curve: final iteration.

A primary scientific goal of Gaia is the determination of the star-formation histories, as described by the temporal evolution of the star-formation rate and the cumulative numbers of stars formed, in the bulge, inner disc, solar neighbourhood, outer disc, and halo of the Milky Way. In general, stellar age-metallicity-extinction degeneracies, convolved with current observational errors and uncertain stellar distances, have made determination of the star-formation history of a mixture of stellar populations unreliable and non-unique. The best available analyses involve comparison of an observed colour-magnitude diagram with a model population. While powerful, such analyses can never be proven unique. The Gaia astrometric, photometric, and spectroscopic data, combined with specifically-developed, direct-inversion tools, will resolve this ambiguity and will make the full evolutionary history of the Galaxy accessible.

The star-formation history defines the luminosity evolution of the Galaxy directly. In combination with the relevant chemical abundance distributions, the accretion history of gas may be derived. Together with kinematics, the merger history of smaller stellar systems can be defined. The sum of these three processes forms what is loosely known as ‘galaxy formation’. Analysis of the Gaia results will provide the first quantitative determination of the formation history of our Galaxy.

The determination of the relative rates of formation and/or accumulation of the stellar populations in a large spiral, typical of those galaxies which dominate the luminosity in the Universe, will provide, for the first time, an ability to test galaxy-formation models in a quantitative manner. Do large galaxies form from accumulation of many smaller systems which have already initiated star formation? Does star formation begin in a gravitational potential well in which much of the gas is already accumulated? Does the bulge pre-date, post-date, or is it contemporaneous with the halo and inner disc? Is the thick disc a mix of the early disc and a later major merger? Is there a radial age gradient in the older stars? Is the history of star formation relatively smooth or highly episodic? In addition to their immediate and direct importance, answers to such questions will provide uniquely a template for analysis of data on unresolved stellar systems, where Gaia-type and -quality data can never be obtained.



Left: estimation of the age of the Hyades at turn-off. Gaia will obtain clean sequences in the Hertzsprung–Russell diagram for many open clusters, allowing stellar-age determinations in the Galactic disc. Right: estimation of the age of 13 halo stars for which high-quality Hipparcos data exists. With Gaia, the number of subgiants with accurate parameters will increase, yielding improved age determinations of the oldest stars.

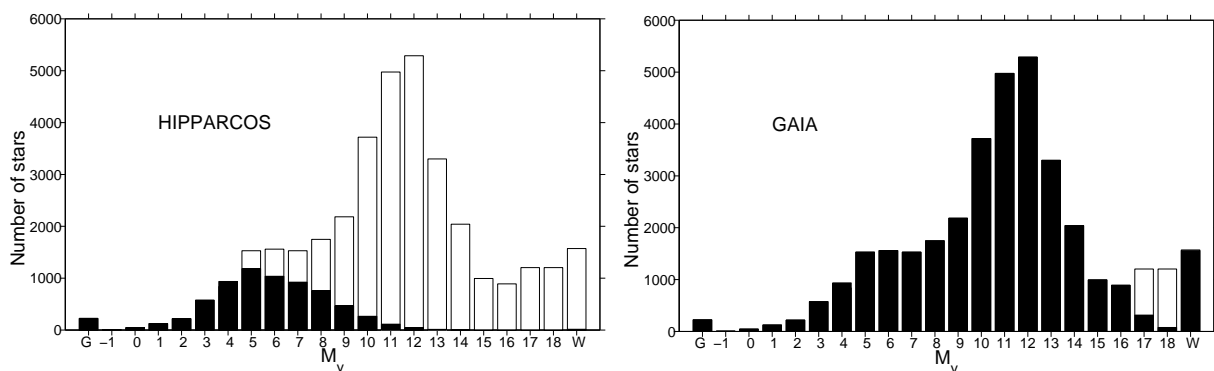
Precise stellar-age determinations are required for various Galactic structure and evolution studies and for cosmological studies. The primary age-determination method relies on comparisons of stellar models or isochrones with the best available data, in particular luminosity, effective temperature, and abundances, for individual stars or stellar groups. The principle of the method is general, but its application to different types of stars requires specific considerations.

**A–F stars, open clusters and Galactic evolution:** Galactic-evolution studies require the determination of the ages of relatively young objects in the Galactic disc, mainly open clusters and main-sequence A–F stars with ages ranging from several million to a few billion years. By providing accurate data for a large number of A–F stars, Gaia will reduce drastically the impact of the distance uncertainty on the age estimates for single stars. Gaia will also provide clean sequences in the Hertzsprung–Russell diagram for many open clusters containing hundreds to thousands of members. Cluster stars with masses spanning a large interval, and assumed to share the same age and chemical composition, constitute a unique tool for age determinations.

**Helium abundance and chemical evolution of the Galaxy:** The position of the zero-age main-sequence in the Hertzsprung–Russell diagram depends critically on the chemical composition of stars. The large sample of non-evolved low-mass stars with determined metallicities and accurate positions in the Hertzsprung–Russell diagram, that will be constituted from Gaia observations of K–M dwarfs, will be a key tool for interpreting the stellar helium abundances and the possible relation between helium and metallicity.

**The oldest stars and the age of the Universe:** The determination of the age of the oldest objects in the Galaxy (Population II) provides a lower limit to the age of the Universe. This can be used to constrain cosmological models and parameters. Currently, the best estimate for the age of the oldest stars is based on the absolute magnitude of the main-sequence turn-off in globular clusters, and is affected by the uncertainty on the cluster distances.

Gaia will improve the age estimate of the oldest stars. The number of subdwarfs with accurate distances will considerably increase in each metallicity interval allowing us to derive the distance of an increased number of globular clusters of various chemical compositions by main-sequence fitting. Furthermore, distances of a substantial number of field subgiants will be measured, improving the age determination of the field halo stars.

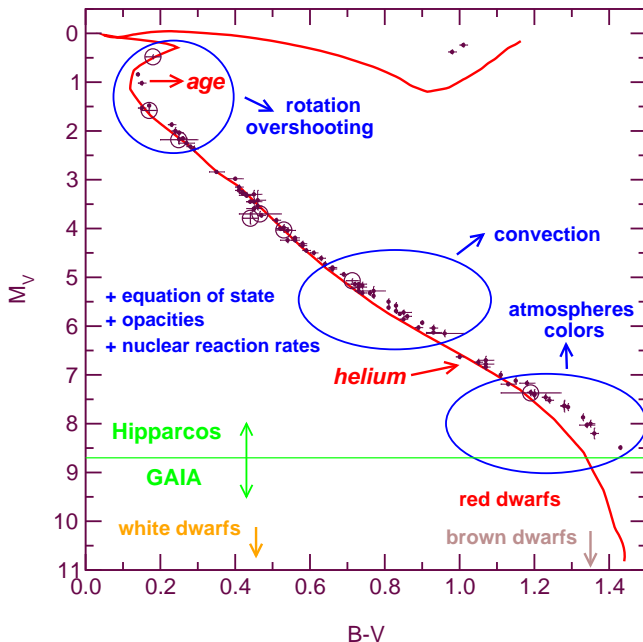


Comparison of the completeness from Hipparcos (left) with the expected completeness from Gaia (right). The plots show the number of star systems (individual stars or binary/multiple systems) within 50 pc of the Sun, as a function of absolute magnitude  $M_V$ , predicted by a systemic luminosity function based on data from the literature. The bar with the letter 'G' (at left) denotes giant stars, and with the letter 'W' (at right) denotes white dwarfs. The black parts of the bars give the number of star systems detected by Hipparcos or by Gaia. Figure courtesy Joan García-Sánchez.

Close or even penetrating passages of stars through the Oort Cloud can in principle deflect large numbers of comets into the inner planetary region, initiating Earth-crossing cometary showers and possible Earth impacts. Although the distribution of long-period cometary aphelia is largely isotropic, some non-random clusters of orbits do exist, and it has been suggested that these groupings record the tracks of recent stellar passages, with dynamical models suggesting typical decay times of around 2–3 Myr. Gaia's complete and accurate census of the distribution and space motions of the stars in the solar neighbourhood will allow a determination of the frequency of such close encounters, and will provide, for the first time, sufficiently accurate astrometric data for a large number of stars to carry out a reliable study of the link between comet showers and past impact events and mass extinctions on Earth.

García-Sánchez et al. (1999) used Hipparcos data to investigate close stellar encounters with the solar system, the consequences for cometary-cloud dynamics, and the evolution of the comet population over the history of the solar system. Effects of individual star passages on comet orbits were studied through dynamical simulations. Algol was the largest perturber in the recent past (although other stars have passed even closer), passing at a distance of about 2.5 pc about 7 Myr ago. Gliese 710 is the most significant known future perturber. At 19 pc from the Sun, and approaching at about  $14 \text{ km s}^{-1}$ , it will pass through the Oort Cloud, at about 69,000 AU from the Sun, in about 1 Myr. But the authors concluded that none of the predicted passages could have caused a significant disruption of the Oort Cloud, which supports the hypothesis that the currently observed flux of long-period comets corresponds to a steady-state value.

The figure above shows the number of star systems (individual stars or binary/multiple systems) within 50 pc of the Sun, as a function of the absolute magnitude. The black parts of the bars give the number of star systems detected by Hipparcos (left) or expected for Gaia (right). 'G' denotes giant stars and 'W' indicates white dwarfs. Hipparcos detected about 20 per cent of the nearby star systems, whereas Gaia will detect nearly all of them. Two explanations for an increased rate of impact events on Earth have been suggested: (i) a collisional breakup of a large asteroid in the asteroid belt that can deliver collision fragments to orbital resonances, resulting in large fragments ejected from the asteroid belt to Earth-crossing orbits; (ii) a comet shower caused by a close stellar passage, increasing significantly the number of comets with Earth-crossing orbits. The reliable determination of a close stellar encounter with the solar system during the time of the impact events would provide strong support to the cometary origin of such impacts, as opposed to the asteroid hypothesis. In particular, an extinction at the end of the Eocene period, 36 Myr ago, is identified with several large impact craters, multiple iridium layers, and other evidence of a prolonged period of increased cometary flux in the inner-planets region. Hipparcos data allowed the study of passages within a few million years. Gaia will enhance this time interval to a geologically interesting range. The encounters predicted by using Gaia data are expected to establish whether the currently observed comet flux corresponds to an enhanced or a steady-state flux, with implications for the size of the Oort-Cloud population. The prediction of future close or penetrating passages through the Oort Cloud may be used to estimate resulting enhancements in the inner-solar-system cometary flux.



Gaia will address a broad range of physical and astrophysical topics related to stellar structure and evolution. Pictured here: the Hipparcos Hertzsprung–Russell diagram of the Hyades compared to a model isochrone. Uncertainties in the stellar parameters and in the calculation of model atmospheres and interiors affect the determination of the cluster age and helium content.

The study of stellar structure and evolution provides fundamental information on the properties of matter under extreme physical conditions as well as on the evolution of galaxies and cosmology. The accurate and homogeneous astrometric and photometric data provided by Hipparcos has resulted in precise characteristics of individual stars and open clusters and the confirmation of certain aspects of internal-structure theory.

Further progress on stellar modelling is required, for example, on atmospheric modelling, transport processes of matter, angular momentum and magnetic fields, microscopic physics, etc. On the observational side, more numerous samples of rare objects, including distant stars and stars undergoing rapid evolutionary phases, an increased number of common objects with high-quality data, and a census over all stellar populations are required.

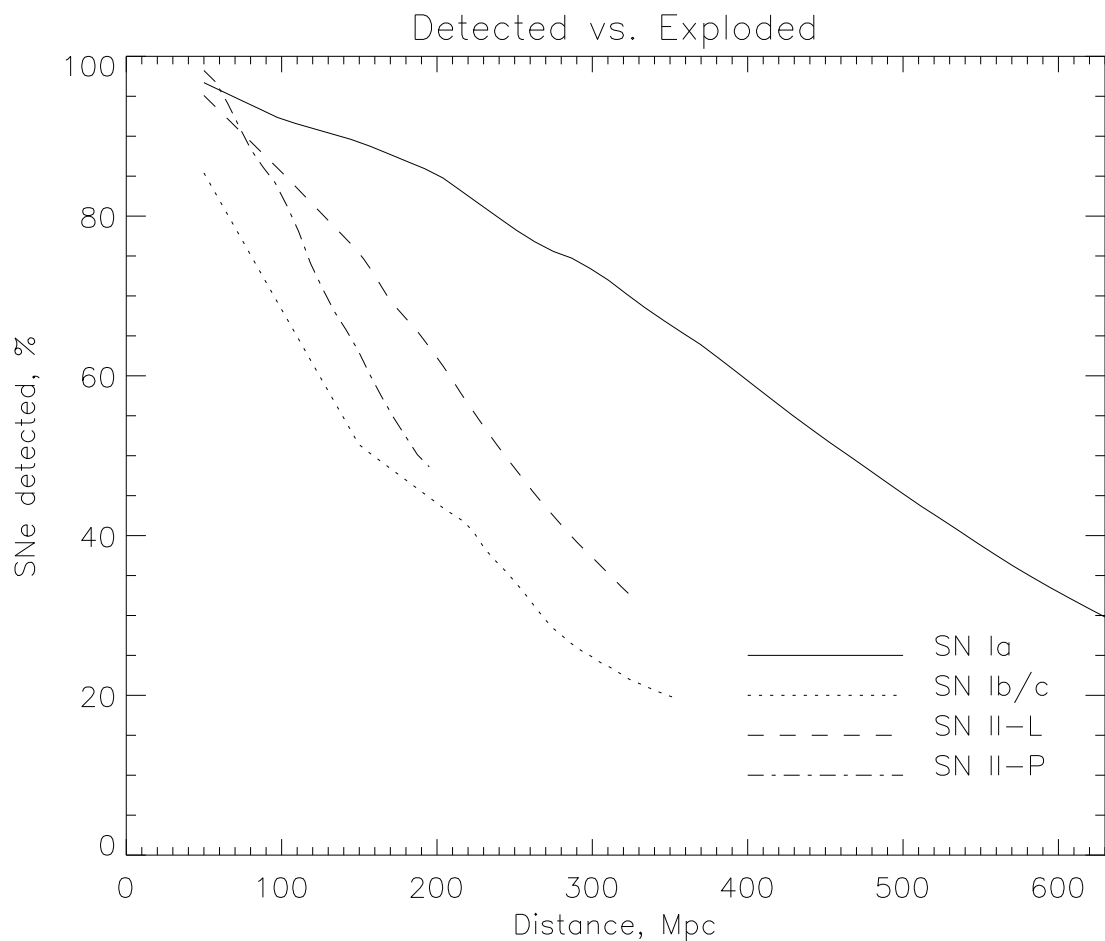
Gaia will return luminosities, surface temperatures, abundances, masses, and determinations of the interstellar extinction for all types of stars. The following are some of the effects that will be probed with the Gaia data:

**The size of convective cores:** Asteroseismic data – obtained from the ground or from the space mission COROT – combined with accurate estimates of global parameters from Gaia can probe the size of stellar convective cores. These define the amount of nuclear material available to sustain the luminosity, playing a crucial role in the evolution of intermediate- and high-mass stars.

**Internal diffusion of chemical elements:** Microscopic and turbulent diffusion of chemical elements in stellar radiative zones may have important consequences for stellar evolution, in particular for stellar ages when fresh helium is brought to the stellar cores. Diffusion may also modify the composition at the surface of stars during their life implying difficulties in linking abundances of elements presently observed to the initial abundances of the protostellar cloud.

The high-precision positions in the Hertzsprung–Russell diagram of stars of known surface abundances, provided by Hipparcos and by high-resolution spectroscopy, have revealed discrepancies between the observations and the predictions of standard stellar models. The large sample of stars with accurate parameters provided by Gaia will help in addressing these discrepancies.

**Outer convective zones:** Most stellar models are still built by treating convection according to the classical parametric mixing-length theory. Asteroseismic analysis of stars combined with the careful calibration of the Hertzsprung–Russell diagram allowed by Gaia for samples of different chemistries, ages, etc., will greatly enhance our capabilities of dealing with non-local convective models for stellar interiors.



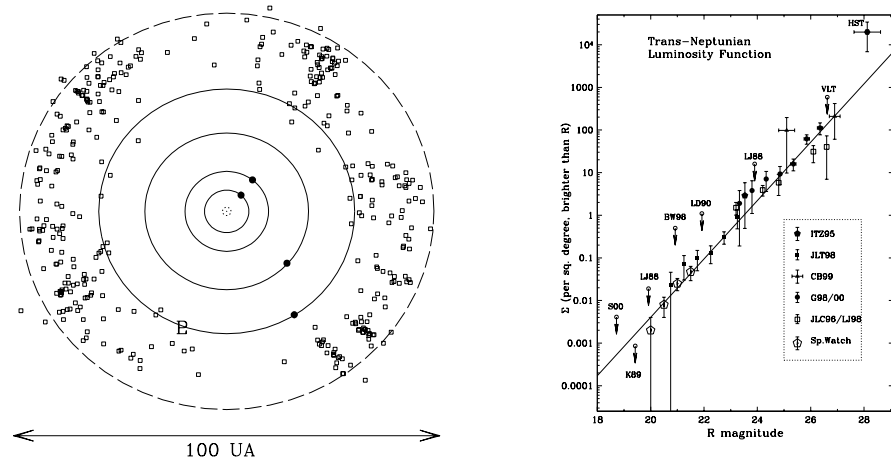
The total number of supernovae detected within distance D as a fraction of the total number exploded. Within 630 Mpc, Gaia detects  $\sim 30\%$  of all type Ia supernovae. Within 355 Mpc, Gaia detects  $\sim 20\%$  of all type Ib/c. For type II-L, Gaia detects  $\sim 31\%$  within 335 Mpc. Finally, for type II-P supernovae, Gaia detects  $\sim 48\%$  within 195 Mpc. Detection is defined as Gaia recording at least one data point on the standard supernova template.

Gaia is an ideal instrument to study nearby supernovae (i.e. within a few hundred Mpc). Gaia will provide a huge dataset of high-quality local type-Ia supernovae in which any deviations from 'standard candles' can be analysed. As the dataset is so large, there will likely also be a good number of relatively rare phenomena, such as sub-luminous supernovae and type Ib/c supernovae.

Gaia will record data on at least 21,400 supernovae during the five-year mission lifetime. This breaks down into  $\sim 14,300$  type Ia,  $\sim 1400$  type Ib/c, and  $\sim 5700$  type II. These supernovae span a redshift range up to  $z \sim 0.14$ .

In the most favourable case, Gaia will alert on all supernovae detected before maximum. These numbers are  $\sim 6300$  type Ia,  $\sim 500$  type Ib/c, and  $\sim 1700$  type II during the whole mission. In other words, Gaia may issue  $\sim 1700$  supernovae alerts a year or  $\sim 5$  alerts a day. Roughly 75% of all alerts will be for type Ia supernovae, while the remainder will be for type Ib/c and II. All these numbers are lower limits since they may be increased by a factor of  $\sim 2$ , depending on the supernova contribution from low-luminosity galaxies.

Supernova rates will be found as a function of galaxy type, as well as extinction and position in the host galaxy. Amongst other applications, there may be about 26 supernovae each year for which detection of gravitational waves is possible and about 180 supernovae each year for which detection of gamma-rays is possible. Gaia's astrometry will provide the supernova position to better than milli-arcseconds, offering opportunities for the identification of progenitors in nearby galaxies and for studying the spatial distribution of supernovae of different types in galaxies.



Left: the Kuiper Belt, as seen looking from the North Pole of our solar system. The 4 solid circles mark the orbits of Jupiter through Neptune, with their position in mid-1999 marked. The 'P' symbol marks the location of Pluto. The squares mark the positions of a sample of Kuiper Belt comets. Right: cumulative luminosity function of the Kuiper Belt. Symbols show several published surveys. The upper limits are 3- $\sigma$  representations at the 50%-limit of the survey.

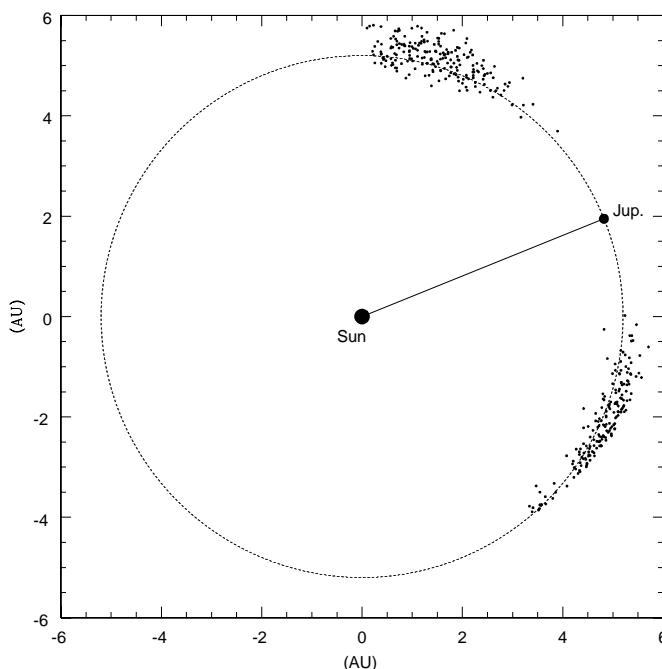
Edgeworth and Kuiper independently suggested the existence of a belt of material in orbits with semi-major axes between 30 and 50 AU, based on the observed distribution of short-period cometary orbits. Dynamical studies showed that after the giant planets reached their current masses the regions between them would be emptied of planetesimals on times scales much smaller than the age of the solar system. However, these studies also showed that outside of Neptune the hypothesised Edgeworth–Kuiper Belt (EKB) was stable, supporting modelling that the short-period comets come from this source via long-term gravitational instability. Today, more than 800 small bodies have been detected in the outer solar system, confirming that there is indeed an EKB. This belt has been found to be dynamically excited (random speeds much larger than would have allowed the accretion of these objects) and heavily depleted (much less material than would have allowed them to accrete).

Due to their large distance to the Sun and Earth, trans-Neptunian objects (TNOs) and Centaurs (objects with perihelia between the orbits of Jupiter and Neptune) are faint objects. Very few of them will be visible by Gaia: currently, only 65 objects are known to be brighter than magnitude 20 (the limit of completeness of Gaia) and 138 are brighter than magnitude 21 (10%-level of detection efficiency). Currently, we estimate to be about 75% complete for objects brighter than  $m_R = 20$ , and at least half complete for objects brighter than  $m_R = 21$ . So Gaia should detect a few tens of objects at most. Most of these should be Centaurs or Scattered Disk Objects (semi-major axis  $>50$  AU and pericentre distance within gravitational reach of Neptune) on their way to the Centaurs region. Only a handful of Classical Kuiper Belt Objects (semi-major axis in the 30–50-AU range, low eccentricity, and low inclination) should be brighter than  $m_R = 21$ , and none should be brighter than  $m_R = 20$ .

Despite this small number, Gaia will provide a valuable contribution to the study of the outer solar system. First of all, it will be the first and only instrument that will survey the whole sky down to magnitude 20, allowing detection of any bright object of the solar system that is currently in front of the Milky Way, or at very high inclination. All ground-based observations have limited detection efficiency in the direction of the Milky Way because of stellar confusion. Starting or foreseen surveys should cover around 90% of the remaining sky. Existence or not of these bright objects will give fundamental clues on the formation mechanism of the EKB and the outer solar system.

For the largest Centaurs which will be cruising at 10 to 30 AU from Gaia, it should be possible to resolve them, providing the only direct measurement of the size of these objects, and hence of their albedo, besides Pluto. All other estimates of size and albedo rely on radio-photometry and thermal modelling.

Among the ~50 objects detected by Gaia, a handful should be binaries. With the astrometric accuracy of Gaia, it will be possible to detect this binarity, and even to determine the orbit of the binary, providing a direct measurement of the mass of these objects. This sample will be a noticeable fraction of masses known at that time, allowing a decently accurate estimate of the volume bulk density.



Schematic view of the locations of the two clouds of a large sample of known Jupiter Trojans around the Lagrangian L4 and L5 points at an arbitrary epoch. The locations of the Trojans have been computed according to their known orbital elements. The orbit of Jupiter, for simplicity approximated by a circle of radius 5.2 AU, is also shown, as are the locations of the planet and the Sun.

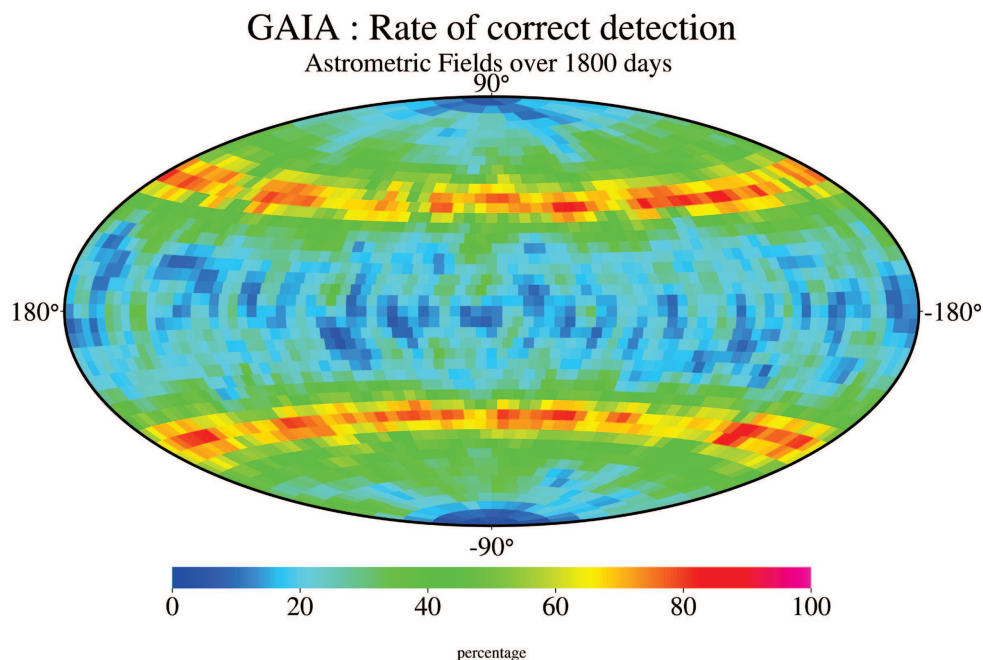
Uniquely among the minor planets, the so-called Jupiter Trojans are made up of small bodies librating around the stable L4 and L5 Lagrangian points of the Sun–Jupiter system on orbits thought to be stable over the age of the solar system. A few Mars and Neptune Trojans are also known to exist, whereas no results have been obtained from searches for Trojans of other planets.

There are many unanswered key questions related to the peculiar locations and orbital properties of Trojans, on which Gaia may cast some light: (i) Did they accrete from planetary grains in the same region where they are found today or were they trapped there in the early stages of the formation of the solar system; (ii) Can Trojans be simply considered as a sub-class of the objects that we collectively call ‘asteroids’, or should we consider them as a separate category of bodies, somehow intermediate between main-belt asteroids and trans-Neptunian objects with distinctive physical properties?

The composition of Trojans constitutes a serious constraint for any study of the original gradient in composition of the planetesimals in the early phase of the solar system. A comparison of their spectral-reflectance properties with those of other classes of minor bodies, including main-belt asteroids, Hildas, Centaurs, trans-Neptunian objects, and comets, is an important task and clearly this is an area where Gaia will contribute significantly.

Another classically-debated problem is the possible systematic difference between the leading (L4) and trailing (L5) clouds. This could reflect a difference in their origin or be the result of a different dynamical and collisional subsequent history. In principle, there should be no difference in the dynamics of the two groups, but it happens that the L4 objects discovered so far are about 1.5 times as numerous as those at L5 (the census as of late July 2009 includes 1850 L4 objects compared with 1404 L5 objects). There are also claims that the distribution of orbital inclinations could be not identical between the two clouds.

Gaia observations of Trojans should help disentangle pieces of the puzzle. Precise astrometric measurements will produce significant improvements in the accuracy of the derived orbits of these objects, leading to the refinement of the statistics of the distribution of orbital elements. The systematic and homogeneous survey of the spectrophotometric properties of Trojans will make it possible to investigate the spectral diversity among Trojans, and to detect possible systematic differences in surface reflectance between the two clouds, as suggested by recent ground-based observations. Moreover, Gaia’s photometric data is expected to produce reliable estimates of rotation periods, spin axis orientations, and overall shapes for a statistically significant sample of the whole population. Regarding object sizes, the large heliocentric distance will restrict that determination to the largest members of the population, such as 624 Hektor and 911 Agamemnon, which have diameters exceeding 100 km.



Probability of recovery, in the end-of-mission data, of a sinusoidal G-band-magnitude variation of period 4h50m and signal-to-noise ratio of 0.75 as function of position on the sky in ecliptic coordinates. The recovery probability varies between nearly 0 per cent and 100 per cent. Gaia's scanning law causes the end-of-mission number of observations to vary with position on the sky, explaining the positional dependency.

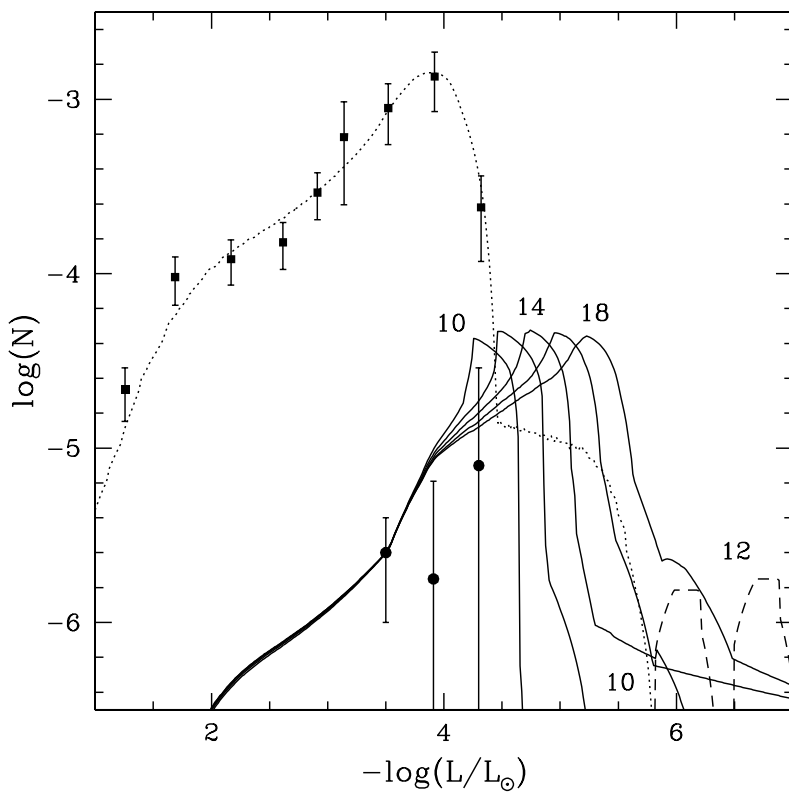
Gaia will provide multi-epoch, multi-colour photometry for all sources brighter than 20-th magnitude. In addition, high-quality broad-band photometric measurements will be made in the astrometric field. The combined photometric data will have the precision necessary to detect diverse variable phenomena and to describe nearly all types of variability. The photometric data will allow a global description of stellar stability and variability across the Hertzsprung–Russell diagram and will permit the identification of the physical processes causing variability.

For a 5-year mission, a sky-averaged number of 70 photometric measurements is expected from the astrometric field and from the Blue and Red Photometers. Expected numbers of variable objects are difficult to predict, but invariably large, with conservative estimates given by Eyer & Cuypers (2000): about 18 million variable stars in total, including 5 million ‘classic’ periodic variables, about 3 million eclipsing binaries, 300,000 with rotation-induced variability, 2,000–8,000 Cepheids, 60,000–240,000 Scuti variables, 70,000 RR Lyrae stars, a significant fraction of these in the bulge, and about 250,000 Miras and SR variables.

Precise physical and orbital parameters of eclipsing binaries will be derived for about 10,000 systems (Zwitter 2003). The pulsating stars include key distance calibrators such as Cepheids, RR Lyrae stars, and long-period variables, for which present samples are incomplete already at magnitudes as bright as 10. A complete sample of objects will allow determination of the frequency of peculiar objects, and will accurately calibrate period-luminosity relationships across a wide range of stellar parameters (i.e. mass, age, and metallicity). Variability on short (seconds) to long (of order 5 years) time scales can be detected.

Several dedicated asteroseismologic space missions (e.g., MOST, COROT, and Kepler) have been launched. Asteroseismological predictions have been achieved from the ground in the case of roAp stars from photometric observations (Matthews et al. 1999) and, for solar-like stars, from radial-velocity measurements (Bouchy & Carrier 2002). Parallax determination is a stringent constraint for testing stellar models when used in asteroseismology; on the other hand, absolute luminosities or masses derived from parallaxes can be used as the starting point for seismological models (Baglin 1997, Favata 1999).

In addition to stellar variability, other ‘time phenomena’ will also be present in the Gaia data: supernovae (estimated at  $\sim 20,000$ ; Belokurov & Evans 2003), microlensing events (though astrometry will be able to detect  $\sim 100$  events, about 1000 stars will have perturbed photometry; Belokurov & Evans 2002), planetary transits ( $\sim 5,000$  detectable transits are expected; Robichon 2003). Finally, non-stellar variable objects will be observed, including gamma-ray bursts, quasars, active galactic nuclei, and small bodies in the solar system.



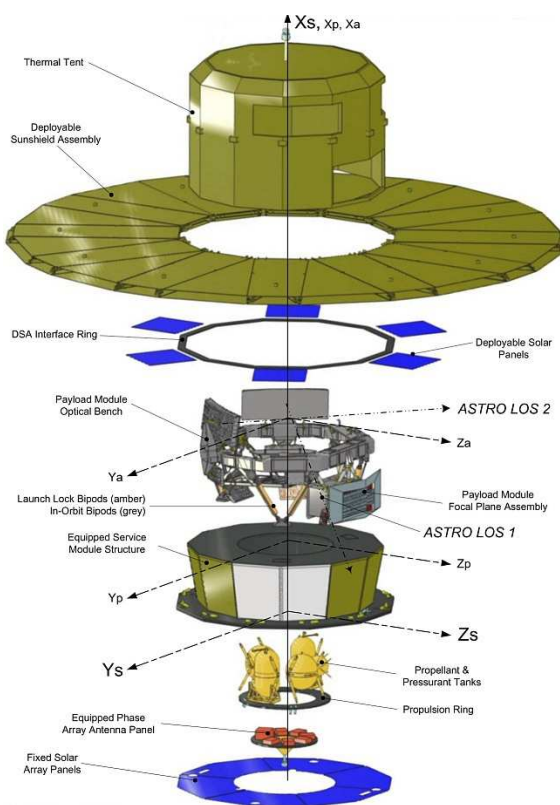
Luminosity functions of disc (dotted line) and halo (solid lines) white dwarfs as a function of luminosity. This figure assumes bursts of star formation at 10, 12, 14, 16, and 18 Gyr that lasted for 0.1 Gyr. The luminosity function of disc white dwarfs was computed assuming a disc age of 9.3 Gyr. The observational data were obtained from Liebert et al. (1988, 1989).

White dwarfs are well-studied objects and the physical processes that control their evolution are reasonably well understood. In fact, most phases of white-dwarf evolution can be successfully characterised as a cooling process. In other words, white dwarfs slowly radiate at the expense of the residual gravothermal energy. The release of this energy occurs over long time scales (of the order of the age of the galactic disc, 10 Gyr).

The mechanical structure of white dwarfs is supported by the pressure of the gas of degenerate electrons, whereas the partially degenerate outer layers control the flow of energy. Precise spectrophotometric data – like those that Gaia will provide – will introduce tight constraints on the models. Specifically, Gaia will allow the mass-radius relationship to be tested. Even today, this relationship is not particularly well constrained. By comparing theoretical models with the observed properties of white dwarfs in binary systems, Gaia will be able to constrain the relation between the mass of the star on the main sequence and the mass of the resulting white dwarf.

Gaia will also provide precise information on the physical mechanisms (crystallisation, phase separation, ...) operating during the cooling process. Given their long cooling time scales, white dwarfs have been used as a tool for extracting information about the past history of our Galaxy. The large number of white dwarfs that Gaia will observe will allow us to determine, with unprecedented accuracy, the age of the local neighbourhood and the star-formation history of the Galaxy. Furthermore, Gaia will be able to distinguish among the thin- and the thick-disc white-dwarf populations, and, in this way, it will be able to provide fundamental insight into the Galactic history. Gaia will also probe the structure and dynamics of the Galaxy and provide new clues about the halo white-dwarf population and its contribution to the mass budget of our Galaxy.

Finally, new constraints on the (hypothetical) rate of change of the gravitational constant ( $G$ ) will be derived by comparing the measured average cooling rates of white dwarfs. More specifically, Gaia will largely reduce the observational errors in the determination of the disc white-dwarf luminosity function. Since the white-dwarf luminosity function measures the average rate of cooling of white dwarfs, and since this rate depends crucially on the rate of change of  $G$ , the Gaia observations will strongly constrain its rate of change.



Schematic view of the adopted design of the Gaia spacecraft. Image courtesy of EADS Astrium.

The Gaia spacecraft provides all necessary support to the payload instrumentation. Generally, the spacecraft subsystems follow well-established spacecraft engineering approaches, although specific innovative features are needed for Gaia, for example for the mechanical and thermal configuration, and for the telecommunication subsystem.

**Mechanical design:** the main structure, of hexagonal conical shape to avoid turning shadows on the sunshield, is an aluminium structure with carbon-fibre reinforced plastic (CFRP) walls, and a central tube supporting the propellant tanks. The deployable solar array is made of 12 panels (CFRP structure back-insulated with multi-layer insulation, and shape-memory alloy hinges) and completed with a sunshield made of multi-layer insulation sheets with Kevlar cables for deployment post launch.

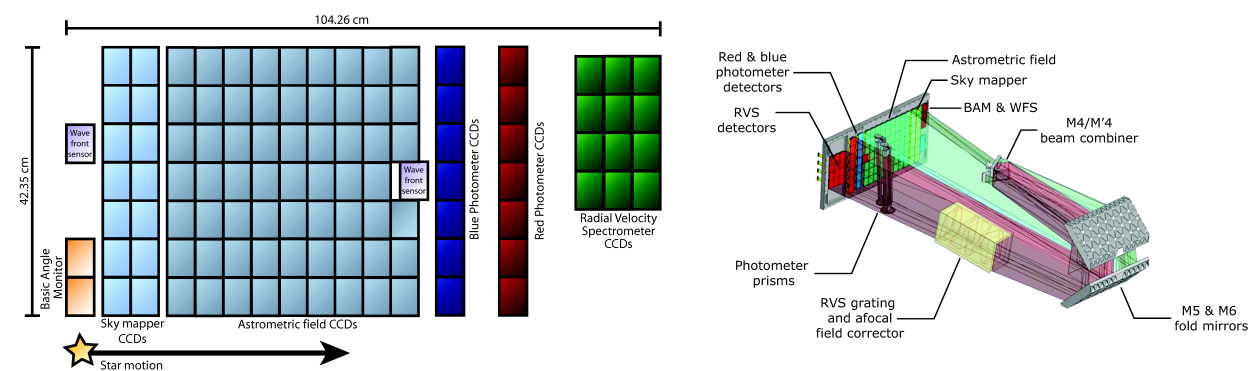
**Thermal control:** the very high stability thermal control is achieved through optical solar reflector material, multi-layer insulation sheets on the outer faces of the service module, and a black painted cavity with a heat pipe network.

**Propulsion and attitude control:** after injection into its L2 transfer orbit, a chemical bi-propellant propulsion system is used for the transfer phase: attitude acquisition, spin control, mid-course corrections, L2 orbit injection, and safe mode. One redundant set of cold-gas thrusters will control the operational orbit and spin motion once at L2. Three Sun acquisition sensors plus one gyroscope provide spin-axis stabilisation during the transfer phase, with one large field of view star tracker plus use of the main instrument for the 3-axis controlled operational phase.

**Payload data handling:** dedicated processing electronics are provided for the computationally intensive tasks of on-board object detection, attitude determination, window allocation, data compression, and temporary storage (a solid state memory of 800 Gbits). The typical (continuous) payload data rate is about 1 Mbps.

**Power and electrical subsystem:** the required solar-array area is split into a number of deployable and fixed panels, with GaAs cells on a CFRP structure. A lithium-ion battery is used for launch and early-orbit operations.

**Communications:** telemetry and telecommand employs X-band up- and down-links with a few kbps capacity and an omni-directional coverage. The science telemetry X-band down-link has a 4–8 Mbps capacity which is used during each ground station visibility period (of about 8 hours per day), based on a set of electronically-scanned phased array antennae accommodated on the service module panels.



Left: the Gaia focal plane. Credit: ESA - A. Short. Right: the Gaia instruments. Credit: EADS Astrium.

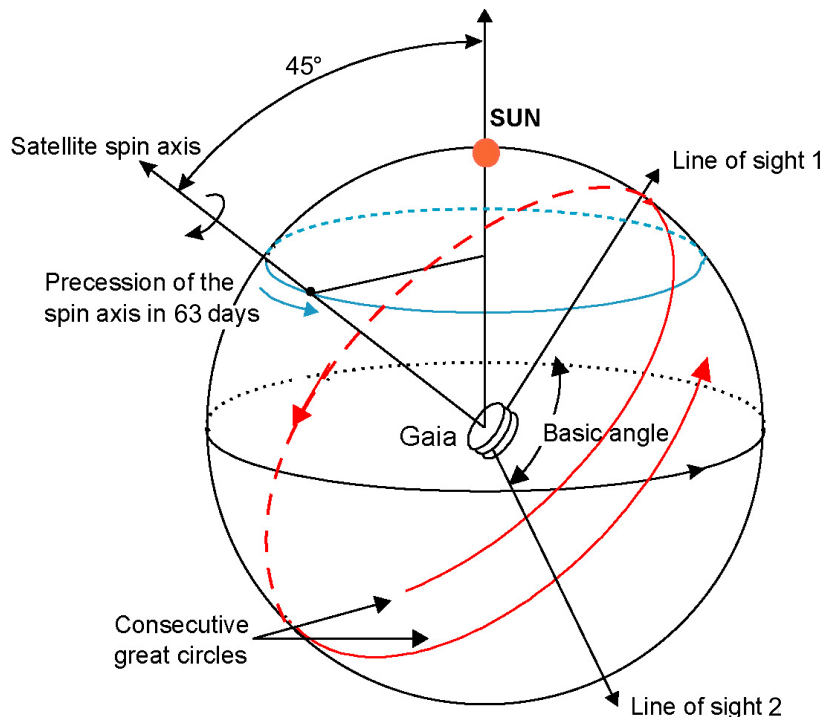
Gaia has two telescopes with two associated viewing directions of size  $0.7^\circ \times 0.7^\circ$  (along scan  $\times$  across scan) each. The two viewing angles are separated by a highly-stable 'basic angle' of  $106.5^\circ$ . The two field of views are combined into a single focal plane covered with CCD detectors. By measuring the instantaneous image centroids from the data sent to ground, Gaia measures the relative separations of the thousands of stars simultaneously present in the combined fields. The spacecraft operates in a continuously scanning motion, such that a constant stream of relative angular measurements is built up as the fields of view sweep across the sky. High angular resolution (and hence high positional precision) in the scanning direction is provided by the primary mirror of each telescope, of dimension  $1.45 \times 0.5 \text{ m}^2$  (along scan  $\times$  across scan). The wide-angle measurements provide high rigidity of the resulting reference system.

The whole sky is systematically scanned such that observations extending over several years yield some 70 sets of relative measurements for each star. These permit a complete determination of each star's five basic astrometric parameters: two specifying the angular position, two specifying the proper motion and one - the parallax - specifying the star distance. A 5-year mission permits the determination of additional parameters, for example those relevant to orbital binaries, extra-solar planets and solar-system objects.

In practice, the *a posteriori* on-ground data processing is a highly complex task, linking all relative measurements and transforming the location (centroid) measurements in pixel coordinates to angular field coordinates through a geometrical calibration of the focal plane, and subsequently to coordinates on the sky through calibrations of the instrument attitude and basic angle. Moreover, corrections for systematic chromatic shifts need to be made, as well as aberration corrections and corrections for general-relativistic light bending due to the Sun, the major planets, some of their moons and the most massive asteroids. Centroid shifts caused, under the influence of radiation damage, by stochastic charge trapping and de-trapping in CCDs also need to be understood and calibrated with high precision.

The astrometric field (AF) in the focal plane is sampled by an array of 62 CCDs, each read out in TDI (time-delayed integration) mode, synchronised to the scanning motion of the satellite. In practice, stars entering the combined field of view first pass across dedicated CCDs which act as a 'sky mapper' (SM) - each object is detected on board and information on its position and brightness is processed in real-time to define the windowed region read out by the following CCDs. Gaia's limiting magnitude is about 20-th magnitude and all objects brighter than this limit at the epoch of observation will be measured. Gaia's observations are thus not limited to stars but also cover quasars, near-Earth objects, asteroids, supernovae, etc.

Before stars leave the field of view, spectra are measured in three further sets of dedicated CCDs. The BP and RP CCDs - BP for Blue Photometer and RP for Red Photometer - record low-resolution prism spectra covering the wavelength intervals 330-680 and 640-1000 nm, respectively. These simultaneous semi-photometric measurements of the spectral energy distribution yield key astrophysical information, such as temperatures, gravities, metallicities and reddenings for each of the vast number of objects observed. In addition to the low-resolution photometric instrument, Gaia features a high-resolution integral-field spectrograph, the so-called Radial Velocity Spectrometer (RVS) instrument. The RVS provides the third component of the space velocity of each star (down to about 17-th magnitude).



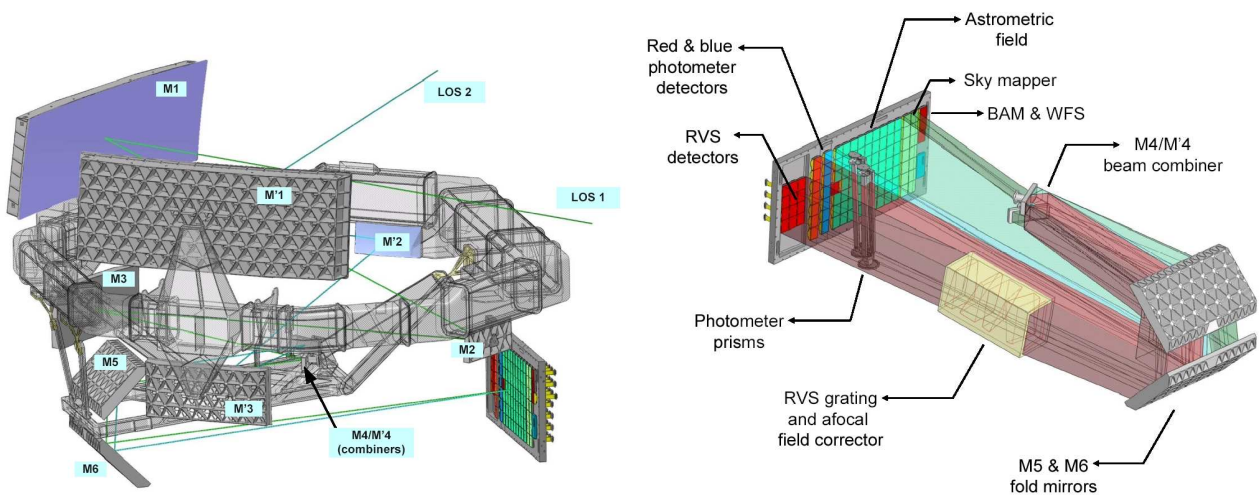
Gaia's two astrometric fields of view scan the sky according to a carefully prescribed 'revolving scanning law'. The constant spin rate of  $60 \text{ arcsec s}^{-1}$  corresponds to 6-hour great-circle scans. The angle between the slowly precessing spin axis and the Sun is maintained at  $45^\circ$ . The basic angle is  $106.5^\circ$ .

Gaia will perform its observations from a controlled Lissajous-type orbit around the L2 Lagrange point of the Sun and Earth-Moon system. During its 5-year operational lifetime, the satellite will continuously spin around its axis, with a constant speed of  $60 \text{ arcsec s}^{-1}$ . As a result, over a period of 6 hours, the two astrometric fields of view will scan across all objects located along the great circle 'perpendicular to' the spin axis. As a result of the basic angle of  $106.5^\circ$  separating the astrometric fields of view on the sky, objects transit the second field of view with a delay of 106.5 minutes compared to the first field.

Gaia's spin axis does not point to a fixed direction in space (or on the sky) but is carefully controlled so as to precess slowly on the sky. As a result, the great circle that is mapped out by the two fields of view every 6 hours changes slowly with time, allowing repeated full sky coverage over the mission lifetime.

The 'scanning law' prescribes how the satellite's spin axis evolves with time during the mission. The optimum scanning law (i) maximizes the angle  $\xi$  between the Sun and the spin axis at all times, and (ii) maximizes the uniformity of the sky coverage after 5 years of operation. The first requirement results from the fact that the parallactic displacement of transiting stars is proportional to  $\sin \xi$ ; a higher value of  $\xi$  thus leads to larger measurable parallaxes and higher end-of-mission astrometric accuracies. Thermal stability and power requirements, however, limit  $\xi$  to about  $45^\circ$ . The best strategy is thus to let the spin axis precess around the solar direction with a fixed angle of  $45^\circ$ . This combination of a spinning satellite, scanning the sky along great circles, and a precession of the spin axis is referred to as 'revolving scanning', and was used for the Hipparcos mission. The actual speed of precession of the spin axis on the sky should be small enough that consecutive great-circle scans overlap 'sufficiently', and large enough that all stars on the sky transit the astrometric fields 'sufficiently often'.

The above requirements have been worked out in detail for Gaia, leading to an optimum nominal scanning law. For a spin rate of  $60 \text{ arcsec s}^{-1}$  and a solar aspect angle of  $45^\circ$ , the precession speed is such that 5 years of operation corresponds to 29 revolutions of the spin axis around the solar direction; the precessional period thus equals 63 days. On average, each object on the sky is observed about 70 times (two astrometric fields combined and 20% total dead time assumed).

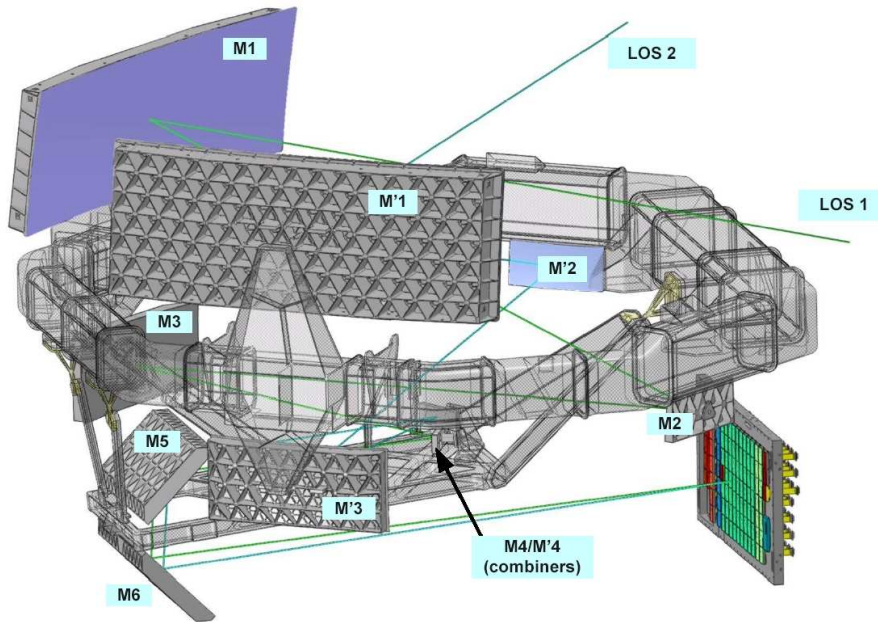


Schematic of the adopted design for the Gaia payload. Left: Two telescope system sharing the same focal plane; right: detail illustrating the radial velocity and photometry functions. Images courtesy of EADS Astrium.

The spacecraft and payload configuration was re-optimised by the industrial teams in their Phase B2/C/D proposal in response to the mission requirements document issued by the ESA project team in 2005. As a result, from early 2006, the final Gaia payload looks somewhat different from the previous design, although all functionality is preserved. The previous design had two separate telescopes, with one comprising the two astrometric viewing directions with a combined focal plane with broad-band photometric filters; the other comprising the medium-band photometry and radial velocity spectrometer. The 'new' Gaia payload combines all functions into a single telescope structure. The photometric measurement concept has also been substantially revised: in place of a series of broad- and medium-band filters, two dispersive prisms now provide full spectral coverage over the entire optical wavelength. The new (post-2006) payload concept is now characterised as follows:

- a dual telescope, with a common structure and common focal plane. Each telescope is based on a three-mirror anastigmatic design with three flat-folding mirrors, the two viewing directions separated by a 106.5 degrees basic angle. Beam combination is achieved in image space with a small beam combiner rather than in object space (saving mass, simplifying accommodation, and eliminating the directional ambiguity of the star transits). The primary mirrors are of dimension  $1.45 \times 0.5 \text{ m}^2$ , the telescope focal length is 35 m, and the astrometric field of view is  $0.7^\circ$  (along scan) by  $0.7^\circ$  (across scan);
- the use of silicon-carbide ultra-stable material for the mirrors and telescope structure, providing low mass, isotropy, thermo-elastic stability, and stability in moving from ground to space. Basic angle stability requirements are largely met with passive thermal control, and a highly robust basic angle measurement system is in place to measure any variations down to  $0.5 \mu\text{as}$  per 5-minute interval;
- the radial velocity spectrometer is an integral field spectrograph with a resolving power of 11 500. It uses a grating plate and an afocal field-corrector lens located close to the focal plane;
- the common focal plane is shared by all instruments, with the astrometric and photometric fields all having the same angular scale. Object detection is carried out using two strips of sky-mapper CCDs, with one pass of object detection applying to all three instruments;
- the same type of CCD (pixel size and format) is used for all three instruments. A total of just over 100 CCDs and accompanying video chains are used, with a pixel size of  $10 \mu\text{m}$  along scan and  $30 \mu\text{m}$  across scan, TDI (time-delayed integration) mode operation, and an integration time of  $\sim 4.4 \text{ s}$  per CCD.

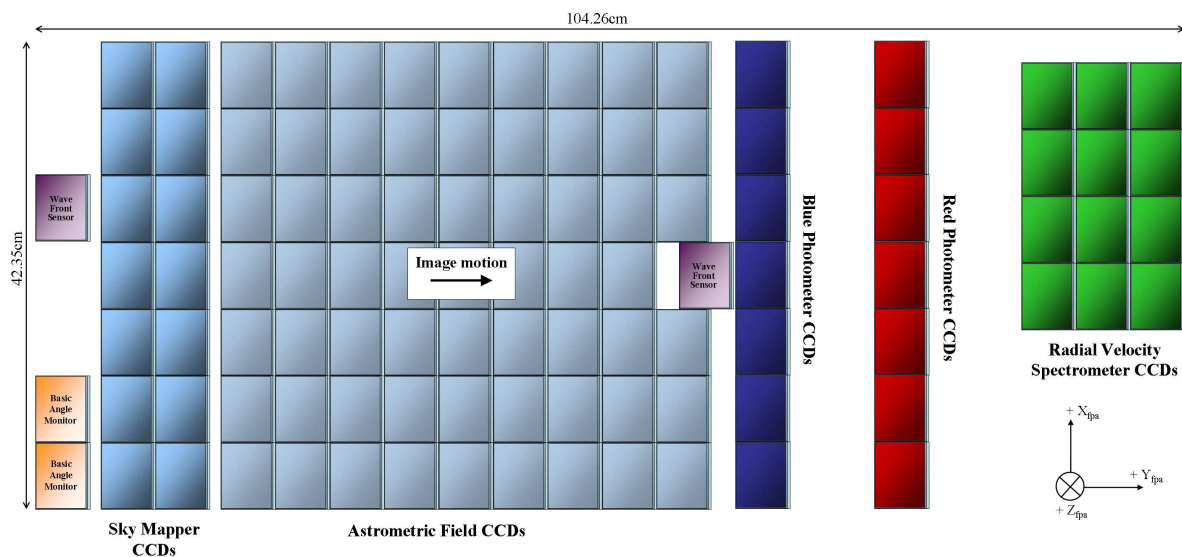
These primary instruments are supported by the opto-mechanical-thermal assembly comprising: (i) the single structural torus supporting all mirrors and focal planes; (ii) a deployable sunshield to avoid direct Sun illumination and rotating shadows on the payload module, combined with the solar array assembly; (iii) control of the heat injection from the service module into the payload module, and control of the focal plane assembly power dissipation in order to provide an ultra-stable internal thermal environment; (iv) an alignment mechanism on the secondary mirror for each astrometric instrument, with micron-level positional accuracy to correct for telescope aberration and mirror misalignment at the beginning of life.



The optical path of both telescopes is composed of six reflectors (M1–M6), two of which are common (M5–M6). The entrance pupil of each telescope is  $1.45 \text{ m} \times 0.5 \text{ m}^2$  and the focal length is 35 m. The payload module features a common focal plane shared by both telescopes. Figure courtesy of EADS-Astrium.

A number of important properties of the Gaia payload are reflected in the adopted optical design:

- (a) The optical configuration reflects a six-mirror anastigmatic design. The two telescopes have rectangular entrance pupils ( $1.45 \times 0.5 \text{ m}^2$ ) and large focal lengths (35 m). A CCD pixel size of  $10 \mu\text{m}$  in the along-scan direction has been selected. With the 35 m focal length, corresponding to a plate scale of  $170 \mu\text{m arcsec}^{-1}$ , this allows a 6-pixel sampling of the diffraction image along scan.
- (b) To ensure the thermal and mechanical stability of the payload, the mirrors – like the optical bench (torus) on which they are mounted – are made of Silicon-Carbide (SiC).
- (c) The optical system is compact, with an optical-bench diameter of about 3 m, and is housed within a mechanical structure adapted to the Soyuz-Fregat launcher fairing.
- (d) The field of view of both telescopes is unvignetted and covers  $0.45 \text{ deg}^2$  per telescope. The across-scan height of  $0.7^\circ$  is sufficient to avoid gaps in the sky coverage resulting from the slow yet continuous precession of the spin axis.
- (e) The optical design allows high-quality imaging, both in terms of wave-front errors (WFEs) and (optical) distortion. The total, effective RMS WFE over the astrometric field of view, including optical design, manufacturing and integration, alignment, and cool-down, is  $\sim 50 \text{ nm}$ . The total, effective RMS distortion over the astrometric field of view, including payload optical design, manufacturing and integration, and in-orbit WFE compensation, is  $1.8 \mu\text{m}$  (0.18 pixel) over a single CCD transit. The latter value is acceptable in terms of causing only limited along-scan blurring of star images during a CCD crossing.
- (f) Although the optical design is fully reflective, based on mirrors only, diffraction effects with residual aberrations induce systematic chromatic shifts of the diffraction images and thus of the measured star positions. This effect, usually neglected in optical systems, was relevant for Hipparcos and is also critical for Gaia. The overall system design is such that these systematic chromatic displacements, which can amount to  $500 \mu\text{as}$  or more, will need to be calibrated as part of the on-ground data analysis using the colour information provided by the photometry on each observed object.

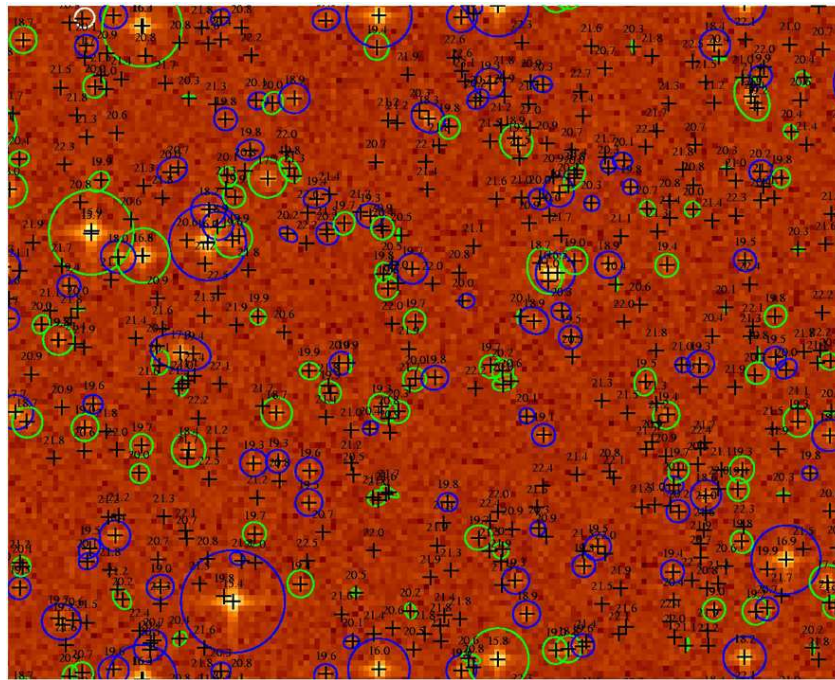


The Gaia focal plane. The viewing directions of both telescopes are superimposed on this common focal plane which features 7 CCD rows, 17 CCD strips, and 106 large-format CCDs, each with 4500 TDI lines, 1966 pixel columns, and pixels of size  $10 \mu\text{m}$  along scan  $\times$   $30 \mu\text{m}$  across scan ( $59 \text{ mas} \times 177 \text{ mas}$ ). Star images cross the focal plane in the direction indicated by the arrow. Figure courtesy of ESA - A. Short.

Given the concept of Gaia as a scanning instrument, the payload focal plane assembly (FPA) is designed around a mosaic of CCD chips operating in TDI (time-delayed integration) mode. During nominal operations, the satellite spin rate, and thus the speed with which objects traverse the focal plane, is continuously synchronised with the fixed TDI period of the CCDs. As a result, stars cross the focal plane at a constant speed ( $60 \text{ arcsec s}^{-1}$ ) and star images are progressively built up as objects cross the CCDs. At the end of each CCD crossing, the generated charge packets are transferred to the serial register for read out and, subsequently, digital processing, temporary on-board storage, and transmission to the ground.

The detailed design of the focal plane is the result of many, often competing, requirements. For example, the FPA-mosaic dimension has been selected large enough to offer a large field of view, and thus a sufficiently large observing time for each object to meet the end-of-mission scientific performance requirements, while keeping the total number of CCDs manageable in the light of manufacturing, testing, integration, power requirements, thermal-stability characteristics, launch schedule, cost, etc. Similarly, the chosen (along-scan) CCD pixel size is small enough to offer sufficient spatial resolution to allow extraction of the centroid position of diffraction images with adequate precision, yet large enough to be feasible with currently available CCD technology in terms of quantum efficiency, modulation-transfer function, noise characteristics at the required read-out rates, manufacturing yield, etc. The number of TDI lines per CCD has been chosen large enough to yield sufficient signal-to-noise for faint stars at the CCD-transit level, yet small enough to avoid performance degradation due to ‘image smearing’ caused by attitude disturbances, scanning-law effects, distortion, radiation-damage driven charge trapping, etc.

The focal-plane assembly is common to both telescopes. It serves five main functions: (i) the wave-front sensor (WFS) and basic-angle monitor (BAM); (ii) the Sky Mapper (SM), autonomously detecting objects entering the fields of view and communicating details of the star transits to the subsequent CCDs; (iii) the main Astrometric Field (AF), devoted to astrometric measurements; (iv) the Blue and Red Photometers (BP and RP), providing low resolution spectrophotometric measurements for each object over the wavelength ranges 330–680 and 640–1000 nm, respectively; and (v) the Radial-Velocity Spectrograph (RVS), registering spectra of all objects brighter than about 17-th magnitude.



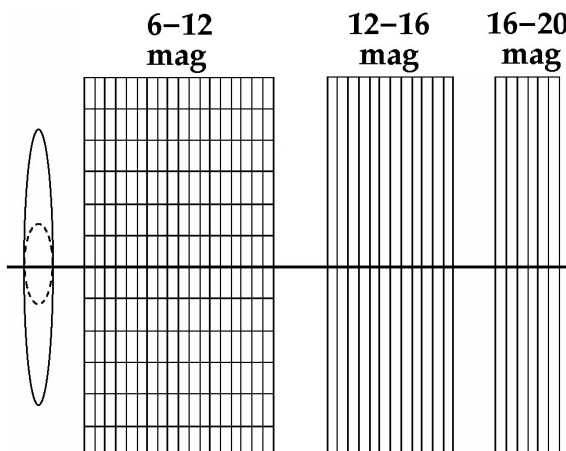
Simulation, based on HST data, of Baade's Window observed by Gaia's Sky Mapper (SM). A sky-mapper sample is composed of  $2 \times 2$  binned pixels. Black crosses indicate all stars up to magnitude 23. Detections are shown with blue and green ellipses, corresponding to objects classified as single and multiple stars, respectively.

Gaia's main goal is to provide an astrometric catalogue of objects complete down to magnitude 20. Since similar catalogues in the Gaia photometric passband and with the Gaia spatial resolution do not exist, Gaia, unlike Hipparcos, cannot operate based on the principle of a pre-compiled input catalogue. Autonomous on-board object detection is thus compulsory, with two associated advantages: (i) on-board detection also allows 'special objects' such as supernovae and near-Earth objects to be naturally detected and observed; (ii) on-board detection allows object selection and object windowing, thus significantly limiting both the number of CCD pixels that have to be read, hence improving CCD noise performances, and the amount of data that have to be transmitted to ground.

The detection algorithm has an impact on the Gaia scientific return: the number and nature of the sources observed and the completeness of the Gaia Catalogue – and any selection biases – will depend on the detailed characteristics of the detection algorithm. Developing a suitable detection algorithm is subject to many trade-offs between scientific requirements (reliable discrimination between stars, double stars, extended non-stellar objects, blended stars, saturated stars, and prompt-particle events such as cosmic rays or solar protons; functional over the magnitude range 6–20; stable under the peculiarities of the real sky, etc.) and operational constraints (operation compliant with real-time constraints; on-board processing architecture; and on-board processing power; robust coupling with AOCS, etc.).

In early studies, several demonstration algorithms have been developed, initially detecting point sources only but subsequently elaborated to cope with extended sources. The latter prototype algorithm, which is based on a thresholding philosophy, features accurate centroiding, accounts for saturated stars, does not generate false detections on stellar diffraction spikes, and is capable of detecting close double stars, thus allowing window patches to be correctly assigned to cover both components. In a field of average stellar density, a 99% detection completeness for single stars is obtained at magnitude 20, with less than one false detection per million samples. Baade's Window is the challenging archetype of a large-scale high-density field which has to be managed in real time. The figure shows a  $13 \times 32$  arcsec $^2$  image simulated with the GIBIS Gaia Simulator (developed by Carine Babusiaux and colleagues) based on a list of stars extracted from a high-resolution HST image. A detection rate of 86% at magnitude 20 without false detections is achieved; the incompleteness is mainly due to faint companions close to bright(er) primaries.

Current developments for the actual flight implementation are focused on providing a mixed hardware/software solution. This has already led to the design of original methods devoted to connected-component searches, deblending schemes for overlapping components, and real-time estimation of sky background.



Samples are read from each CCD inside a ‘window’ centred on each star detected and selected at the beginning of a field transit. The default astrometric field windows are shown here. The dashed ellipse shows the ‘Airy diffraction disc’ of a single star; the solid ellipse shows the maximum smearing of the ‘Airy ellipse’ in the across-scan direction, integrated over a single CCD transit, resulting from the precession of the spin axis.

The function of the Sky Mapper (SM) CCDs is to autonomously detect all objects brighter than 20-th magnitude in the Gaia photometric passband (G). After SM, stars traverse the main Astrometric Field (AF), which is composed of 9 CCD strips (AF1–AF9), the Blue and Red Photometers (BP and RP), and the Radial-Velocity Spectrograph (RVS).

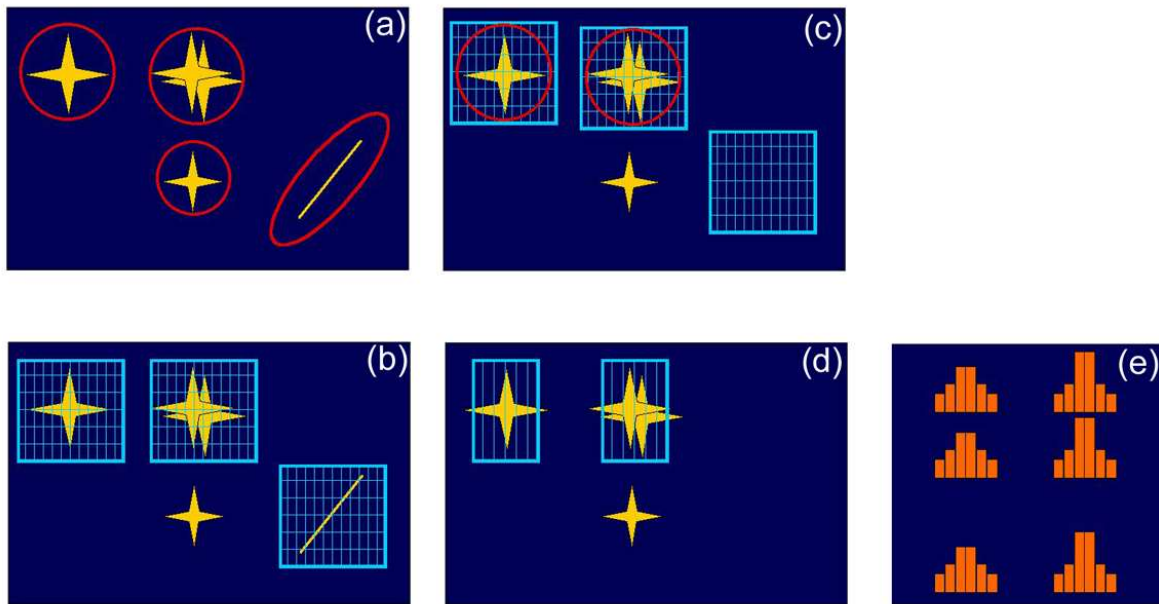
The concept of on-board detection of objects allows the active application of ‘windows’ to them, thereby significantly limiting both the number of CCD pixels that has to be read, hence improving CCD noise performances, and the amount of data that has to be transmitted to ground. The sample and window sizes for the different CCD strips and magnitude intervals have been chosen to give optimal astrometric, photometric, and spectroscopic results for all stars, taking into account the resolution of the star images, the smearing of these images in the across-scan direction due to the continuous precession of the spin axis, the scientific interest in double stars, and the (variable) sky background.

In order to optimise the signal-to-noise ratio of the measurements, pixels that are read from the CCDs are generally binned on-chip in the across-scan direction to form samples. Normally, no on-chip (hardware) binning takes place in the along-scan direction, thus preserving the full angular resolution of the images in this fundamental direction. The collection of samples related to an individual star is referred to as a ‘window’. Normally, samples are transmitted to the ground as they are read, although numerical (software) binning of read samples is applied in some cases before transmission to the ground in order to reduce telemetry.

The default AF windows are shown above. For stars with  $G = 12\text{--}20$  mag, read samples consist of  $1 \times 12$  pixels; the sample size across scan (12 pixels) is sufficiently large to contain nearly all star light. AF windows typically contain 12 of these samples for  $G = 12\text{--}16$  mag and 6 samples for  $G = 16\text{--}20$  mag. In AF2, AF5 and AF8, windows are currently projected to cover 12 samples, allowing the *a posteriori* on-ground measurement of the local sky background and the mapping of the surroundings of each star out to a few arcsec down to  $G \sim 23$  mag. In AF1, read samples are composed of  $1 \times 2$  pixels; this across-scan resolution is essential for the AOCS feedback loop and for speed measurements of solar-system objects.

It is currently foreseen to avoid saturated pixels and samples for bright stars ( $G = 6\text{--}12$  mag) by limiting the CCD integration time for these objects by the use of TDI gates and by sampling the images of these objects with single-pixel-resolution windows (see figure). These windows are also planned to be used for the calibration of the PSF and of CTI effects as function of star colour, time, and position in the focal plane.

Dedicated sampling and windowing schemes similarly exist for BP, RP, and RVS, aimed at optimally covering the spectra and, at the same time, allowing the on-ground determination and subtraction of the sky background.



The on-board data handling consists of a sequence of operations starting with (a) object detection, (b) first selection, (c) actual observation in the next CCD strip and confirmation, (d) final selection, (e) observation in the following CCD strips, post-processing with packetisation, and compression for subsequent downloading.

Since Gaia will perform a continuous all-sky survey at high angular resolution, the on-board processing, which must operate autonomously, needs to be able to cope with virtually all the varieties and peculiarities of the real sky, both in terms of the nature of objects (bright stars, multiple stars, nebulosities, solar-system objects, planets, etc.) and object densities (Galactic pole, Baade's Window, cores of globular clusters, etc.). Generic and adaptive algorithms are therefore required.

Given real-time processing constraints, limits on the acceptable CCD read-out noise, and the limited telemetry bandwidth, not all CCD pixel data can be read and subsequently transmitted to the ground. A limited number of 'windows', regions of interest around target objects, are therefore observed in the focal plane, thus effectively removing the 'empty space between the stars' from the data stream. The object detection and confirmation tasks, aimed at distinguishing real objects from prompt-particle events such as cosmic rays and solar protons, thus have to be accompanied by a selection step which decides which sources are tracked in the remaining CCDs and how these objects are observed.

From a scientific point of view, a statistical analysis of the final Gaia Catalogue, and especially of selection effects, requires that the on-board selection process is entirely and exactly reproducible on the ground. For this reason, some detection parameters will need to be downloaded for objects which are detected and confirmed but not observed because of selection criteria.

In general, the on-board data handling should allow the observation of the maximum number of objects in the best possible conditions. Multiple stars in particular pose a challenge in this respect, given the limited number of windows available. Similarly, optimum window placement in dense fields is non-trivial given the fact that the computing requirements should remain modest.

A Payload Data Handling Electronics demonstration study under an industrial contract has been conducted. This was aimed at designing a possible overall implementation architecture, and developing and integrating a representative breadboard, taking constraints in terms of scientific requirements and mass, volume, and power budgets into account. Based on this study, the current implementation architecture distributes the on-board processing between dedicated hardware (field programmable gate arrays) for 'pixel-based operations' and software for 'floating-point operations'.



Pictured above is part of the team from the e2v wafer fabrication area that produced the initial batch of Gaia demonstrator CCDs. Inset: Two CCD91-72 CCDs on a silicon wafer. Each CCD comprises  $4500 \times 1966$  pixels, each  $10 \times 30 \mu\text{m}^2$  in size. Test structures are visible on either side of the CCDs. Images courtesy of e2v technologies.

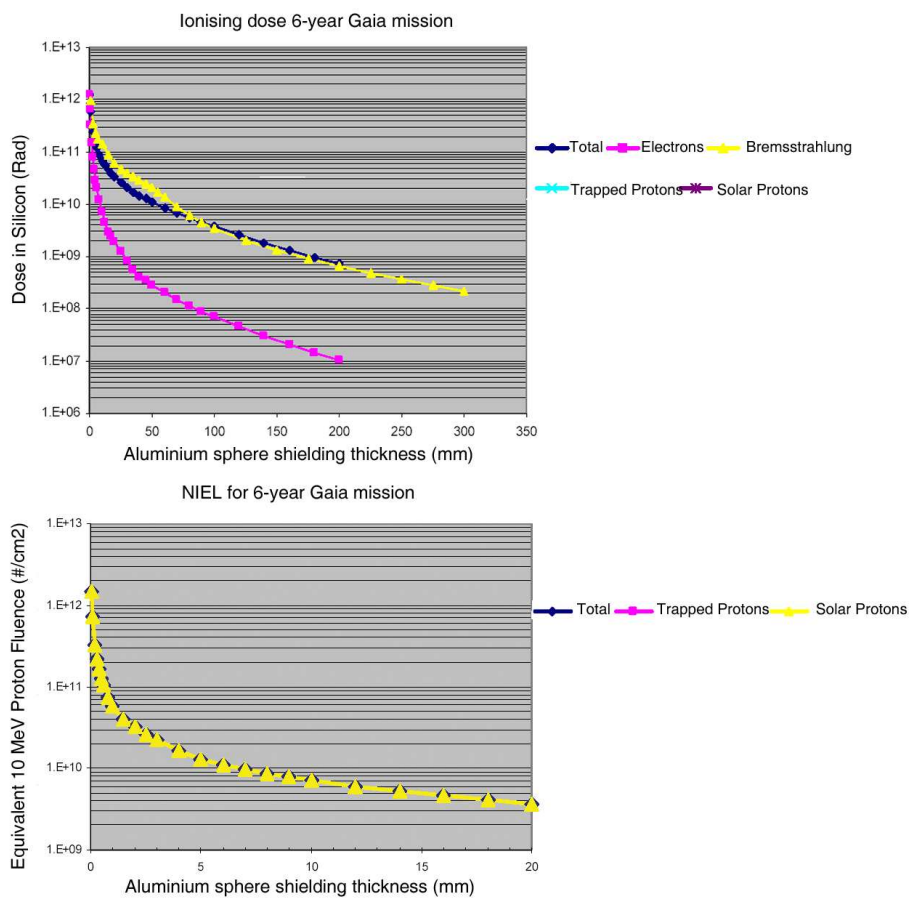
Charge-Coupled-Device (CCD) detectors form the core of the Gaia payload. Their development and manufacture represents one of the key challenges for the programme. The design of the Gaia CCDs has been tailored to the needs of the mission. Compared with contemporary scientific space missions, Gaia's CCDs will need to be produced in unprecedented numbers. In order to meet this challenge, Gaia has enlisted the services of e2v technologies, the world's leading scientific CCD manufacturer.

Gaia features a focal-plane assembly of nearly  $0.4 \text{ m}^2$ . This FPA will be populated with 106 back-illuminated devices, each with an active area of  $45 \times 59 \text{ mm}^2$  corresponding to 4500 TDI lines and 1966 pixel columns. All CCDs will be operated in time-delayed integration (TDI) mode with a TDI period  $982.8 \mu\text{s}$ . Stars will thus cross a CCD in 4.4s. All CCDs will be individually packaged and each CCD will be driven by a dedicated proximity electronics module mounted below it and connected to it via a thermally isolating flex circuit.

All of the Gaia CCDs are large area, back-illuminated, full frame devices. They all have a 4-phase electrode structure in the image section and a 2-phase structure in the readout register, leading to a single, high-performance, two-stage, buffered output node. A noise performance better than 10 electrons RMS is expected. The CCDs will be operated at  $-115^\circ\text{C}$ , selected to minimise dark current and charge-trapping effects.

Gaia will observe objects over a very wide range of apparent magnitude and the CCDs must therefore be capable of handling a wide dynamic signal range. In order to observe all objects as efficiently as possible, the CCD quantum efficiency has been optimized, while keeping acceptable modulation-transfer-function performance. A number of features have been incorporated in the CCD design in order to cope with bright stars. These include a large full-well capacity ( $> 190,000$  electrons), an anti-blooming drain, and 12 TDI gates which effectively reduce the integration time for bright objects. The CCDs also feature a summing well, a supplementary buried channel, and a charge-injection structure.

The pixel size of the CCDs has been specified in order to correctly sample the point spread functions of the astrometric instrument in the along- and across-scan directions. The resulting pixel dimensions are  $10 \times 30 \mu\text{m}^2$ . Whilst the QE of the main-field astrometric CCDs has been chosen to give good overall response in the centre of the band, the photometric and spectroscopic CCDs require a response biased towards the red or blue ends of the band. This is achieved in part by selecting appropriate surface passivation processes and anti-reflection coatings. However, for the red-enhanced CCDs, it is also necessary to fabricate thicker devices on high-resistivity silicon.



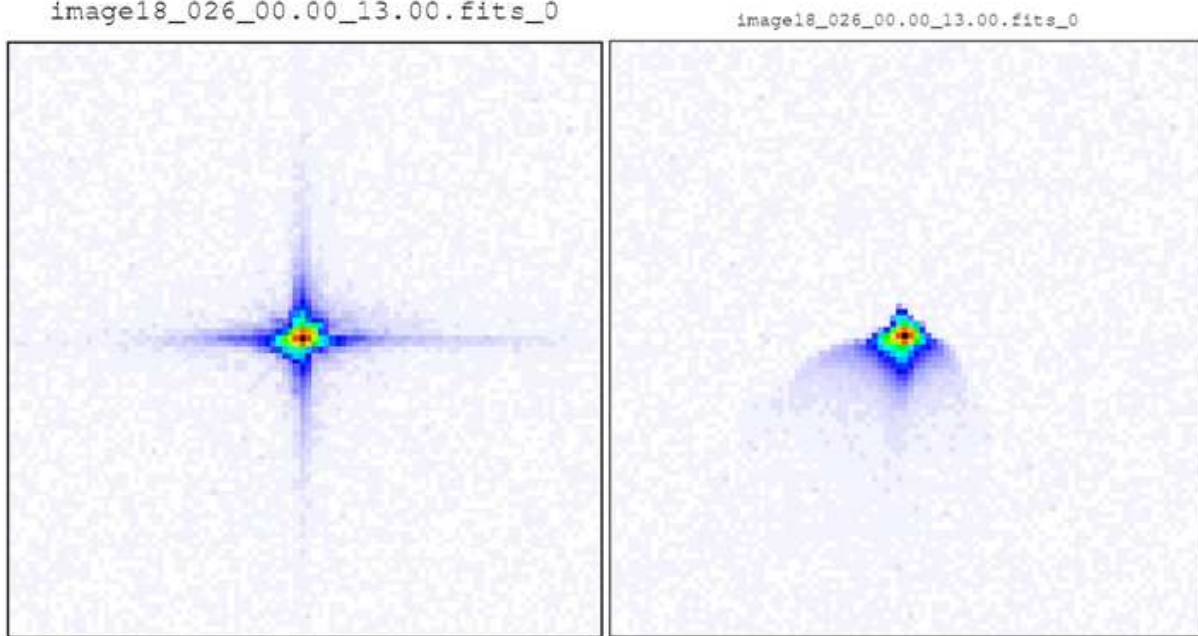
The radiation environment at L2 is an important factor in optimising Gaia's CCD operations. These figures show the ionising dose (above) and non-ionising energy loss (below) as a function of spherical shielding thickness for a 6-year (extended) Gaia mission at L2. Images courtesy H. Evans.

The Gaia satellite will continuously spin around its axis, causing the field of views of both telescopes to scan across all objects located along the great circle which is perpendicular to the spin axis. Data is continuously read as the telescopes sweep out these great circles on the sky. For this reason, the CCDs will operate in time-delayed integration (TDI) mode. This means that the CCD electrodes are clocked at the same speed as the image scans along the focal plane. Since the integration time for each TDI-line transfer is  $982.8 \mu\text{s}$ , images cross the 4500 TDI lines of a CCD in the focal plane in 4.4 s. The along-scan dimensions of the four phases of a single CCD pixel are 2, 3, 2, and  $3 \mu\text{m}$ , respectively. The  $982.8\text{-}\mu\text{s}$  TDI period is therefore sub-divided between the four phases as 196.6, 294.8, 196.6, and  $294.8 \mu\text{s}$ , respectively, to give the closest possible match between the motion of the incoming optical image and the motion of the integrating measured (electronic) image.

The CCD output node has a high-performance, two-stage, buffered design. At typical Gaia frequencies, the CCD is quite capable of a noise performance better than 5 electrons RMS. This performance is expected to be degraded by the electronics bandwidth and increased capacitance due to inverted mounting (required for back illumination). However, a noise performance better than 10 electrons RMS is still expected.

Another important operational consideration is the radiation environment in which the CCDs will operate. At the L2 Lagrange point, this environment is essentially an interplanetary environment dominated by solar-flare protons. Due to the size of the focal plane, it is only possible to incorporate minimal shielding for the astrometric CCDs. Whilst this will be sufficient to reduce the total ionising radiation dose (TID) to about 5 krad, the non-ionising (displacement-damage) dose (NIEL) is expected to be high ( $\sim 4.0 \times 10^9$  protons 10 MeV equivalence).

In order to reduce the effects of radiation damage, the CCDs have a supplementary buried channel (SBC) which reduces the interaction cross section between electrons and traps. The CCDs will be operated at  $-115^\circ\text{C}$ , which causes the maximum number of traps to remain full, and therefore inactive. The CCDs also feature a charge-injection structure to periodically re-fill the traps for the same reason.



Output from the Gaia CCD model showing the effects of radiation damage. Left: Image of a 13-th mag G2V star before radiation damage. Right: Image of the same star after a  $10^{10}$  proton (10 MeV equivalent) displacement damage dose.

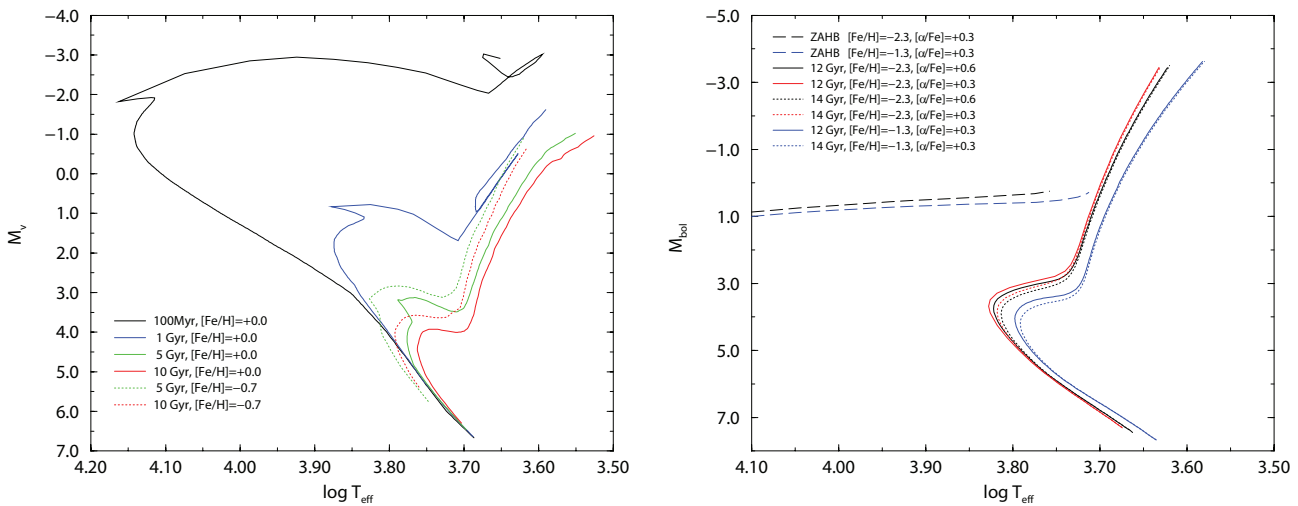
In order to better predict Gaia's performance, a number of (Monte–Carlo) simulation tools have been developed. One of these covers the detailed behaviour of the Gaia CCDs. This tool is being used to assess the centroiding accuracy of the real instrument in TDI mode, the impact of particle background events on centroiding accuracy, and the effects of degradation due to radiation damage during the course of the mission. A sufficiently detailed model enables predictions of Gaia performance and capability on the basis of CCD performance parameters and characteristics, which have been measured in the laboratory. It also serves as a tool for generating large quantities of simulated data with which to exercise the Gaia data processing chain.

From the outset, the model is tailored to Gaia-specific CCD operation (TDI mode, back illumination, anti-blooming structure, etc.) The aim is to satisfactorily handle all characteristics of the CCDs that are going to change during the course of the mission due to ionising and non-ionising radiation damage. This requires a dynamic treatment of electron trapping and de-trapping, charge injection, beneficial charge packets, the supplementary buried channel, and so on. Modelling CCDs like this in a meaningful, physical way is rather challenging.

The model implementation comprises two arrays, 4500 pixels (lines) long by 1966 pixels (columns) wide. The first array represents the immobile CCD, containing traps and trapped electrons. The second array represents the 'conveyor-belt' of mobile electron packets. Each model cycle corresponds to a CCD line transfer (982.8  $\mu$ s). During this period, the model carries out three steps:

1. Generate mobile electrons due to signal (e.g. PSF photons) and noise (e.g. protons or stray light). This step encompasses not only the interactions of photons and particles within the CCD, but also the spreading of resultant electron clouds due to charge diffusion and mapping to pixels.
2. Transfer electrons between the mobile and trapped arrays according to trap occupancy, time constants, etc. This step is sub-divided into four parts corresponding to the four electrode phases of the CCD.
3. Translate the mobile charge by one pixel along scan and read out one TDI line in the serial register with appropriate binning, noise, etc.

The characteristics of the model are currently being checked and verified against laboratory data. This will lead to adjustment of parameters, and possibly more fundamental refinements in some areas, until sufficient confidence in the model has been established.



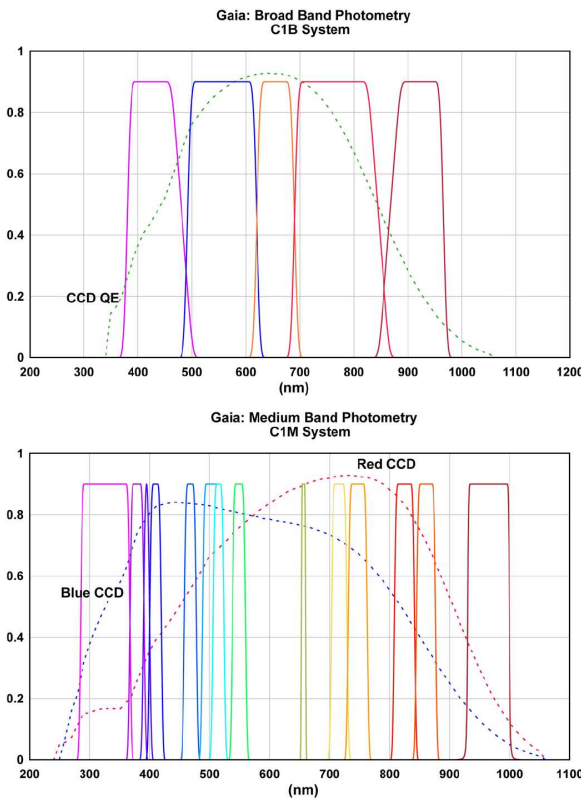
Gaia photometry will allow chemical-abundance and age determination of the Galactic stellar populations over the entire Hertzsprung–Russell diagram. Left: isochrones of 0.1, 1, 5, and 10 Gyr covering the thin disc and the bulge. Right: isochrones of 12 and 14 Gyr and zero-age-horizontal-branch loci for several  $[Fe/H]$  and  $[\alpha/Fe]$  abundances suitable for the halo and the thick disc.

If Gaia's astrometric measurements would be unsupported by appropriate diagnostic data, the final Catalogue would contain immense numbers of positions and velocities of objects whose astrophysical nature would otherwise be unknown. With such limited data, the key objective of the mission – the study of the structure and history of the Milky Way – could not be met. Therefore, Gaia has therefore been equipped with a photometric instrument with the goal of measuring the spectral energy distributions of all objects. From these measurements, astrophysical quantities such as luminosity, effective temperature, mass, age, and chemical composition can be derived.

In order to meet the astrometric performance requirements, the measured centroid positions must be corrected for systematic chromatic shifts induced by the optical system. This is only possible with the knowledge of the spectral energy distribution of each observed target in the wavelength range covered by the CCDs of the main astrometric field ( $\sim 330\text{--}1000\text{ nm}$ ). The photometric instrument also covers this requirement.

Photometric measurements are indispensable in providing the basic tools for classifying stars across the entire Hertzsprung–Russell diagram, as well as in identifying specific and peculiar objects. To achieve this, it is necessary to observe a broad spectral domain, extending from the ultraviolet to the infrared. Gaia's photometric measurements must be able to determine, among others, (i) effective temperatures and reddenings for early-type stars, which serve both as effective tracers of Galactic spiral arms and as reddening probes; (ii) effective temperatures and abundances for late-type stars; and (iii) luminosities for stars with large relative parallax errors. Moreover, in order to be able to reconstruct the Galactic formation history, the distribution function of stellar abundances must be determined to  $\sim 0.2$  dex, while effective temperatures must be obtained to  $\sim 5\%$ . These accuracies allow separation of stars belonging to the various stellar populations in the Galaxy (i.e. thin disc, thick disc, and halo). The determination of abundances of Fe and  $\alpha$ -elements is essential for mapping Galactic chemical evolution. Photometric measurements will be performed for every target transiting the focal plane. Hence, astrophysical information will not be limited to stars but will also be available for quasars, solar-system objects, and many other celestial bodies.

A broad-band magnitude, and its time dependence, can be obtained from the analysis and rigorous calibration of the primary mission data (i.e. by determination of the ‘amplitudes’ of star images in the main astrometric field). Combined with parallaxes and with estimates for interstellar absorption, these so-called G-band magnitudes give a measure of the absolute magnitude. Gaia will provide reliable absolute magnitudes for several hundred million stars.



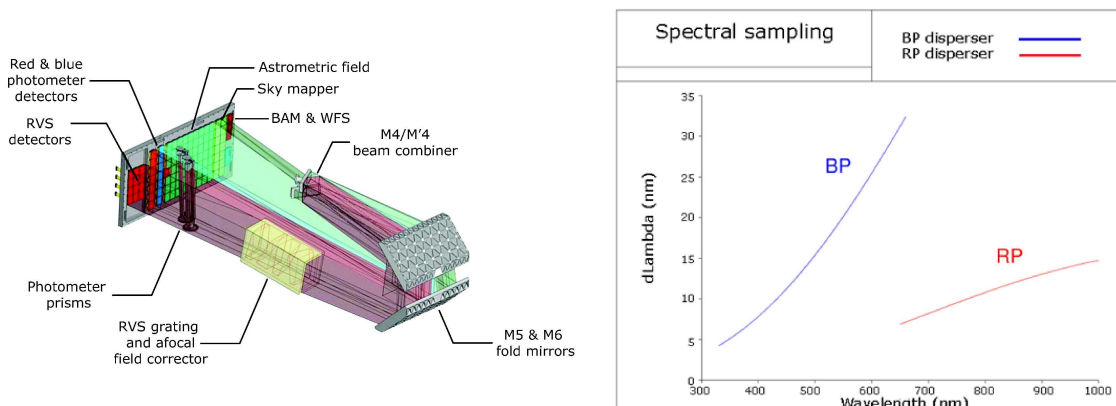
The originally proposed broad-band (top) and medium-band (bottom) photometry filters for Gaia. The dashed line corresponds to the response curve of the CCDs. The design of Gaia's photometric instrument has since been changed from interference filters to dispersive prisms. Photometric data are thus no longer limited to a finite number of bands but consist of low-resolution spectra covering the interval  $\sim 330\text{-}1000\text{ nm}$ .

Many ground-based photometric systems exist but none satisfies all the requirements of a space-based mission such as Gaia. Portions of the optical/near-infrared spectrum blocked by atmospheric O<sub>3</sub> and H<sub>2</sub>O bands, and therefore not covered in ground-based systems, are observable with Gaia. Classical photometric systems have often been designed for specific spectral-type intervals or objects, while Gaia must cover the entire Hertzsprung-Russell diagram, quasar and galaxy photometry, solar-system object classification, and many more diverse objects. In addition, Gaia allows the extension of stellar photometry to yet-unexplored Galactic areas where classical classification schemes lose validity because of systematic variations in element abundances in stellar atmospheres and interstellar matter.

Considerable effort has therefore been devoted to the selection of an optimum photometric system for Gaia. In optimising the design of this system, the Photometry Working Group defined a set of scientific targets - single stars belonging to the Galactic halo, the thin and thick disc and the bulge - for which the photometric system should be optimised. These targets were selected so as to ensure that the scientific goals of the Gaia mission are met. In general terms, the selected photometric system should allow for the precise determination of the astrophysical parameters (e.g. T<sub>eff</sub>, log g, [M/H] and A<sub>v</sub>) of stars from all Galactic populations.

In December 2004, the Photometry Working Group recommended the implementation of a 19-band baseline photometric system based on interference filters, referred to as the C1B system with 5 broad bands covering the spectral region  $\sim 380\text{-}1000\text{ nm}$  and the C1M systems with 14 medium bands covering the range  $\sim 300\text{-}1000\text{ nm}$  (see figure). This recommendation, however, was made under the explicit assumption of a specific payload design featuring two telescopes (Astro and Spectro) with different spatial resolutions and two photometric instruments (BBP and MBP) with different main aims, fields of view, focal-plane layouts, observing times, etc.

With the selection of EADS Astrium as Gaia prime contractor, the design of the scientific payload has been optimised further. Gaia's photometric instrument is now based on a dispersive-prism approach such that starlight is not focused in a PSF-like image and observed through an interference filter, but dispersed along the scan direction in a low-resolution spectrum. These spectra cover the wavelength range  $\sim 330\text{-}1000\text{ nm}$ . This approach provides optimum flexibility since it not only allows to reconstruct, *a posteriori*, the 19 photometric bands of the C1B and C1M systems but also arbitrary new bands, including ones 'intermediate' to those originally foreseen. For further details see the information sheet on the *Photometric Instrument*.



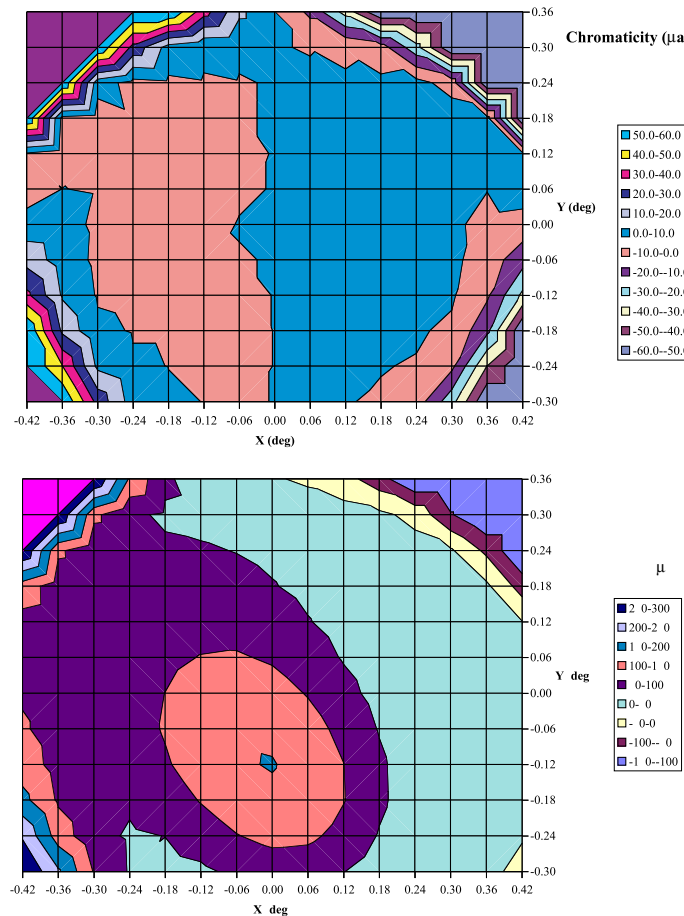
Left: Schematic view of the photometric instrument and the Gaia focal plane. Right: BP and RP dispersion properties (see text). Figures courtesy of EADS Astrium.

The primary aim of the photometric instrument is to measure the spectral energy distribution of all observed objects. This measurement is mission critical in two respects: it serves (i) to correct the measured centroid positions in the main astrometric field for systematic chromatic shifts, and (ii) to determine astrophysical characteristics, such as effective temperature, mass, age, and chemical composition, for all stars.

Gaia's photometric instrument is based on a dispersive-prism approach such that starlight is not focused in a PSF-like spot but dispersed along the scan direction in a low-resolution spectrum. The instrument consists of two low-resolution fused-silica prisms dispersing all the light entering the field of view. One disperser – called BP for Blue Photometer – operates in the wavelength range 330–680 nm; the other – called RP for Red Photometer – covers the wavelength range 640–1000 nm. Both prisms have appropriate broad-band filters for blocking unwanted light. The photometric instrument is integrated with the astrometric and spectroscopic instruments and telescopes; the photometric CCDs are located in the Gaia focal plane. As a result, light and objects coming from the two viewing directions of the two telescopes are superimposed on the photometric CCDs. The prisms are located between the last telescope mirror (M6) and the focal plane, close to the latter, and are physically supported by the CCD radiator (see the figure above).

Two CCD strips are dedicated to photometry, one for BP and one for RP. Both strips cover the full astrometric field of view in the across-scan direction. Since BP and RP use the (astrometric) Sky Mapper (SM) function for object detection and confirmation, all objects selected for observation in the astrometric field will also be selected for observation in BP and RP. All BP and RP CCDs are operated in TDI (time-delayed integration) mode. The CCDs have 4500 TDI lines and 1966 pixel columns ( $10 \times 30 \mu\text{m}^2$  pixels). Anti-reflection coatings and device thicknesses, and thus quantum efficiencies, are optimised separately for BP and RP.

The spectral resolution is a function of wavelength as a result of the natural dispersion curve of fused silica; the dispersion is higher at short wavelengths, and ranges from 4 to 32 nm/pixel for BP and from 7 to 15 nm/pixel for RP (see figure). The variation across-scan does not exceed  $\pm 9\%$  for BP and  $\pm 4\%$  for RP. The BP and RP dispersers have been designed in such a way that BP and RP spectra have similar sizes (on the order of 45 pixels along scan). BP and RP spectra will be binned on-chip in the across-scan direction; no along-scan binning is used. For bright stars, single-pixel-resolution windows are allocated, in combination with TDI gates. RP and BP will be able to reach object densities on the sky of at least 750,000 objects  $\text{deg}^{-2}$ . Window extensions meant to measure the sky background have been implemented.



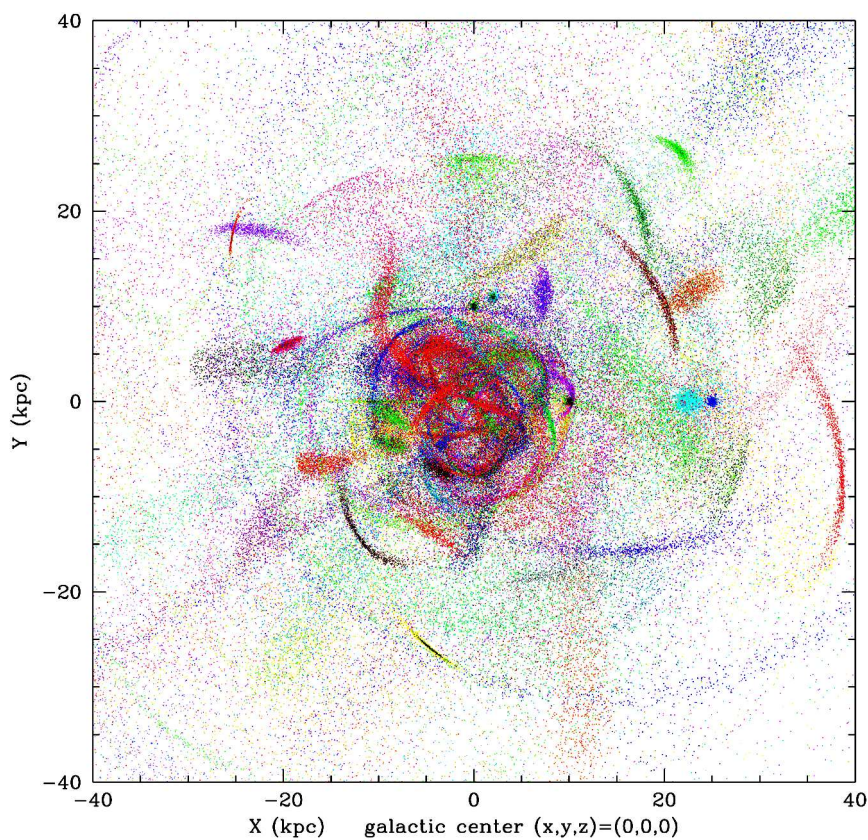
Above: Chromaticity map for the nominal system of an early Gaia telescope design.

Below: Chromaticity map when all sources of wave-front errors are included.

Although the Gaia optical design only employs mirrors, diffraction effects with residual (achromatic) aberrations induce a small chromatic shift of the diffraction peak. This effect is usually neglected in optical systems, but was relevant for Hipparcos and becomes even more critical for Gaia. The chromatic image displacement depends on position in the field, and on the star's spectral energy distribution, but not on its magnitude. The overall system design must either reduce these chromatic displacements to levels below those relevant for the final mission accuracies - which proved to be impossible for Gaia's selected flight design - or ensure that they can be calibrated as part of the data analysis. One purpose of the photometric instrument is to provide colour information on each observed object in the astrometric field to enable the chromaticity bias calibration on ground.

For a rough quantitative assessment of the effect of chromaticity, a chromaticity measure can be defined which corresponds to the relative displacement (in  $\mu\text{as}$ ) of the diffraction peak between two stars of extreme spectral types (say B3V and M8V). This measure can be calculated by means of a simple formula for any WFE (wave-front error) map. WFE maps for different points in the field of view can thus be transformed into a 'chromaticity map' showing the variation of the effect across the field of view for a given set of alignment and polishing errors.

A chromaticity map for the nominal system of an early Gaia telescope design is given in the top figure above. In the field of view, where the RMS optical-design WFE is assumed to be  $\lambda/30$ , chromatic shifts reach  $\sim 30 \mu\text{as}$ . However, the actual chromaticity error will include all sources of WFE, i.e. including optical misalignments and residual polishing residual errors. The lower figure shows an example of a chromaticity map obtained by including all sources of WFE, assuming that polishing errors are  $\lambda/30$  RMS for the primary mirror and  $\lambda/50$  RMS for the secondary. For constructing this map, the polishing errors were arbitrarily distributed over 3-rd and 5-th order Zernike polynomials. This is a worst case scenario, since the actual polishing error will be distributed over a much larger number of polynomials (the actual spectrum depends sensitively on the polisher and the polishing technique), and since high-spatial-frequency wavefront errors contribute marginally to chromaticity. Nevertheless, this example shows that chromatic shifts of several hundred  $\mu\text{as}$  should be expected. This is confirmed by recent simulations of the EADS Astrium Gaia flight-model design. With the aid of the photometric data these shifts can be accurately calibrated by the data processing on ground, thus not impacting the final mission performance.



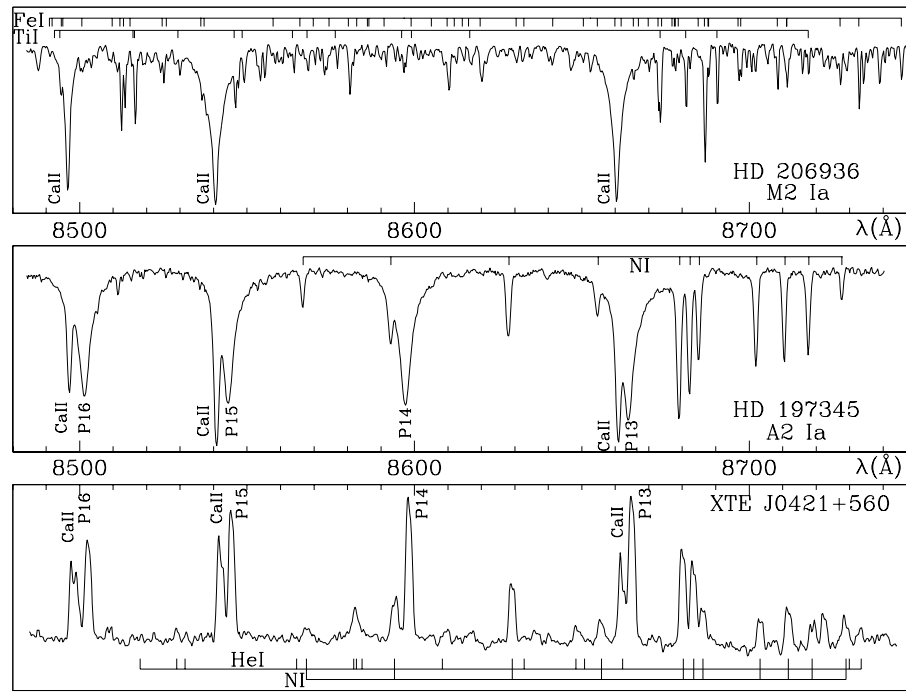
Simulation of a galactic halo formed by accretion of 50 dwarf galaxies over a period of 10 Gyr. Each colour represents an accreted satellite galaxy. Gaia's data will allow astronomers to identify and characterise the accretion events that have taken place in the halo of the Milky Way. Image courtesy of A. Helmi and the 'Spaghetti Project Survey' team.

The primary objective of the Gaia's Radial Velocity Spectrometer (RVS) instrument is the acquisition of radial velocities. These line-of-sight velocities complement the proper-motion measurements provided by the astrometric instrument. Together, these data provide the means to decipher the kinematical state and dynamical history of our Galaxy.

The RVS will provide the radial velocities of about 100-150 million stars up to 17-th magnitude with precisions ranging from  $15 \text{ km s}^{-1}$  at the faint end to  $1 \text{ km s}^{-1}$  or better at the bright end. Gaia's data will radically improve our understanding of the Milky Way. It will allow us to probe the gravitational potential and the distribution of dark matter throughout the Galaxy, to map the spiral structure of the Galactic disc, to disentangle, characterise, and constrain the origin and evolution of the stellar populations of the Galaxy, to recover the history of the halo accretion events, and to test the paradigm of the hierarchical formation of galaxies.

The RVS will collect, on average,  $\sim 40$  (transit) spectra per star over the 5 years of the mission. The associated multi-epoch radial-velocity information will be ideally suited for identification and characterisation of double and multiple systems. In particular, Gaia will provide masses and radii accurate to a few per cent for thousands of eclipsing binaries. The RVS will also monitor the radial motions of the outer layers of pulsating stars. It will provide pulsation curves for RR Lyrae stars, Cepheids and Miras up to  $\sim 14$ -th magnitude. Radial velocities will also be used to correct the astrometric data of nearby, fast-moving stars for the effects of 'perspective acceleration'.

The RVS wavelength range, 847–874 nm, is a rich domain. It will not only provide radial velocities, but also many stellar and interstellar diagnostics. The RVS data will effectively complement the astrometric and photometric observations of Gaia's targets, improving object classification. RVS data will also contribute to the derivation of stellar atmosphere parameters, in particular effective temperature, surface gravity, and overall metal abundances. Individual abundances of key chemical elements, e.g. Ca, Mg and Si, will be derived for millions of stars up to  $\sim 12$ -th magnitude, bringing major improvement in our knowledge of the chemical history and the enrichment processes of the Galaxy. Information on many facets of stellar physics will be extracted from the spectroscopic observations, for example, stellar rotation, chromospheric activity, and mass loss. Finally, from the 862-nm Diffuse Interstellar Band (DIB), RVS data will allow astronomers to derive a 3-dimensional map of interstellar reddening.



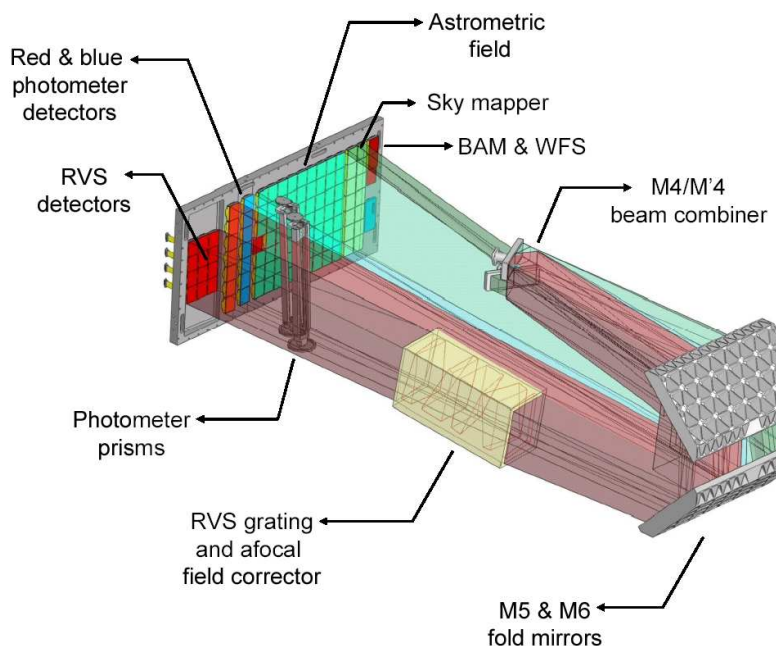
Spectra of the late-type star HD 206936 (top), of the early-type star HD 197345 (middle), and of the X-ray-transient star XTE J0421+560 (bottom), obtained with the echelle spectrograph mounted on the Asiago 1.82-m telescope. The different morphologies of the spectra outline the classification potential of the RVS wavelength range. Figure courtesy of U. Munari.

The Radial Velocity Spectrometer (RVS) is an integral-field spectrograph dispersing the light of the field of view with a resolving power  $R \sim 11,500$ . The RVS instrument, like the astrometric and photometric instruments, operates in TDI (time-delayed integration) mode, observing each source about 40 times during the 5 years of the mission. The RVS wavelength range, 847–874 nm, has been selected to coincide with the energy-distribution peaks of G- and K-type stars which are the most abundant RVS targets. For these late-type stars, the RVS wavelength interval displays, besides numerous weak lines mainly due to Fe, Si, and Mg, three strong ionised Calcium lines (at around 849.8, 854.2, and 855.2 nm). The lines in this triplet allow radial velocities to be derived, even at modest signal-to-noise ratios. In early-type stars, RVS spectra may contain weak lines such as Ca II, He I, He II, and N I, although they will generally be dominated by Hydrogen Paschen lines.

Over the 5 years of the mission, the RVS will observe  $\sim 5$  billion (transit) spectra of the brightest 100–150 million stars on the sky. The on-ground analysis of this spectroscopic data set will be a complex and challenging task, not only because of the data volume but also because the spectroscopic data analysis relies on the multi-epoch photometric and astrometric data. As a consequence, the extraction of radial velocities and astrophysical parameters from Gaia's observations will be performed in a fully automated fashion. Automated methods will also be used to analyse the RVS spectra to extract, for example, chemical-element abundances, rotational velocities, and interstellar reddening.

Radial velocities will be obtained by cross-correlating observed spectra with either a template or a mask. An initial estimate of the source atmospheric parameters derived from the astrometric and photometric data will be used to select the most appropriate template or mask. Iterative improvements of this procedure are foreseen. For stars brighter than  $\sim 15$ -th magnitude, it will be possible to derive radial velocities from spectra obtained during a single field-of-view transit. For fainter stars, down to  $\sim 17$ -th magnitude, accurate summation of the  $\sim 40$  transit spectra collected during the mission will allow the determination of mean radial velocities.

Atmospheric parameters will be extracted from observed spectra by comparison of the latter to a library of reference-star spectra using, e.g., minimum-distance methods, principal-component analyses, or neural-network approaches. The determination of the source parameters will also rely on the information collected by the other two instruments: astrometric data will constrain surface gravities, while photometric observations will provide information on many astrophysical parameters. Details of the procedures with which to optimally 'combine' Gaia's astrometric, photometric, and spectroscopic data are currently being studied.



Schematic figure illustrating the location of the RVS optical module and CCDs. Figure courtesy of EADS Astrium.

The primary aim of the Radial Velocity Spectrometer (RVS) instrument is the acquisition of spectra for the brightest 100–150 million stars on the sky, down to 17-th magnitude. These spectra, mainly through extracted radial-velocity information, are crucial for the study of the kinematical and dynamical history of the Milky Way.

The RVS instrument is a near-infrared (847–874 nm), medium-resolution ( $R = \lambda/\Delta\lambda \sim 11,500$ ), integral-field spectrograph dispersing all the light entering the field of view. The RVS instrument is integrated with the astrometric and photometric instruments and telescopes; the RVS CCDs are located in the Gaia focal plane. RVS uses the (astrometric) Sky Mapper function for object detection and confirmation. Objects will be selected for RVS observation based on measurements made slightly earlier in the Red Photometer. Light from objects coming from the two viewing directions of the two telescopes is superimposed on the RVS CCDs.

The spectral dispersion of objects in the field of view is materialised by means of an optical module physically located between the last telescope mirror (M6) and the focal plane. This module contains a grating plate, a filter plate, and four fused-silica lenses which correct the main aberrations of the off-axis field of the telescope. The RVS module has unit magnification which means that the effective focal length of the RVS equals 35 m. Spectral dispersion is oriented in the along-scan direction. A dedicated passband filter restricts the throughput of the RVS to the desired wavelength range. The total throughput of the telescope (6 Silver reflections), the grating plate, the four dioptric elements, and the bandpass rejection filter is  $\sim 30\%$  at the central wavelength of the spectrograph (this value includes the CCD quantum efficiency).

The RVS-part of the Gaia focal plane contains 3 CCD strips and 4 CCD rows. With an assumed dead time of 20%, each source will thus typically be observed during  $\sim 40$  field-of-view transits throughout the 5-year mission. On the sky, the RVS CCD rows are aligned with the astrometric and photometric CCD rows; the resulting semi-simultaneity of the astrometric, photometric, and spectroscopic transit data will be advantageous for variability analyses, scientific alerts, spectroscopic binaries, etc. All RVS CCDs are operated in TDI (time-delayed integration) mode. The RVS CCDs have 4500 TDI lines and 1966 pixel columns ( $10 \times 30 \mu\text{m}^2$  pixels) and are red enhanced with high resistivity.

RVS spectra will be binned on-chip in the across-scan direction. All single-CCD spectra are transmitted to the ground without any further on-board (pre-)processing. For bright stars, single-pixel-resolution windows will be used. The RVS will be able to reach object densities on the sky of at least  $36,000$  objects  $\text{deg}^{-2}$ .